

AD-A202 438 DOCUMENTATION PAGE

ATTC FILE COPY

2

1a. REPORT SECURITY CLASSIFICATION

UNCLASSIFIED

1b. RESTRICTIVE MARKINGS

2a. SECURITY CLASSIFICATION AUTHORITY

3. DISTRIBUTION / AVAILABILITY OF REPORT  
Approved for public release;  
distribution is unlimited.

2b. DECLASSIFICATION / DOWNGRADING / DEREGISTRATION

4. PERFORMING ORGANIZATION / REPORT NUMBER(S)

5. MONITORING ORGANIZATION REPORT NUMBER(S)

AFOSR-TR-88-1006

6a. NAME OF PERFORMING ORGANIZATION

Colorado State University

6b. OFFICE SYMBOL  
(if applicable)

7a. NAME OF MONITORING ORGANIZATION

AFOSR/NP

6c. ADDRESS (City, State, and ZIP Code)

Fort Collins, CO 80523

7b. ADDRESS (City, State, and ZIP Code)

Building 410, Bolling AFB DC  
20332-6448

8a. NAME OF FUNDING / SPONSORING ORGANIZATION

AFOSR

8b. OFFICE SYMBOL  
(if applicable)

NP

9. PROCUREMENT INSTRUMENT IDENTIFICATION NUMBER

AFOSR-86-0096

8c. ADDRESS (City, State, and ZIP Code)

Building 410, Bolling AFB DC  
20332-6448

10. SOURCE OF FUNDING NUMBERS

PROGRAM ELEMENT NO.  
61102FPROJECT NO.  
2301TASK NO.  
A8WORK UNIT  
ACCESSION NO.

11. TITLE (Include Security Classification)

(U) STUDY OF THE GENERATION OF INTENSE PULSED ELECTRON BEAMS USING A  
GLOW DISCHARGE

12. PERSONAL AUTHOR(S)

Dr. Jorge J. Rocca

13a. TYPE OF REPORT  
FINAL13b. TIME COVERED  
FROM 1 Mar 86 TO 29 Feb 88

14. DATE OF REPORT (Year, Month, Day)

88 Feb 88

15. PAGE COUNT  
109

16. SUPPLEMENTARY NOTATION

17. COSATI CODES

FIELD GROUP SUB-GROUP

20.09

18. SUBJECT TERMS (Continue on reverse if necessary and identify by block number)

19. ABSTRACT (Continue on reverse if necessary and identify by block number)

The electric field distribution in the cathode sheath of an electron-beam glow discharge has been measured and calculated. The electron yield of various cathode materials under helium ion bombardment has been measured. Current densities in excess of 10 amps per sq-cm have been generated from cold cathode glow discharges. The plasma of a pulsed high current density electron beam glow discharge has been characterized. Negative glow plasmas have been studied as electron sources for the generation of high current density electron beams.

SEARCHED  
DEC 09 1988  
SERIALIZED  
H

20. DISTRIBUTION / AVAILABILITY OF ABSTRACT

 UNCLASSIFIED/UNLIMITED  SAME AS RPT.  DTIC USERS

21. ABSTRACT SECURITY CLASSIFICATION

UNCLASSIFIED

22a. NAME OF RESPONSIBLE INDIVIDUAL

D. J. BARKER

22b. TELEPHONE (Include Area Code)

(202) 767-5011

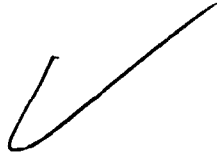
22c. OFFICE SYMBOL

AFOSR/NP

DD FORM 1473, 84 MAR

83 APR edition may be used until exhausted.  
All other editions are obsolete.SECURITY CLASSIFICATION OF THIS PAGE  
UNCLASSIFIED

88 128 \$15



STUDY OF THE GENERATION OF INTENSE  
PULSED ELECTRON BEAMS USING GLOW DISCHARGES  
GRANT AFSOR-86-0096

**AFOSR-TR. 88-1006**

FINAL REPORT

PERIOD: MARCH 1, 1986 - FEBRUARY 29, 1988

JORGE J. ROCCA  
PRINCIPAL INVESTIGATOR  
ELECTRICAL ENGINEERING DEPARTMENT  
COLORADO STATE UNIVERSITY  
FORT COLLINS, CO 80523



5) "A Reflex Electron Beam Discharge as a Plasma Source for Electron Beam Generation", C. Murray, B. Szapiro, and J.J. Rocca, Submitted for Publication, IEEE Journal of Plasma Sciences.

6) "Electron Yield of Glow Discharge Cathode Materials Under Helium Ion Bombardment", B. Szapiro, J.J. Rocca<sup>(a)</sup>, and Prabhurham T., Submitted for Publication, Appl. Phys. Lett..

Conference Papers

1) "Generation of Intense Large Area Electron Beams by Glow Discharges", H.F. Ranea-Sandoval, N. Reesor, B. Szapiro, B. Wernsman and J.J. Rocca, Thirty-Ninth Annual Gaseous Electronics Conference, 1986.

2) "Quadratic Stark Laser Spectroscopy Determination of the Electric Field Distribution in the Cathode Sheath of an Electron Beam Glow Discharge", S.A. Lee, L.-U.A. Andersen, J.J. Rocca, M. Marconi, and N.D. Reesor, Gaseous Electronics Conference, 1987.

3) "A Reflex Glow Discharge as a Plasma Source for Broad Area Electron Beam Generation", J.J. Rocca, C. Murray, and B. Szapiro, IEEE Conference on Plasma Science, 1988.

4) "Electric Field Distribution in a Glow Discharge by Quadratic Stark Laser Spectroscopy", S.A. Lee, L.-U.A. Andersen, J.J.

Rocca, M. Marconi, and N.D. Reesor, Conference on Lasers and  
Electro Optics, 1988.

### Project Summary

We have studied the generation of high current density electron beams using glow discharges. The objective of this work has been to study fundamental aspects of high voltage glow discharges and to demonstrate the generation of high current density ( $> 10 \text{ A/cm}^2$ ) electron beam using cold cathode glow discharges. To achieve this goal we have completed the following studies.

- 1) Measurement and calculation of the electric field distribution in the cathode sheath of an electron beam glow discharge.

The energy distribution, current density and efficiency of the electron beams generated in the cathode sheath of high-voltage glow discharges are closely dependent on the electric field in that region. We have measured for the first time the electric field distribution in the cathode sheath of an electron beam helium glow discharge using laser saturation spectroscopy to determine the quadratic Stark shift produced by the electric field. A model of the cathode sheath was developed. Our calculations were made by solving Poisson's equation and the equations of continuity, in a self-consistent way, for the flux of energetic charged and neutral particles. The measured electric field value agrees within 10% with the calculations of the model.

- 2) Measurement of the electron yield of cathode materials for helium ion bombardment.

In the generation of electron beams by secondary emission of electrons from cold cathode surfaces the secondary emission coefficient of the cathode material is an important quantity. We have observed that oxidation of an aluminum cathode surface significantly increases the electron beam current density and efficiency as a consequence of the increase of the secondary electron emission coefficient. We measured the secondary electron emission coefficient of materials for helium ion bombardment in the energy range 0.5-20 keV for the surface conditions of cathodes in high voltage glow discharges. The materials studied are oxidized aluminum, oxidized magnesium, a molybdenum-aluminum oxide sintered composite, molybdenum, stainless steel, copper and graphite. Each sample was surface conditioned by operating it as cathode of a helium glow discharge shortly before the electron yield measurement. Oxidized magnesium and aluminum present the higher yields, followed by the sintered composite. This result is in agreement with observations of the current intensity emitted by high power d.c. cold cathode electron guns that use the same materials.

- 3) Generation of high current density ( $> 10 \text{ A/cm}^2$ ) electron beams from cold cathode glow discharges.

Our work has emphasized the use of high electron yield cathode materials in the generation of intense pulsed electron beams. We have studied the use of aluminum, magnesium and molybdenum cathodes in helium, nitrogen and oxygen atmospheres at pressures up to 720 mTorr and at voltages up to 100 kV. The oxidized aluminum and magnesium cathodes produced similar results, and the molybdenum cathode operated at considerably lower current in agreement with our electron yield measurements. Electron beam currents up to 900 A were produced at 65 kV using oxidized aluminum cathodes having an emitting surface area of  $44 \text{ cm}^2$ . This corresponds to a current density of  $20 \text{ A/cm}^2$ . The maximum electron beam current densities and energies are limited by the development of arcs occurring mainly in the periphery of the cathode, in the gap between the cathode and ceramic shield surrounding it. The electron beam generation was measured to be very efficient; the electron beam discharge current and the total discharge current were measured to differ in only a few percent.

The duration of the electron beam current pulses was limited by the energy stored in the capacitors of the Marx generator used to excite the discharges. At large electron beam current densities ( $20 \text{ A/cm}^2$ ) the pulse durations obtained were approximately  $0.2 \mu\text{s}$ , while at small current densities ( $1 \text{ A/cm}^2$ ) electron beam pulses lasted several  $\mu\text{s}$ .

The fraction of the electron beam current measured to be transmitted by a  $7.7 \mu\text{m}$  thick aluminum foil at a discharge

voltage of 100 kV was 80%. This value can be considered to be in reasonable agreement with our glow discharge model prediction, considered that the acceptance angle of our detection system was  $12^\circ$ , and consequently electrons scattered by the foil at large angles were not detected.

The radial and axial variation of the electron beam current density was measured. At low electron beam currents (100 A) the electron beam current profile is only slightly more intense at the axis. In contrast, the measurements performed at large currents show a distribution that is sharply peaked at the center. The electron beam current density at the axis is seen to increase as a function of the distance from the cathode due to self-constriction of the electron beam by the self-generated magnetic field. No external magnetic field was applied to compensate for this effect and at a current of 300 A the entire beam focuses in an area of a few  $\text{cm}^2$  at 17 cm from the electron gun. The location of the region of maximum current density at the axis approaches the cathode as the electron beam current increases.

- 4) Study of the plasma of a pulsed high current density electron beam glow discharge.

Electrostatic probe measurements showed that the negative glow plasma density and the electron beam current have a similar spatial distribution. The plasma density ( $8.5 \cdot 10^{11} \text{ cm}^{-3}$  at 450 A) was measured to depend linearly on the

discharge current. Electron temperatures between 1 and 1.5 eV were measured at 7 cm from the cathode. In discharges at high current densities a denser and higher temperature plasma was observed to develop at approximately 20 cm from the cathode, in the region where the electron beam current density increases due to self-constriction. The energy of the thermal electrons in this high luminosity region was found to be between 2 and 6 eV, depending on the discharge conditions. In this region secondary electrons produced by ionization are likely to be heated as a result of beam-plasma interactions. The plasma density was also found to be significantly higher. Values between  $5 \cdot 10^{12}$  and  $7 \cdot 10^{13} \text{ cm}^{-3}$  were measured at electron beam currents between 160 and 400 A. This phenomena can be avoided by placing the foil through which the electron beam might be extracted at less than 20 cm from the electron gun.

We have modeled the process of electron beam generation in the high current density helium glow discharges. The model was used to predict the density and energy distribution of the electron beam. Experimental values of the plasma density and temperature in the negative glow were used to calculate the flux of ions entering the cathode sheath. The electric field and the fluxes of charged particles in the cathode fall region were calculated in a self-consistent manner. Charge particle creation in the sheath resulting from ionization by fast ions and beam electrons was included. The electron beam current densities predicted by the model using the measured

plasma parameters are in good agreement with the experimental values. Fast neutral atoms created by charge transfer in the cathode sheath, are found to be at least as important as ions in causing the emission of electrons from the cathode surface. The emission due to neutral atoms results in electron beam current densities above those corresponding to the Child-Langmuir space charge limit ion flux for a given voltage and sheath thickness. The calculated electron beam energy distributions show that 95% of the electron beam energy is carried by electrons having an energy that is within 10% of that corresponding to the discharge voltage.

- 5) Study of negative glow plasmas as electron sources for the generation of high current density electron beams.

In addition to studying the direct generation of intense electron beams from the cathode fall region of a glow discharge, we demonstrated that thermal electrons from a negative glow plasma can be accelerated by an externally applied electric field to generate intense beams.

To demonstrate the feasibility of this scheme we used a hollow cathode discharge to create a 5 cm diameter negative glow plasma, and a potential difference between a pair of grids to accelerate the electrons and form a beam. We have obtained electron beam current densities greater than  $30 \text{ A/cm}^2$  and a total beam current of 92 A in 5  $\mu\text{s}$  pulses. The current of energetic electrons (2 keV) was measured at 15 cm

from the electron gun and does not include the electrons accelerated in the gap, but intercepted by the 40% opaque acceleration grid. The electron current density emitted by the plasma source is larger and approaches  $45 \text{ A/cm}^2$ . The ratio of electron beam current to discharge current is close to 1.

We have demonstrated the use of pulsed glow discharge electron beams to create extended plasmas, and the subsequent acceleration of thermal electrons from this plasma by an externally applied electric field could be a useful method for the generation of large area large current density electron beam pulses of several  $\mu\text{s}$  duration. For this purpose a reflex electron beam glow discharge has been used as a plasma source for the generation of broad area electron beams. An electron current of 120 A ( $12 \text{ A/cm}^2$ ) was extracted from the plasma in 10  $\mu\text{s}$  pulses and accelerated to energies greater than 1 keV in the gap between two grids. The scaling of the scheme for the generation of multikiloamp high energy electron beams is discussed.

Appendix 1

Journal Publications  
and  
Conference Papers

**Study of Intense Electron Beams Produced by High-  
Voltage Pulsed Glow Discharges**

**H. F. Ranea-Sandoval, N. Reesor, B. T. Szapiro, C. Murray,  
and J. J. Rocca**

Reprinted from  
IEEE TRANSACTIONS ON PLASMA SCIENCE  
Vol. PS-15, No. 4, AUGUST 1987

# Study of Intense Electron Beams Produced by High-Voltage Pulsed Glow Discharges

H. F. RANEA-SANDOVAL, N. REESOR, B. T. SZAPIRO, C. MURRAY, AND  
J. J. ROCCA, MEMBER, IEEE

**Abstract**—We report the generation of high-current-density ( $20 \text{ A/cm}^2$ ) pulsed electron beams from high-voltage (48–100 kV) glow discharges using cathodes 7.5 cm in diameter. The pulse duration was determined by the energy of the pulse generator and varied between 0.4  $\mu\text{s}$  and several microseconds, depending on the discharge current. The largest electron beam current (900 A) was obtained with an oxidized aluminum cathode in a helium-oxygen atmosphere. An oxidized magnesium cathode produced similar results, and a molybdenum cathode operated at considerably lower currents. A small-diameter ( $< 1 \text{ mm}$ ) well-collimated beam of energetic electrons of very high current density ( $> 1 \text{ kA/cm}^2$ ) was also observed to develop in the center of the discharge. Electrostatic probe measurements show that the negative glow plasma density and the electron beam current have a similar spatial distribution. Electron temperatures of 1–1.5 eV were measured at 7 cm from the cathode. The plasma density ( $8.5 \cdot 10^{11} \text{ cm}^{-3}$  at 450 A) was found to depend linearly on the discharge current. In discharges at high currents a denser and higher temperature plasma region was observed to develop at approximately 20 cm from the cathode. We have modeled the process of electron beam generation and predicted the energy distribution of the electron beam. More than 95 percent of the electron beam energy is calculated to be within 10 percent of that corresponding to the discharge voltage.

## I. INTRODUCTION

GLow DISCHARGES can be used to generate energetic beams of electrons by accelerating through the cathode fall the electrons emitted at the cathode surface by the bombardment of ions and fast neutrals [1]–[4]. There is no limit to the duration of the electron beam pulse, and it is possible to produce dc electron beams at current densities of  $> 0.1 \text{ A/cm}^2$  [5]. A detailed study of pulsed high-voltage glow discharges (40–80 kV) at currents of the order of  $10 \text{ mA/cm}^2$  was conducted by McClure [6]. O'Brien [7] has generated electron beam current densities in excess of  $1 \text{ A/cm}^2$  over large areas, for durations of the order of 20  $\mu\text{s}$ . His results were obtained using aluminum or stainless steel electrodes in different gaseous atmospheres. The largest current densities

Manuscript received November 26, 1986; revised May 22, 1987. This work was supported by the U.S. Air Force. J. Rocca was supported by a National Science Foundation Presidential Young Investigators Award. B. Szapiro was supported by a fellowship from the Universidad Nacional de Buenos Aires.

The authors are with the Electrical Engineering Department, Colorado State University, Fort Collins, CO 80523. H. F. Ranea-Sandoval is on leave from Centro de Investigaciones Opticas, (CIC-BA) Rep. Argentina. B. T. Szapiro is on leave from Programa de Fisica Experimental Tandil, (UNCPBA) Rep. Argentina.

IEEE Log Number 8716399.

that he obtained were  $5 \text{ A/cm}^2$  (in nitrogen at 20 mtorr) and  $3 \text{ A/cm}^2$  (in helium at 180 mtorr). Isaacs *et al.* [8] obtained electron beam current densities up to  $0.2 \text{ A/cm}^2$  using large-area ( $> 100 \text{ cm}^2$ ) aluminum cathodes in helium atmospheres up to pressures of 45 mtorr.

In the generation of dc electron beams by glow discharges it is known that oxidation of an aluminum cathode can significantly increase the electron beam current density and efficiency [3]. Surface nitridation causes a similar effect. This is a consequence of an increased secondary electron emission at the cathode surface. Thus, high secondary electron cathode materials are desirable. This work puts emphasis on studying the use of high-electron-yield cathode materials in the generation of intense pulsed electron beams.

We present in Section III results of operating aluminum and magnesium cathodes in helium, nitrogen and oxygen atmospheres at pressures up to 720 mtorr and at voltages between 48 and 100 kV. A small amount of oxygen ( $< 10 \text{ mtorr}$ ) was added to maintain the cathode oxidation in the helium discharges during long periods of operation. Electron beams with currents up to 900 A were produced at 65 kV using cathodes with an emitting surface area of  $44 \text{ cm}^2$ . This corresponds to a current density at the cathode of nearly  $20 \text{ A/cm}^2$ . A current density of  $9 \text{ A/cm}^2$  was measured passing through a  $7.7\text{-}\mu\text{m}$ -thick aluminum foil in the axis of the beam operating the discharge at 100 kV. The beam generation is very efficient; the electron beam current and the total discharge current were measured to differ by only a few percent. The duration of the electron beam current pulses was limited by the energy stored in the capacitors (5-nF erected capacitance) of the pulse generator. At large electron beam current densities ( $20 \text{ A/cm}^2$ ) the pulse duration is approximately 200 ns, while at small current densities ( $1 \text{ A/cm}^2$ ), it is several microseconds. We compare these results with those obtained using a molybdenum cathode that does not form a high secondary electron yield oxide or nitride layer.

In Section III-B the radial and axial distribution of the electron beam current is discussed. The radial profiles show the presence of a high-current-density ( $> 1 \text{ kA/cm}^2$ ) small-diameter ( $< 1 \text{ mm}$ ) beam in the axis of the discharge. This phenomenon is further discussed in Section III-D. Measurements of the plasma density and electron temperature in the negative glow region of the discharge were obtained using electrostatic probes. The

110 results are presented in Section III-C. The model of Section  
111 IV uses these data and predicts the electron energy  
112 distribution.

## 113 II. EXPERIMENTAL APPARATUS

115 A two-stage Marx generator capable of delivering 25 J  
116 at 100 kV was built using commercially available spark-  
117 gaps, pressurized with dry nitrogen. Both stages of the  
118 Marx generator are triggered by a transmission line dis-  
119 charged by a third spark-gap. This spark-gap is switched  
120 by discharging a second transmission line through a  
121 grounded-grid hydrogen thyatron.

122 The experimental setup is schematically shown in Fig.  
123 1. The Marx generator is enclosed in a metal tank filled  
124 with transformer oil. The vacuum chamber consists of a  
125 stainless steel cylinder 50 cm long, 20 cm ID in which  
126 the cathode is placed 13 cm from one end. The vacuum  
127 chamber is grounded and constitutes the anode of the dis-  
128 charge. The electron gun is connected to the Marx gen-  
129 erator by a high-voltage high-vacuum feedthrough. The  
130 cathode holder includes a water refrigeration system for  
131 high repetition rate operation. However, most of the re-  
132 sults presented herein were obtained at 1-Hz repetition  
133 rate.

134 The vessel is pumped to  $10^{-6}$  torr by a 200 l/s turbo-  
135 molecular pump. Pressure is measured by an ionization  
136 gauge. The gases are flowed at a slow rate into the cham-  
137 ber through needle valves, and circulated by means of a  
138 rotary pump to minimize impurities in the gas mixture.  
139 Working gas pressures are measured with a capacitance  
140 manometer.

141 A diagram of the electron gun is presented in Fig. 2.  
142 The cathode is enclosed in a closely spaced (1 mm) di-  
143 electric shield to avoid emission from surfaces other than  
144 the front one. The enclosure was made of polycarbonate  
145 due to its ability to support surface flashover without sig-  
146 nificant deterioration. A ceramic shield protects the plas-  
147 tic from direct exposure to the discharge by avoiding pos-  
148 sible carbon sputtering from the polycarbonate, due to ion  
149 bombardment. The electron gun structural design allows  
150 for the easy replacement of cathodes. Cathodes made of  
151 oxidized aluminum, magnesium, and molybdenum were  
152 tested. They are 7.5-cm-diameter 3.5-cm-long cylinders  
153 with rounded edges at their front surfaces.

154 The front cathode surfaces are hand-polished, but the  
155 results do not show any significant dependence on the sur-  
156 face finishing except when pores are present. Pores can  
157 cause the development of arcs on the cathode front sur-  
158 face, and consequently the collapse of the higher imped-  
159 ance glow discharge. In the case of magnesium, devel-  
160 opment of pores was observed as a consequence of the  
161 chemical attack caused by a detergent used during the  
162 cleaning procedure. After this was realized, only acetone  
163 and methanol were used as cleaning agents.

164 The electron beam current was measured using a com-  
165 mercially available pulse current monitor coil mounted in-  
166 side the discharge chamber. The coil inside diameter is 5  
167 cm. It was placed coaxial with the beam, 7 cm from the

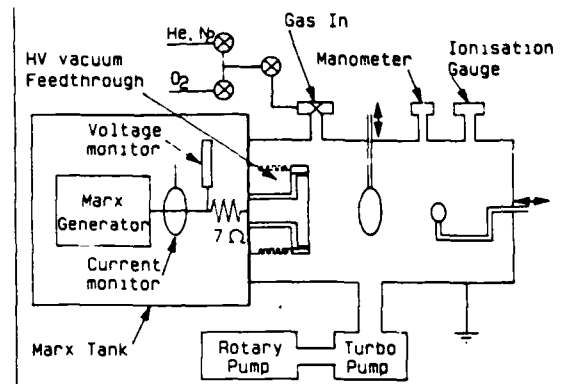


Fig. 1. Schematic diagram of the experimental apparatus. The electron beam current monitors could be alternatively replaced by movable Langmuir probes to measure electron temperature and plasma density. A 7- $\Omega$  resistor is in series with the discharge. A detailed diagram of the electron gun and high voltage vacuum feedthrough is shown in Fig. 2.

cathode surface, and gave a signal proportional to the electron beam current passing through it. The calibrated sensitivity of the coil is 0.1 V/A. A second coil having an inner diameter of 1.25 cm and a sensitivity of 1 V/A was also used in measuring electron beam current density profiles. The coils could be displaced along the diameter of the beam by a dynamic vacuum feedthrough shown in Fig. 1. The smaller coil could also be displaced along the axis of the discharge chamber when mounted in a second vacuum feedthrough placed at the end of the chamber. The introduction of the probes in the negative glow region of the plasma, that is almost field free, does not perturb the discharge. As shown by current transmission measurements through a filtering aluminum foil practically all (>95 percent) of the current going through the coil is composed by energetic beam electrons.

The total discharge current was measured by a third coil mounted inside the tank of the Marx generator. The discharge voltage was monitored using a 5000:1 resistive voltage divider. The plasma density and electron temperature were measured using electrostatic probes. Both single and double probes were used in these measurements. They were made of 0.25-mm-diameter tungsten wire, and were biased with batteries. Probe currents were measured with a commercially available current transformer. Spatially resolved plasma parameter measurements were obtained by displacing the probes with dynamic vacuum feedthroughs.

## III. EXPERIMENTAL RESULTS

### A. Electron Beam Generation

Glow discharges created using three different cathode materials were studied. Cathodes made of aluminum, magnesium, and molybdenum were alternately tested in oxygen, nitrogen, and helium-oxygen atmospheres. The largest electron beam current, 900 A, was obtained at 65 kV from a aluminum cathode in a helium-oxygen gas mixture. The electronic component of the glow discharge current was measured with the 5-cm-diameter current

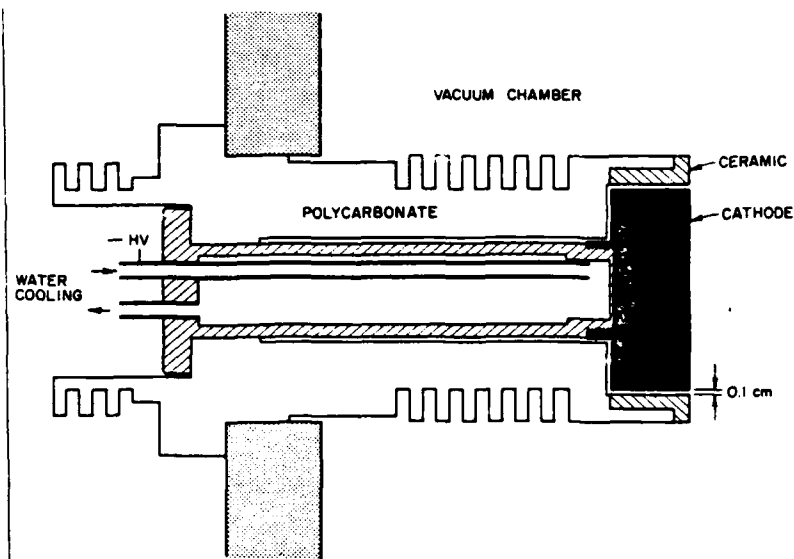


Fig. 2. Schematic diagram of the electron gun and high-voltage vacuum feedthrough. The cathode diameter is 7.5 cm.

207 monitoring coil placed at 7 cm from the cathode surface.  
 208 The active area of the coil is 20 cm<sup>2</sup>, approximately half  
 209 of the cathode area. It is shown in Section III-B that at  
 210 low currents (< 100 A) the electron beam current density  
 211 distribution across the cathode is approximately uniform.  
 212 Consequently, at low beam currents the electron flux  
 213 measured by the coil represents nearly half of the electron  
 214 beam current generated by the electron gun. At high currents,  
 215 almost all the electron beam flux is measured by the coil  
 216 due to the self-constriction of the electron beam, as  
 217 evidenced by the fact that this current is practically equal  
 218 to the total discharge current.

219 Fig. 3 shows the dependence of the electron beam current  
 220 generated by an aluminum cathode in a helium-oxygen  
 221 atmosphere on discharge conditions. The variation  
 222 of the electron beam current  $I$  (amperes) with  
 223 pressure  $P$  (torr) and discharge voltage  $V$  (kilovolts)  
 224 can be described by the empirical expression,  $I = CV^k P^m$ ,  
 225 where  $C = (4.8 \pm 0.1) 10^{-3}$ ,  $k = (3 \pm 0.15)$ , and  $m =$   
 226  $(2.2 \pm 0.2)$ .

227 The electron beam current increases sharply with in-  
 228 creasing pressure and discharge voltage. The maximum  
 229 values of voltage and pressure at which the electron beam  
 230 discharge may be operated is limited by the occurrence  
 231 of arcs in the gap between the cathode and the ceramic  
 232 shield. At a Marx generator voltage of 65 kV, the dis-  
 233 charge was operated at pressures up to 600 mtorr. At these  
 234 conditions, the electron current measured through the  
 235 monitoring coil was 900 A. This value corresponds to an  
 236 electron beam current density at the cathode of approxi-  
 237 mately 20 A/cm<sup>2</sup>. At a voltage of 100 kV the maximum  
 238 operating pressure at which an electron beam was ob-  
 239 tained was 320 mtorr, resulting in an electron beam cur-  
 240 rent of 300 A.

241 Fig. 4(a), (b) shows a 680-A electron beam current

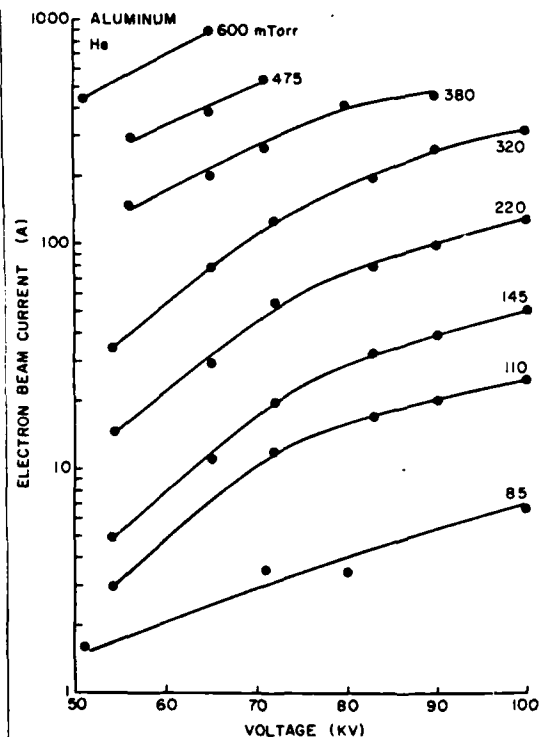


Fig. 3. Electron beam peak current versus initial voltage of the erected Marx generator, with pressure as a parameter. An aluminum cathode was used in He + 10 mtorr of O<sub>2</sub>. A 5-cm-ID pulse transformer was used to measure the current at 7 cm from the cathode.

pulse obtained operating the discharge at a pressure of 720 Mtorr and the discharge voltage for the same discharge conditions. The electron beam pulsewidth of 200 ns full width at half maximum (FWHM) is limited by the charge stored in the Marx generator. Fig. 5(a), (b) illus-

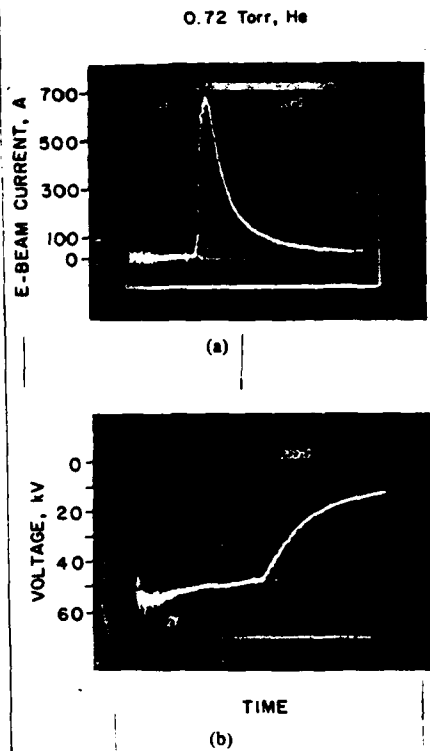


Fig. 4. (a) Electron beam current pulse. (b) Corresponding evolution of the discharge voltage. An aluminum cathode was used at 710 mtorr of He + 10 mtorr of O<sub>2</sub>. The photographs were obtained in different pulses at the same discharge conditions. Pulse-to-pulse variation was negligible. The change in the slope of the voltage pulse corresponds to the instant of discharge breakdown; the initial linear drop is due to charge losses from the Marx generator capacitors before breakdown.

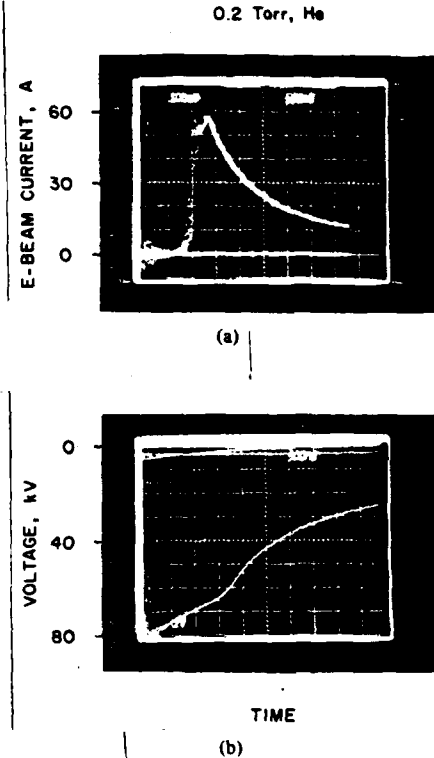


Fig. 5. (a) Electron beam current pulse. Three superimposed traces can be seen. (b) Corresponding evolution of the discharge voltage. An aluminum cathode was used at 190 mtorr of He + 10 mtorr of O<sub>2</sub>. The photographs were obtained in different pulses at the same discharge conditions. Pulse-to-pulse variation was negligible. The change in the slope of the voltage pulse corresponds to the instant of discharge breakdown; the initial linear drop is due to charge losses from the Marx generator capacitors before breakdown.

247 trates a lower current electron beam pulse of 1.6  $\mu$ s  
 248 FWHM and the discharge voltage variation. At lower dis-  
 249 charge currents electron beam pulses of longer duration,  
 250 lasting a few tens of microseconds, were recorded.

251 The electron beam current passing through a 7.7- $\mu$ m  
 252 thick aluminum foil was measured using the 5-cm-ID cur-  
 253 rent monitor. The foil was mounted on a stainless steel  
 254 plate having an orifice of 2.8 cm in diameter placed in the  
 255 axis of the discharge between the cathode and the coil.  
 256 Results obtained operating the discharge at 100 kV at  
 257 pressures between 100 mtorr and 300 mtorr are shown in  
 258 Fig. 6. A transmitted beam current density of 9 A/cm<sup>2</sup>  
 259 was measured at 300 mtorr. The energy cutoff of the fil-  
 260 tering foil is 28 keV [9]. The results of the sheath model  
 261 presented in Section IV show that the major part of the  
 262 electron beam energy is carried by high-energy electrons  
 263 with energy within 10 percent of that corresponding to the  
 264 discharge voltage.

15 The aluminum cathode was also operated in pure oxy-  
 16 gen and pure nitrogen atmospheres. Fig. 7(a), (b) shows  
 17 the variation of the electron beam current passing through  
 18 the 5-cm-diameter current monitoring coil as a function  
 19 of discharge pressure and voltage. For both molecular  
 20 gases, the maximum pressures at which an electron beam  
 21 was generated were below 60 mtorr, and the maximum

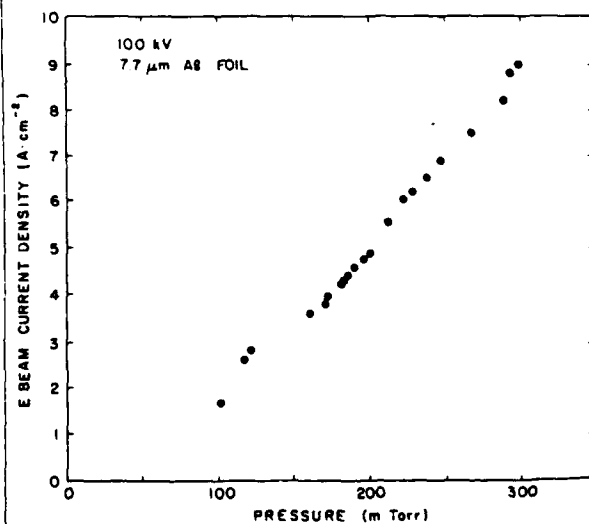


Fig. 6. Electron beam peak current density passing through a 7.7- $\mu$ m-thick aluminum foil placed at 7 cm from the cathode as function of discharge pressure. The filtering foil has an energy cutoff of 28 keV. Measurements were made through an on-axis aperture 2.8 cm in diameter. Increasing pressure corresponds to increasing discharge current. An aluminum cathode was used in a He + 10 mtorr O<sub>2</sub> atmosphere. The Marx output voltage was 100 kV.

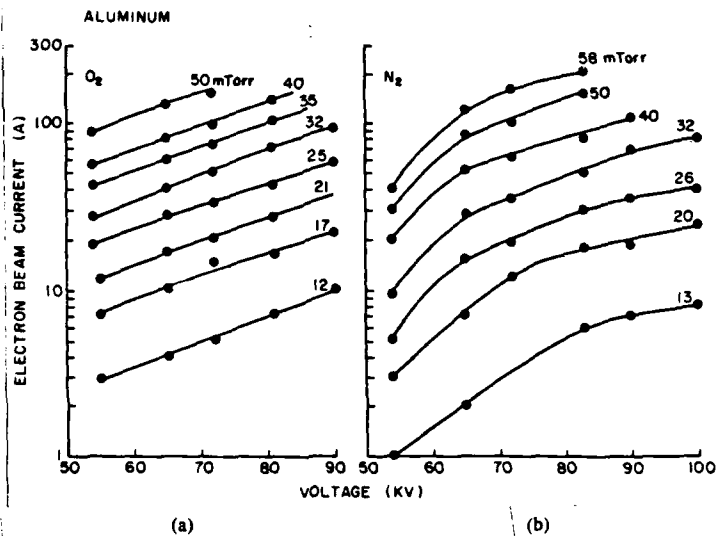


Fig. 7. Electron beam peak current versus initial voltage of the erected Marx generator, with pressure as a parameter. An aluminum cathode was used in (a) pure  $O_2$ , (b) pure  $N_2$ . In both cases a 5-cm-ID pulse transformer was used to measure the current at 7 cm from the cathode.

22 electron beam current obtained in both cases was below  
23 200 A.

24 The use of magnesium as a cathode material was also  
25 investigated. As in the case of aluminum, magnesium  
26 forms oxide or nitride layers that constitute efficient em-  
27 itters of electrons following ion bombardment. Fig. 8  
28 shows the variation of the electron beam current as a func-  
29 tion of discharge voltage and pressure. As in Fig. 3, the  
30 gas mixture contained 10 mtorr of oxygen, the balance  
31 being helium. The electron beam currents passing through  
32 the 5-cm monitoring coil are comparable to the values ob-  
33 tained with the aluminum cathode. A maximum current  
34 of 700 A was obtained at 65 kV and a pressure of 520  
35 mtorr.

36 Fig. 9(a), (b) shows the electron beam currents ob-  
37 tained operating the magnesium cathode in pure oxygen  
38 and nitrogen atmospheres, respectively. In these experi-  
39 ments the maximum electron beam current measured  
40 through the 5-cm coil was below 200 A. As in the case of  
41 aluminum, the electron beam currents obtained in the ox-  
42 ygen and nitrogen atmospheres are considerably lower  
43 than those obtained in the helium-oxygen mixture.

44 We also studied glow discharges generated using a mo-  
45 lybdenum cathode. In contrast with aluminum and mag-  
46 nesium, molybdenum does not form oxide or nitride lay-  
47 ers that significantly increase electron emission. Fig. 10  
48 summarizes the electron beam currents obtained in a he-  
49 lium atmosphere. Fig. 11(a), (b) shows the results ob-  
50 tained in experiments in pure oxygen and nitrogen atmo-  
51 spherics, respectively. In all cases, the currents emitted  
52 by the molybdenum cathode are significantly lower than those  
53 obtained with the oxidized cathodes. All the results dis-  
54 cussed in the following sections were obtained using alu-  
55 minum cathodes.

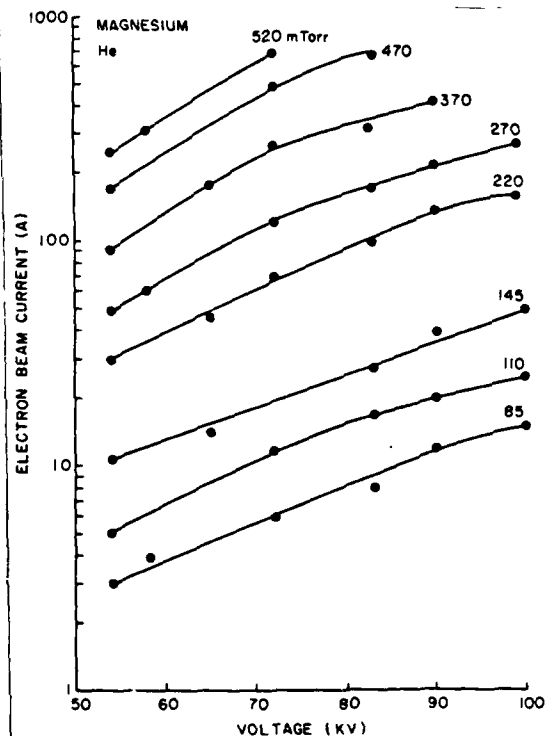
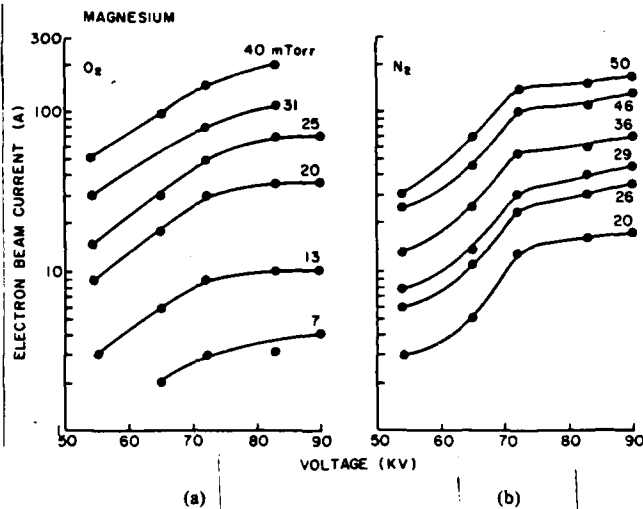


Fig. 8. Electron beam peak current versus initial voltage of the erected Marx generator, with pressure as a parameter. The magnesium cathode was used in He + 10 mtorr of  $O_2$ . A 5-cm-ID pulse transformer was used to measure the current at 7 cm from the cathode.

### B. Spatial Distribution of the Electron Beam Current

We have studied the radial and axial variation of the electron beam current. All the experiments discussed in this section were performed in a helium-oxygen atmo-



177 Fig. 9. Electron beam peak current versus initial voltage of the erected  
178 Marx generator, with pressure as a parameter. A magnesium cathode was  
179 used in (a) pure O<sub>2</sub>, (b) pure N<sub>2</sub>. In both cases a 5-cm-ID pulse  
180 transformer was used to measure the current at 7 cm from the cathode.  
181

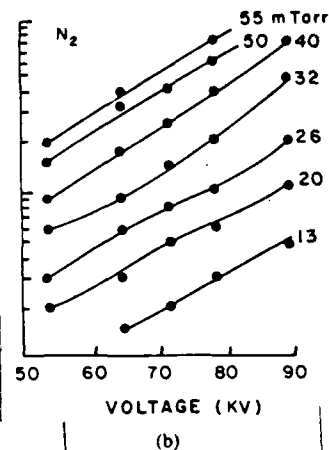
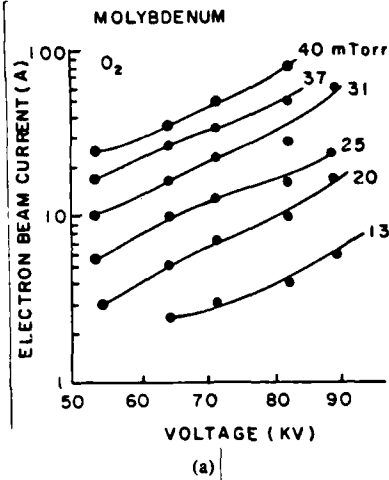
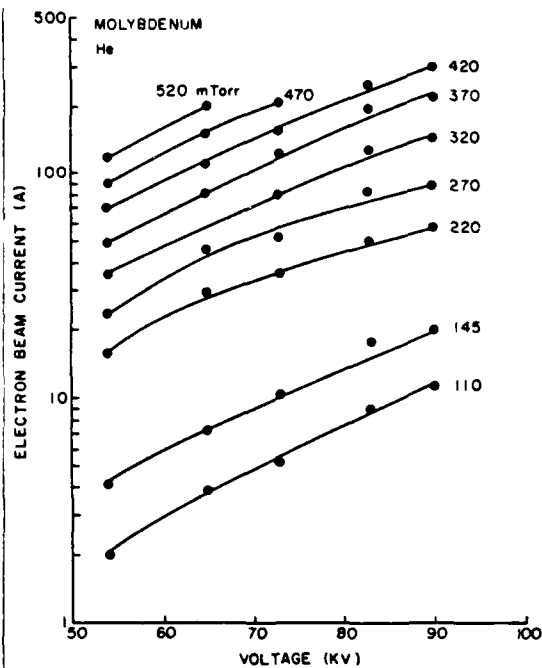


Fig. 11. Electron beam peak current versus initial voltage of the erected Marx generator, with pressure as a parameter. A molybdenum cathode was used in (a) pure O<sub>2</sub>, (b) pure N<sub>2</sub>. In both cases a 5-cm-ID pulse transformer was used to measure the current at 7 cm from the cathode.



185 Fig. 10. Electron beam peak current versus initial voltage of the erected  
186 Marx generator, with pressure as a parameter. A molybdenum cathode  
187 was used in He + 10 mTorr of O<sub>2</sub>. A 5-cm-ID pulse transformer was  
188 used to measure the current at 7 cm from the cathode.  
189

61 sphere. The radial distribution was measured displacing  
62 the 1.25-cm-diameter coil masked by a stainless steel plate  
63 across a cathode diameter by means of a vacuum feed-  
64 through. The plate supported two blades defining a 1.25  
65 × 0.2 cm<sup>2</sup> slot that provided good spatial resolution. The  
66 electron beam current profile was measured monitoring  
67 the current passing through the slot at different positions.  
68 When using this configuration to measure the electron

beam current in the region close to the axis of the discharge two very distinct groups of current pulses were observed for a given discharge condition. One group of plates is distinguished by an anomalously high current. These pulses were determined to be due to the presence of a small-diameter (0.5 mm) high-current-density (1000 A/cm<sup>2</sup>) beam of electrons. The position of this mini-beam was observed to change slightly from shot to shot, but was always observed to appear near the center of the discharge. Even if the current contribution of this small beam is only several amps, it can distort the electron beam current radial profiles and should be taken into account in analyzing the current distribution profiles. Anomalously high currents pulses were measured in the shots in which the position of this minibeam was coincident with the slot. The characteristics of this small diameter beam of electrons is further discussed in Section III-D.

The solid lines in Fig. 12 show the radial distributions of the electron beam current measured at 7 cm from the cathode corresponding to discharge currents of 100 and

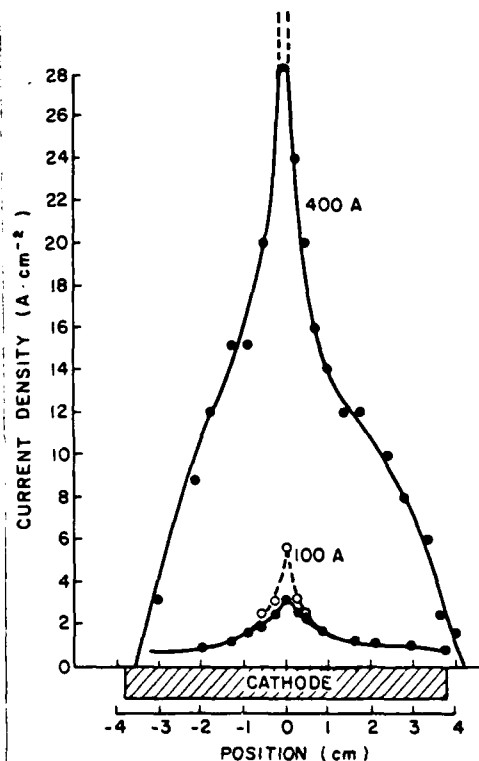


Fig. 12. Radial distribution of electron beam peak current density measured at 7 cm from the aluminum cathode for two values of the discharge current. A slotted mask of  $1.25 \times 0.2 \text{ cm}^2$  was used in front of the current monitor. The full lines correspond to data obtained in the absence of the minibeam. The dashed lines relate data points obtained in the presence of the minibeam. In the 400-A profile, the near axis values in the presence of the minibeam reach  $80 \text{ A/cm}^2$  and fall out of scale. The shadowed region in the abscissas identifies the relative position of the cathode.

400 A in the absence of the minibeam. The shape of the profile measured by O'Brien [7] for a  $180\text{-cm}^2$  aluminum cathode operated at a current of 34 A was very uniform. Our measurements at a larger current of 100 A show an electron beam profile that is slightly more intense at the axis. When the current was further increased to 400 A a distribution sharply peaked at the axis was obtained. The current calculated by integrating the 5-cm central region under the respective profiles agrees within 10 percent with the current measured with the 5-cm-diameter pulse transformer, at the same discharge conditions.

The dashed lines in Fig. 12 relate to measurements in which the position of the minibeam was coincident with the slot and were obtained in several pulses by displacing the current probe as described above. The data points symbolized with open circles include the current contribution of the minibeam and appear to increase the current density of the electron beam in the axis of the discharge. However, a better description of the current distribution for a given pulse is the one described by the solid lines with the addition of a very narrow (0.5 mm) peak at some specific location near the axis of the discharge within the region corresponding to the dashed lines in Fig. 12.

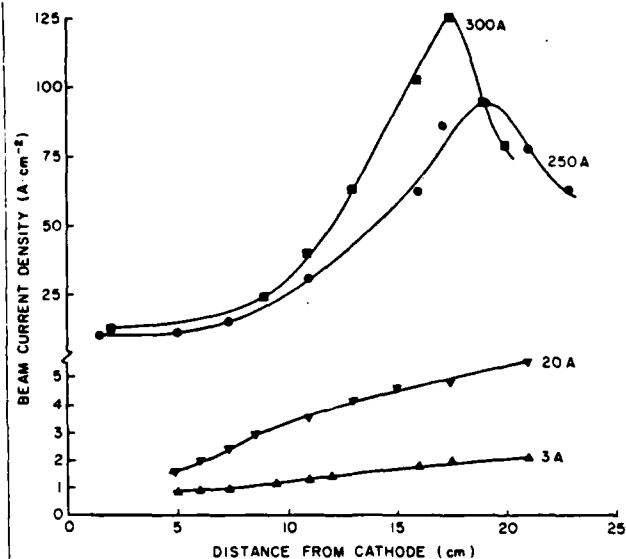


Fig. 13. Electron beam current density profile along the axis of the beam, measured using a 1.25-cm-diameter coil. The discharge voltage was 72 kV. A change of scale was used in the current density axis, to allow the comparison of the four curves. Peak discharge currents are indicated.

Fig. 13 shows the current density variation along the electron beam axis for four values of the discharge current measured with the 1.25-cm-diameter coil. The electron beam current density at the axis is seen to increase as a function of the distance from the cathode. At 300 A the entire beam focuses into a spot of a few square centimeters at 17.5 cm from the cathode surface. The location of the region of maximum current density at the axis approaches the cathode as the electron beam current increases. The variation of this location with discharge conditions agrees well with results of simple calculations of the beam constriction due to the self-generated magnetic field.

At high currents ( $>150 \text{ A}$ ) a bright, pink plasma is observed in the region where the highest current densities are attained. The electrostatic probe measurements discussed in Section III-C confirm that a higher density plasma ( $>5 \times 10^{12} \text{ cm}^{-3}$ ) develops in this region. Strong beam-plasma interactions are likely to occur there. This phenomenon was previously observed in the focal region of glow-discharge-generated dc electron beams [10]. By this mechanism a significant fraction of the electron beam energy is transferred to the plasma, which increases both its density and temperature. Simultaneously, the electron beam spectrum degrades [10] and the beam diverges.

We have also studied the radial profiles of the beam after passing through a  $7.7\text{-}\mu\text{m}$ -thick aluminum foil at 7 cm from the cathode. Figs. 14 and 15 compare the beam profiles with and without the foil at the same set of discharge voltage and He-O<sub>2</sub> operating pressure: at 100 kV and 100 mtorr, and at 100 kV and 200 mtorr, respectively. In both cases the integrated current passing through the foil is approximately 80 percent of the current evaluated from the profile without the foil. The acceptance an-

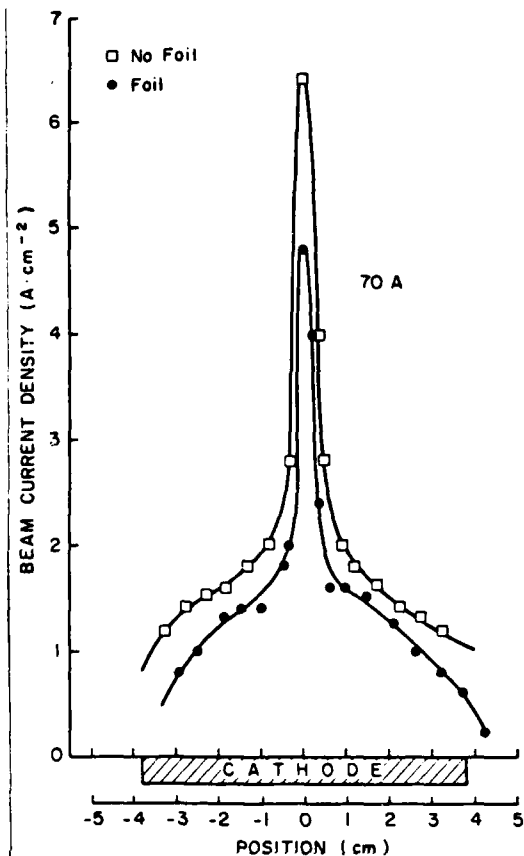


Fig. 14. Electron beam current radial profile measured with (lower trace) and without (upper trace) a 7.7- $\mu\text{m}$ -thick Al foil placed between the cathode and the coil. The profile was measured with a slotted aperture of  $0.2 \times 1.25 \text{ cm}^2$  placed in front of a current monitoring coil at 7 cm from the cathode. The peak discharge current was 70 A.

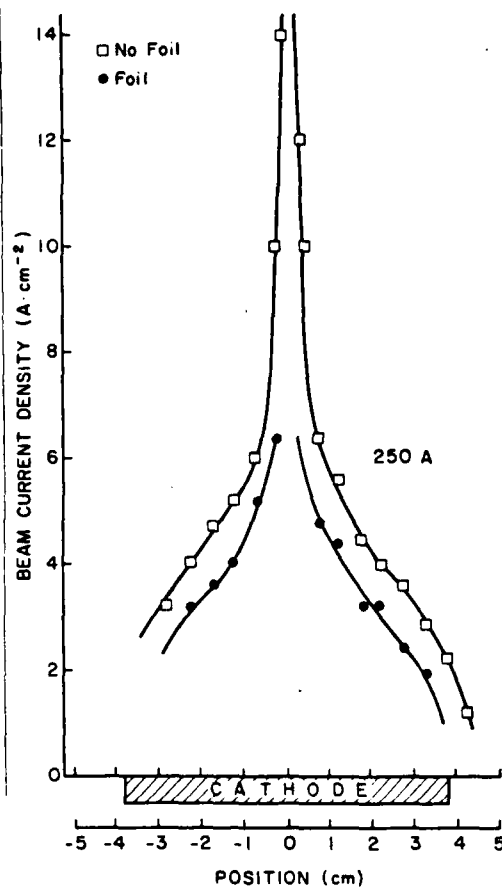


Fig. 15. Electron beam current radial profile measured with (lower trace) and without (upper trace) the 7.7- $\mu\text{m}$ -thick Al foil placed between the cathode and the coil. The profile was measured with a slotted aperture of  $0.2 \times 1.25 \text{ cm}^2$  placed in front of a current monitoring coil at 7 cm from the cathode. The peak discharge current was 250 A.

213  
214  
215  
216  
217  
218

146 gle of our detection system composed by the slot and the  
147 pulse transformer is rather small ( $12^\circ$ ). At 100 kV the  
148 fraction of fast electrons that are scattered by the foil at  
149 larger angles, thereby not reaching the detector, is cal-  
150 culated to be approximately 15 percent. Consequently, 95  
151 percent of the total current is estimated to be composed  
152 by fast electrons that pass through the foil.

153 Sharp peaks in the electron beam current density distri-  
154 butions are observed at the axis of the electron beam in  
155 Figs. 14 and 15. As previously discussed, the origin of  
156 this phenomenon is the presence of a very small diameter  
157 ( $< 1 \text{ mm}$ ) beam of energetic electrons approximately  
158 coincident with the axis of the high-current-density dis-  
11 charge. Thus, during the high-current-density measure-  
11 ments with the foil we avoided the axial region because  
€ the minibeam could perforate the foil. For this reason, the  
€ lower trace in Fig. 15. This phenomenon is further dis-  
€ cussed in Section III-D.

### 64 C. Electron Density and Temperature

66 The electron energy distribution in the negative glow of  
67 the discharge is non-Maxwellian, containing high-speed  
electrons that have been accelerated in the cathode fall

[11]. A large fraction of these electrons have an energy  
corresponding to approximately the entire discharge volt-  
age. The calculated energy distribution of these high-  
speed electrons is discussed in Section IV. Nevertheless,  
the majority of the electrons in the negative glow region  
have low energy. This low-energy group, which practi-  
cally determines the plasma density, is made of secondary  
electrons produced by the beam electrons in ionizing col-  
lisions [11]. The energy distribution of these slow elec-  
trons is approximately Maxwellian [6], [7], [10].

The knowledge of the plasma density and electron tem-  
perature in the negative glow region of the discharge is  
relevant to the process of electron beam generation. These  
parameters determine the ion flux from the negative glow  
to the cathode fall region. These ions, which are subse-  
quently accelerated in the cathode fall region, and the fast  
neutral atoms created by charge transfer collisions, are  
responsible for the emission of secondary electrons at the  
cathode surface. In the rest of this section we discuss the  
measurement of the temperature and density of the ther-  
malized electrons. In Section IV we use these experimen-  
tal values in a model of the discharge to predict the energy

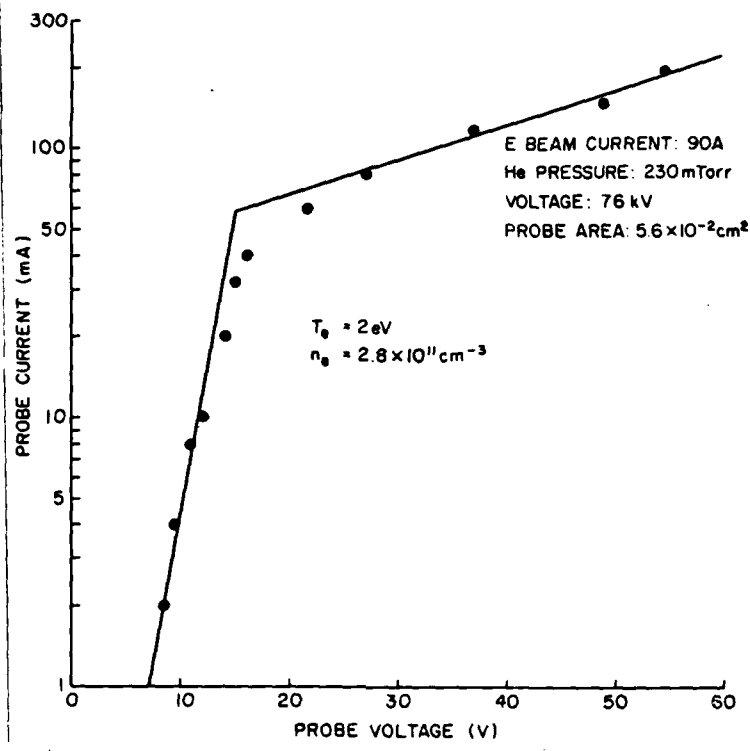


Fig. 16. Langmuir single-probe characteristic yielding plasma density and electron temperature. The measurements were performed at 20 cm from the cathode, at a discharge voltage of 76 kV, using an aluminum cathode in a helium-oxygen atmosphere at 230 mtorr.

91 distribution and density of beam electrons produced in the  
 92 glow discharge.

93 McClure [6] and O'Brien [7] have previously measured  
 94 the plasma density and electron temperature in the nega-  
 95 tive glow region of pulsed discharges. Their measure-  
 96 ments correspond to low-discharge current densities  
 97 ( $< 0.3 \text{ A/cm}^2$ ). We have measured these parameters at  
 98 glow discharge current densities up to  $10 \text{ A/cm}^2$ .

99 Our measurements were made using single and double  
 200 electrostatic probes. The probe traces were obtained by  
 201 sequentially changing the probe bias on a shot-by-shot ba-  
 202 sis. The double probe was used to measure in the high-  
 density plasma region, where the electron beam focuses.  
 The single probe, giving a larger signal, was used to mea-  
 sure in the lower density regions. Our double probe has a  
 better frequency response than our single probe. How-  
 ever, in measurements made in the plasma regions where  
 it was possible to compare both probes, the values of the  
 plasma parameters agree within a factor of two. Fig. 16  
 is a typical single probe trace, and corresponds to a mea-  
 surement taken at 20 cm from the cathode.

212 Radial profiles of the plasma densities measured at 7  
 213 cm from the cathode using a single probe are shown in  
 214 Fig. 17. The measurements were made at a discharge  
 215 voltage of 72 kV and at currents of 180 and 450 A. The  
 216 general shape of the plasma density profiles resembles the  
 217 radial distribution of the electron beam current density  
 218 shown in Fig. 12. The maximum plasma density is at the

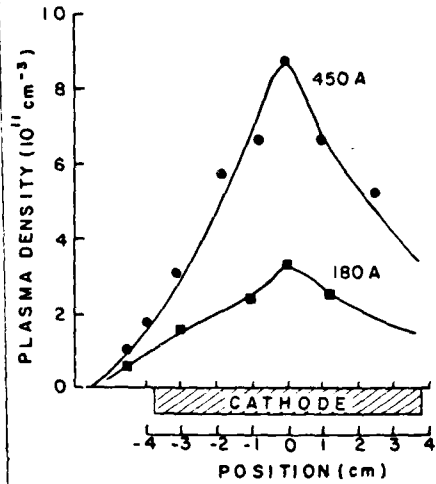


Fig. 17. Radial profiles of the plasma density measured at 7 cm from the cathode. Peak values of the discharge current are indicated.

axis of the beam, where the electron beam current density  
 peaks. Values of the electron temperature obtained from  
 the same measurements were all between 1 and 1.5 eV.

The variation of the plasma density on the axis of the  
 beam, at 7 cm from the cathode, as a function of dis-  
 charge current is illustrated in Fig. 18. The measurements  
 were obtained at a discharge voltage of 56 kV. In the range  
 of currents investigated, the plasma density was observed

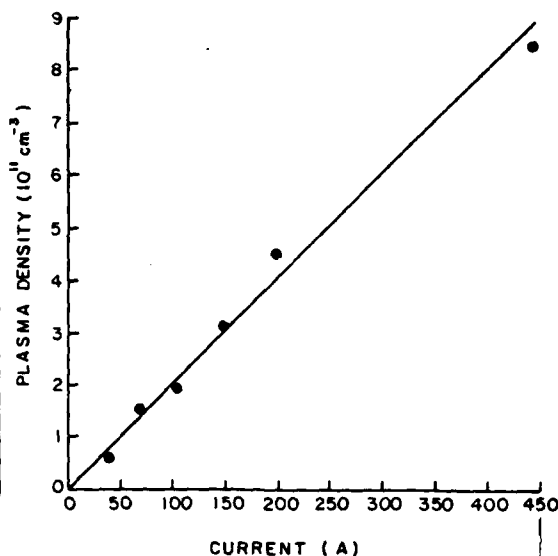


Fig. 18. On-axis plasma density as a function of the peak discharge current.

to increase linearly with the current, from a value of  $6 \times 10^{10} \text{ cm}^{-3}$  at 40 A to  $8.5 \times 10^{11} \text{ cm}^{-3}$  at 450 A. The electron energy values obtained from the same probe traces were also between 1 and 1.5 eV. In all the measurements made in the negative glow region of the discharge the plasma potential was between 5 and 10 V above anode potential, confirming that practically all the discharge voltage drops in the cathode sheath.

We also measured the plasma parameters at 20 cm from the cathode where at high currents a high luminosity plasma is observed. This is the region where, as shown in Fig. 13, the electron beam current density increases due to self-constriction. The energy of the thermal electrons in this region was observed to be consistently higher than closer to the cathode, where the electron beam current density is considerable lower. The measured electron energies in the high luminosity region are between 2 eV and 6 eV. Secondary electrons produced by ionization in the high luminosity region are likely to be heated as a result of beam-plasma interactions [10]. The plasma density in this region is also significantly higher. Values between  $5 \times 10^{12}$  and  $7 \times 10^{13} \text{ cm}^{-3}$  were measured at electron beam currents between 160 and 400 A.

Measurements were also made in a pure nitrogen atmosphere at 7 cm from the cathode and 72 kV of discharge voltage. At a pressure of 30 mtorr and discharge current of 60 A ( $1.3 \text{ A/cm}^2$ ), we obtained an electron temperature  $kTe = 1.2 \text{ eV}$  and a plasma density of  $1.1 \times 10^{11} \text{ cm}^{-3}$ . At a pressure of 40 mtorr and discharge current of 100 A ( $2.2 \text{ A/cm}^2$ ), these values were 1.4 eV and  $2 \times 10^{11} \text{ cm}^{-3}$ . These electron temperatures compare well with the value of  $kTe = 1 \text{ eV}$  measured by O'Brien [7] at lower current densities ( $0.3 \text{ A/cm}^2$ ). The plasma densities measured in both experiments indicate the same linear increase with the current density.

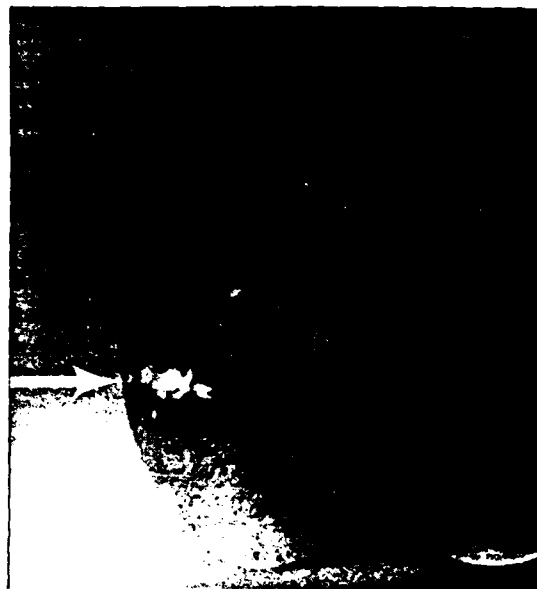


Fig. 19. Photograph of the plasma spot (arrow) generated when the mini-beam impinges the brass wall of the 1.25-cm-ID pulse transformer. The coil was rotated  $45^\circ$  with respect to the beam axis to make it more visible. Discharge voltage was 82 kV, and the He + 10 mtorr  $\text{O}_2$  pressure was 375 mtorr. The peak beam current was 300 A.

#### D. High Current Density Mini Electron Beam

As mentioned in Section III-B, a high-current-density electron beam of small diameter develops approximately in the axis of the discharge. This small beam made marks of less than 1 mm in diameter in the stainless steel blades used as collimators in the current profile measurements. As the coil was moved vertically across the cathode diameter, a line of similar dots was etched on the stainless steel plate used to protect the pulse transformer from electron bombardment.

Where this well-collimated minibeam impinges on a metallic surface, a bright plasma spot is observed. This effect is shown in Fig. 19. To obtain this photograph the coil was rotated  $45^\circ$  with respect to the axis of the discharge to permit viewing of the minibeam-created plasma. The photograph was obtained at a discharge voltage of 82 kV, in an He- $\text{O}_2$  mixture at 375 mtorr.

When the time evolution of the electron beam in the axial region of the beam was measured, the pulse shape shown in Fig. 20 was observed. This signal was obtained with a 1.25-cm-diameter current monitoring coil aligned with the axis of the discharge. A short pulse, having a width of approximately 20 ns, is apparent in the leading edge of the electron beam pulse. This feature is only observed in the axial region of the discharge where the minibeam is present, and consequently it is attributed to it.

Using data from Figs. 15 and 20 it is possible to obtain a rough estimate of the current and energy density of the minibeam. In Fig. 15 the current density at the center of the profile made without the aluminum foil is out of scale. The value there is  $32 \text{ A/cm}^2$ , and the major fraction is attributed to the minibeam. The corresponding measured

234  
236  
237

247  
248  
249  
250  
251  
252  
253  
254  
255  
256  
257  
258  
259  
260  
261

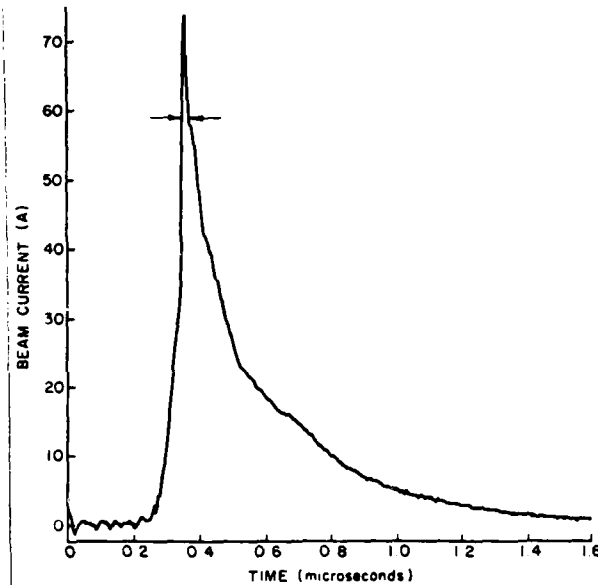


Fig. 20. Time evolution of the current in the central region of the electron beam. The signal was digitalized in 512 channels with 5-ns resolution. The minibeam is apparent between the arrows, and lasts about 20 ns. The He + 10 mtorr O<sub>2</sub> pressure was 430 mtorr and the discharge voltage was 72 kV.

18 current through the  $0.2 \times 1.25 \text{ cm}^2$  slot was 8 A. The  
 19 base of the narrow peak in Fig. 15 can be estimated to be  
 20  $7.5 \text{ A/cm}^2$ , corresponding to a current of approximately  
 21 2 A. Consequently, the current of the minibeam at these  
 22 discharge conditions is estimated to be 6 A. From the  
 23 marks left in the stainless steel plate the diameter of the  
 24 minibeam is estimated to be 0.5 mm. The corresponding  
 25 current density is of the order of  $1 \text{ kA/cm}^2$ . Considering  
 26 a pulsewidth of 20 ns and a discharge voltage of 100 kV,  
 27 the energy density of this small beam can be estimated to  
 28 be of the order of several joules per square centimeters.

29 Similar effects were also observed in magnesium cathodes  
 30 when the discharge currents were above a few  
 31 hundreds amperes. Moreover, the plasma spot shown in  
 32 Fig. 19 was found independent of the axial position of the  
 33 target. A more detailed study is needed to determine the  
 34 mechanism of formation of this high-current-density very-  
 35 small-area electron beam.

#### 36 IV. MODEL OF THE ELECTRON BEAM GENERATION

38 The pulsed glow discharges discussed in the previous  
 39 section were operated at high current densities ( $1\text{--}20$   
 40  $\text{A/cm}^2$ ) and at relatively high helium pressures. The  
 41 mechanisms of electron beam generation at these condi-  
 42 tions have not been previously studied.

43 We have modeled the process of electron beam genera-  
 44 tion in these high-current-density helium glow dis-  
 45 charges. The model was used to predict the density and  
 46 energy distribution of the electron beam. The results also  
 47 show that fast neutral atoms bombarding the cathode make  
 48 a major contribution to the total electron emission. We

constructed a model of the cathode fall region similar to  
 that previously developed by McClure [12] for a deuterium  
 discharge. Our experimental values of the parameters  
 of the negative glow region of the discharge were used to  
 calculate the flux of ions entering the cathode sheath. The  
 electric field and the fluxes of charged particles in the  
 cathode fall region were calculated in a self-consistent  
 manner. Charged particle pair creation in the sheath  
 resulting from ionization by fast ions and beam electrons  
 was included. The collisional processes considered in the  
 cathode fall region include the creation of fast neutral  
 atoms by charge transfer and are summarized in Table I.  
 The sources of the cross-section data used are also indi-  
 cated.

The secondary electron emission coefficients for alu-  
 minum under He<sup>+</sup> bombardment measured by Bourne *et al.*  
 [13] were used. The secondary emission yields due to  
 fast helium atoms and ions of the same energy were as-  
 sumed to be equal for energies above 20 keV [14], but  
 electron emission due to atoms was assumed to be negli-  
 gible for energies below 500 eV.

The electron beam energy distribution resulting from  
 running the model at 52 kV and 370 mtorr of helium is  
 shown in Fig. 21. The conditions correspond to a mea-  
 sured negative glow plasma density at  $4.5 \times 10^{11} \text{ cm}^{-3}$ ,  
 and electron energy of 1.5 eV. By integrating the data  
 shown in Fig. 21, we calculated that 97 percent of the  
 electron beam energy is carried by electrons having an  
 energy that is within 10 percent of that corresponding to  
 the discharge voltage. The low-energy peak is due to elec-  
 trons created by ionization in the sheath. The integration  
 of the total electron flux density amounts to a current den-

TABLE I  
COLLISIONAL PROCESSES IN THE CATHODE SHEATH

REACTION	PROCESS	REFERENCE
$e + He \rightarrow He_s^+ + 2e$	Ionization by electrons	[15], [16]
$e + He \rightarrow He_s^{++} + 3e$	Double ionization by electrons	[17]
$He_f^+ + He \rightarrow He_s^+ + He + e$	Ionization by fast neutrals	[18], [19]
$He_f^+ + He \rightarrow He_f^+ + He^+ + e$	Ionization by fast ions	[18], [19], [20]
$He_f^{++} + He \rightarrow He_s^+ + He_f^{++} + e$	Ionization by double ions	[17]
$He_f^+ + He \rightarrow He_f^{++} + He + e$	Ionization of fast ions	[18]
$He_f^+ + He \rightarrow He_f^+ + He^+$	Ion-neutral charge-transfer	[18], [21], [22]
$He_f^{++} + He \rightarrow He_f^+ + He^{++}$	Double ion-neutral double charge transfer	[23], [24], [25]
$He_f^{++} + He \rightarrow He_f^+ + He^+$	Double ion charge-transfer	[23], [24], [25]

s : slow particle

f : fast particle

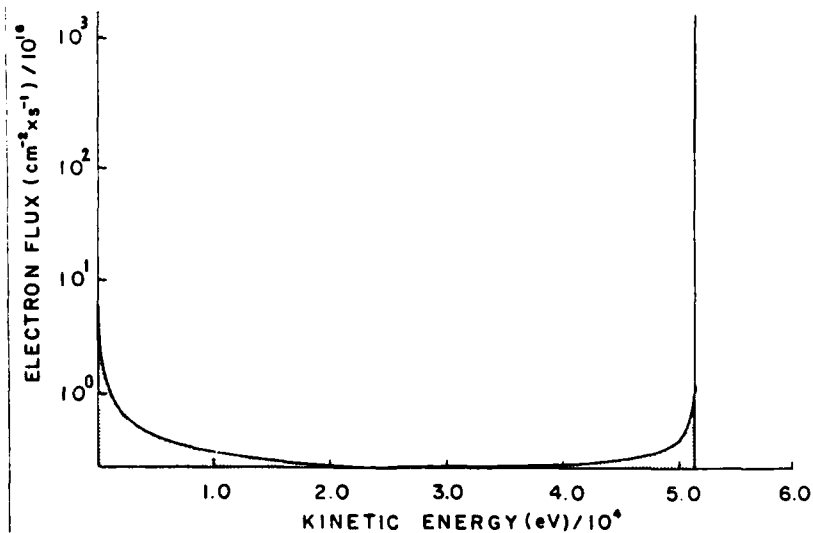


Fig. 21. Calculated electron flux energy distribution corresponding to a discharge voltage of 52 kV and a helium pressure of 350 mtorr.

111 sity of  $4.1 \text{ A/cm}^2$ . This value is in good agreement with  
112 the experimentally measured value of  $4.5 \text{ A/cm}^2$ .

113 Fig. 22(a), (b) is the predicted energy spectra of the  
114 fluxes of  $He^+$  and fast He atoms at the cathode. The emis-  
115 sion rate of electrons is calculated by the convolution of  
116 these curves with the corresponding secondary electron

emission data. For the above conditions the emission of  
electrons at the cathode due to fast neutrals is calculated  
to be 65 percent of the total electron emission at the cath-  
ode.

The model results can be summarized as follows. The  
electron beam current densities predicted using measured

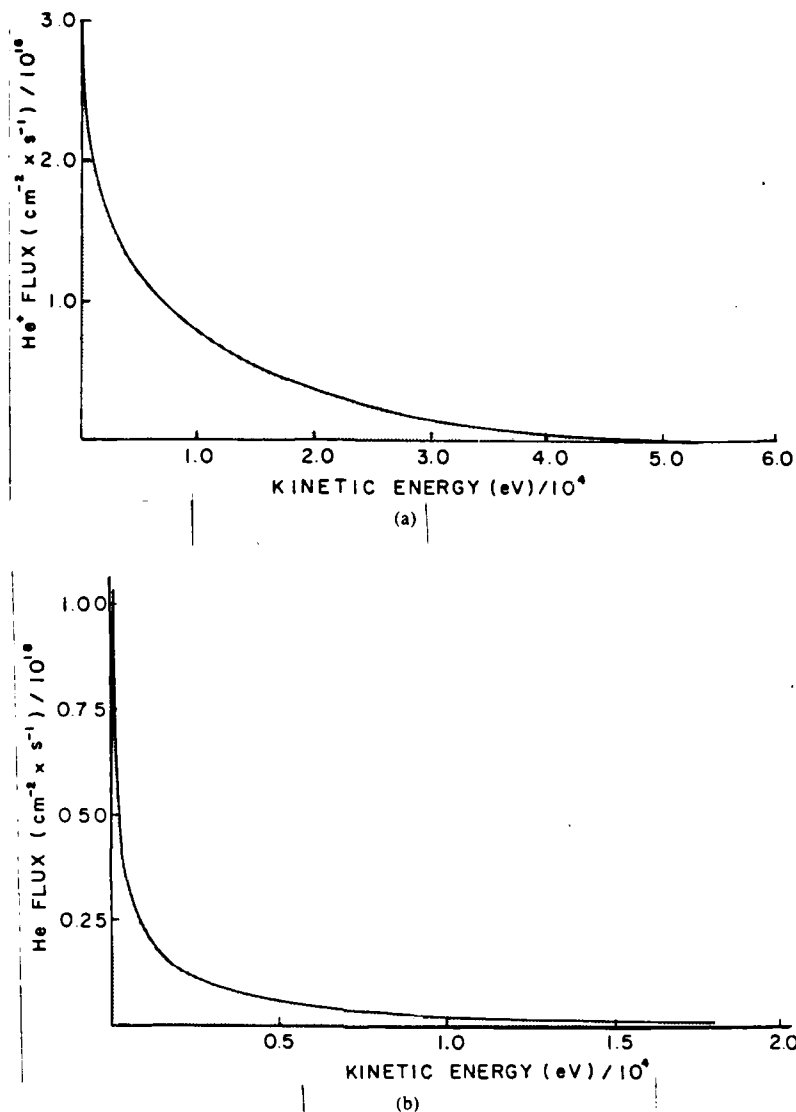


Fig. 22. (a) Calculated  $\text{He}^+$  flux energy distribution at the cathode surface. (b) Calculated neutral helium flux energy distribution at the cathode surface. The distributions corresponds to a discharge voltage of 52 kV and a helium pressure of 350 mtorr.

123 negative glow plasma parameters are of the same order as  
 124 the experimental values. Fast neutral atoms, created by  
 125 charge transfer in the cathode sheath, are at least as im-  
 126 portant as ions in causing the emission of electrons from  
 127 the cathode surface. The emission due to neutrals results  
 128 in electron beam current densities above those corre-  
 129 sponding to the Child-Langmuir space-charge-limited ion  
 130 flux for a given voltage and sheath thickness. More than  
 131 95 percent of the electron beam energy is carried by elec-  
 132 trons having an energy that is within 10 percent of that  
 133 corresponding to the discharge voltage.

#### 34 V. SUMMARY

36 We studied the generation of intense pulsed electron  
 37 beams in glow discharges at voltages between 48 and 100

kV using cathodes 7.5 cm in diameter. An aluminum  
 cathode in a helium-oxygen atmosphere produced elec-  
 tron currents up to 900 A ( $20 \text{ A/cm}^2$ ). Pulse duration was  
 limited by the stored energy in the Marx generator. A cur-  
 rent density of  $9 \text{ A/cm}^2$  was measured through a  $7.7\text{-}\mu\text{m}$ -  
 thick aluminum foil in the axis of a 100-kV discharge.  
 Similar current densities were obtained using an oxidized  
 magnesium cathode. Arcs developing between the cath-  
 ode and the ceramic shield set a limit for the maximum  
 electron beam current and voltage. The electron beam  
 currents obtained operating the discharge in pure oxygen  
 and nitrogen atmospheres were lower than those obtained  
 in the helium-oxygen mixture. A molybdenum cathode,  
 that does not have a high electron yield oxide layer, de-  
 livered considerably lower current densities.

153 Simultaneously, the glow discharges were observed to  
154 generate a small-diameter ( $< 1$  mm) short-duration (20  
155 ns) beam of energetic electrons of very high current density  
156 ( $> 1$  kA/cm<sup>2</sup>) in the axis. Its energy density ( $> 1$   
157 J/cm<sup>2</sup>) is enough to etch marks on metallic targets. The  
158 understanding of the mechanism of formation of this intense  
159 small beam requires further studies.

60 Electron beam current distribution measurements show  
61 that the beam is relatively uniform at low ( $< 100$  A) currents.  
62 At large currents, self-constriction increases the axial beam  
63 density. Electrostatic probe measurements show that the negative  
64 glow plasma density and the electron beam current have a similar  
65 radial distribution. The plasma density measured at the axis of  
66 the discharge at 7 cm from the cathode increases linearly with  
67 discharge current. The electron temperature in the same region  
68 was measured to be between 1 and 1.5 eV. A bright high-density  
69 plasma was observed in the region where the highest electron  
70 beam current densities occur. Electrostatic probe measurements  
71 show that both the plasma density and the electron temperature  
72 are higher there than in the other regions of the discharge. This  
73 is possibly due to the onset of beam-plasma instabilities.

174 A model of the cathode sheath predicts electron beam current  
175 density values in agreement with the experiments. According to the  
176 model results, more than half of the electron current emitted at  
177 the cathode is due to the bombardment of fast neutrals created  
178 by charge transfer in the cathode sheath. The calculated energy  
179 distribution shows that  $> 95$  percent of the electron beam is  
180 carried by electrons having an energy within 10 percent of the  
181 discharge voltage.

#### 185 ACKNOWLEDGMENT

186 The authors want to thank the experimental assistance  
187 of B. Wernsman and the skillful machining by J. Davis. The  
188 support and the helpful comments by A. Garscadden and P. Haland  
189 are gratefully acknowledged.

#### 190 REFERENCES

- [1] A. S. Pokrovskaya-Soboleva and B. N. Kliarfel'd, "Ignition of the high voltage discharge in hydrogen at low pressures," *Sov. Phys. - JETP*, vol. 5, pp. 812-818, Dec. 1957.
- [2] R. A. Dugdale, "Soft vacuum processing of materials with electron beams," *J. Mater. Sci.*, vol. 10, pp. 896-902, 1975.
- [3] J. J. Rocca, J. D. Meyer, M. R. Farrell, and G. J. Collins, "Glow-discharge-created electron beams: Cathode materials, electron gun designs, and technological applications," *J. Appl. Phys.*, vol. 56, pp. 790-797, Aug. 1984.
- [4] B. Wernsman, H. F. Ranea-Sandoval, J. J. Rocca, and H. Mancini, "Generation of pulsed electron beams by simple cold cathode plasma guns," *IEEE Trans. Plasma Sci.*, vol. PS-14, no. 4, 518-522, Aug. 1986.
- [5] J. J. Rocca, J. D. Meyer, Z. Yu, M. Farrell, and G. J. Collins, "Multikilowatt electron beams for pumping CW lasers," *Appl. Phys. Lett.*, vol. 41, pp. 811-813, Nov. 1982.
- [6] G. W. McClure, "High-voltage glow discharges in D<sub>2</sub> gas. I. Diagnostic measurements," *Phys. Rev.*, vol. 124, pp. 969-982, Nov. 1961.
- [7] B. B. O'Brien, Jr., "Characteristics of a cold cathode plasma electron gun," *Appl. Phys. Lett.*, vol. 22, pp. 503-505, May 1973.
- [8] G. G. Isaacs, D. L. Jordan, and P. J. Dooley, "A cold-cathode glow discharge electron gun for high-pressure CO<sub>2</sub> laser ionisation," *J. Phys. E: Sci. Instrum.*, vol. 12, pp. 115-118, 1979.
- [9] M. J. Berger and S. M. Seltzer, *Tables of Energy-Losses and Ranges of Electrons and Positrons*, NAS-NRC Pub. 1133, p. 205, 1964.
- [10] Z. Yu, J. J. Rocca, and G. J. Collins, "Studies of a glow discharge electron beam," *J. Appl. Phys.*, vol. 54, pp. 131-136, Jan. 1983.
- [11] Z. Yu, J. J. Rocca, G. J. Collins, and C. Y. She, "The energy of thermal electrons in electron beam created helium discharges," *Phys. Lett.*, vol. 96A, pp. 125-127, Jun. 1983.
- [12] G. W. McClure and K. D. Granzow, "High-voltage glow discharges in D<sub>2</sub> gas. II. Cathode fall theory," *Phys. Rev.*, vol. 125, pp. 3-10, Jan. 1962.
- [13] H. C. Bourne, Jr., R. W. Cloud, and J. G. Trump, "Role of positive ions in high-voltage breakdown in vacuum," *J. Appl. Phys.*, vol. 26, pp. 596-599, May 1955.
- [14] F. Schwitzke, "Ionisierungs- und Umladequerschnitte von Wasserstoff-Atomen und Ionen von 9 bis 60 keV in Wasserstoff," *Z. Physik*, vol. 157, pp. 510-522, 1960.
- [15] W. Lotz, "Electron-impact ionization cross sections and ionization rate coefficient for atoms and ions," *Astrophys. J. (Suppl. Ser. XIV)*, no. 128, pp. 207-237, May 1967.
- [16] L. J. Kiefer and G. H. Dunn, "Electron impact ionization cross section data for atoms, atomic ions and diatomic molecules: I. Experimental data," *Rev. Mod. Phys.*, vol. 38, pp. 1-35, Jan. 1966.
- [17] M. J. Van Der Wiel, F. J. DeHeer, and G. Wiebes, "Double ionization of helium," *Phys. Lett.*, vol. 24A, pp. 423-424, Apr. 1967.
- [18] S. K. Allison, "Experimental results on charge-changing collisions of hydrogen and helium atoms and ions at kinetic energies above 0.2 keV," *Rev. Mod. Phys.*, vol. 30, pp. 1137-1138, Oct. 1958.
- [19] L. J. Puckett, G. O. Taylor, and D. W. Martin, "Cross sections for ion and electron production in gases by 0.15-1.00 MeV hydrogen and helium ions and atoms," *Phys. Rev.*, vol. 136, pp. 379-385, Oct. 1964.
- [20] R. A. Langley, D. W. Martin, D. S. Harmer, J. W. Hooper, and E. W. McDaniel, "Cross sections for ion and electron production in gases by fast helium (0.133-1.0 MeV): I. Experimental," *Phys. Rev.*, vol. 36, pp. 379-385, Oct. 1964.
- [21] S. W. Nagy, W. J. Savloa, Jr., and E. Poylack, "Measurements of the total cross section for symmetric charge exchange in Helium from 400-2000 eV," *Phys. Rev.*, vol. 177, pp. 71-76, Jan. 1969.
- [22] J. B. Hasted, in *Atomic and Molecular Processes*, D. R. Bates, Ed. New York: Academic, 1962, pp. 496-720.
- [23] K. H. Berkner, R. V. Pyle, J. W. Stearns, and J. C. Warren, "Single and double electron capture by 7.2 to 181 keV He<sup>++</sup> ions in He," *Phys. Rev.*, vol. 166, pp. 44-46, Feb. 1968.
- [24] G. R. Hertel and W. S. Koski, "Cross sections for the single charge transfer of doubly charged rare gas ions in their own gases," *J. Chem. Phys.*, vol. 40, pp. 3452-3453, 1964.
- [25] L. I. Pivovarov, M. T. Novikov, and V. M. Tubaev, "Electron capture of helium ions in various gases in the 300-1500 keV energy range," *Sov. Phys. - JETP*, vol. 15, pp. 1035-1037, Dec. 1962.

# Generation of Pulsed Electron Beams by Simple Cold Cathode Plasma Guns

B. WERNSMAN, H. F. RANEA-SANDOVAL, J. J. ROCCA, AND H. MANCINI

**Abstract**—Electron-beam pulses of current up to 20 A have been generated using glow discharge electron guns of simple construction. Beam pulses of 1–20  $\mu$ s long at energies between 2 and 15 keV have been created at helium pressures between 1 and 5 torr. Results obtained using 3-cm diameter aluminum cathodes of two different geometries are discussed. As an example of the use of these electron guns for laser excitation, we have excited an He–Zn metal vapor mixture. Three new infrared laser transitions in ZnII are reported.

**P**REVIOUSLY WE OBTAINED dc electron-beam currents up to 1 A using glow discharge electron guns [1]. Here we report the pulsed operation of electron guns of two different cold cathode geometries at currents one order of magnitude above those obtained for dc operation. The generation of electron beams in a gas environment can find applications in laser excitation [2] and material processing [3]. The electron guns are of very simple construction; each consisting of an aluminum cathode 3 cm in diameter surrounded by an insulating ceramic tube. The oxide layer covering the surface of the aluminum cathode provides a high secondary electron emission coefficient following the bombardment by ions and fast neutral atoms [1]. This allows for high electron-beam generation efficiencies.

The geometry of one of the cathodes is the same as the one previously used for dc electron-beam generation. It is shown in Fig. 1(a). The geometry and position of the anode is not too critical to the operation of the gun. In our experiment, the metallic vacuum chamber is used as the anode for the glow discharge. When the discharge is operated in helium at a pressure of a few torr, a large cathode fall develops. Most of the voltage drop applied between the electrodes occurs in this region adjacent to the cathode and the rest of the discharge is a nearly field free negative glow. Consequently, practically all of the electron acceleration occurs in the cathode fall region. If the anode is placed at a distance from the cathode several times larger than the cathode fall thickness, the shape of

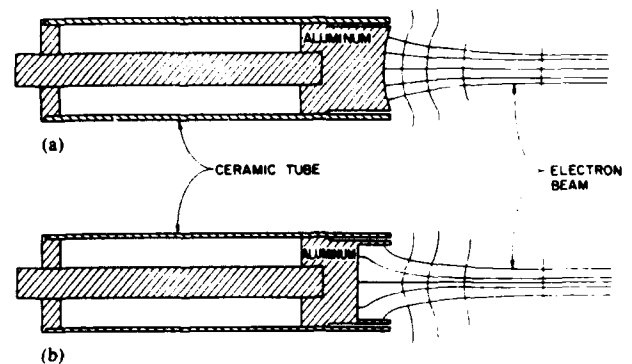


Fig. 1. Schematic representation of the electron guns. (a) and (b) show two different cathode geometries. The radius of curvature of the cathode front surface in (a) is 6 cm.

the electric-field lines in the cathode dark space is mainly dependent on the cathode geometry. Consequently, the electron beam can be focused by tailoring the cathode shape. In the gun of Fig. 1(a), electron-beam focusing is achieved by making the cathode surface concave [3].

The second cathode geometry used in our experiments is shown in Fig. 1(b). It consists of an aluminum cylindrical cavity 3 cm in diameter and 1 cm in depth. Electron emission is achieved following ion bombardment of the inner walls of the cylindrical cavity. The cavity shapes the electric-field lines as indicated in Fig. 1(b). The emitted electrons are accelerated along the field lines to form the well collimated beam shown in Fig. 2.

With this cathode geometry, good electron-beam focusing is achieved at pressures between 1 and 3 torr. At lower pressure, the cathode fall region broadens; the equipotential surfaces become flatter, and the focusing effect decreases. At pressures above 4 torr, the equipotential lines penetrate too deeply inside the cavity and follow the contour of the metal walls. This decreases electron-beam extraction, and the discharge collapses into a hollow cathode discharge.

The experiments were conducted in a stainless steel vacuum chamber which had a 4-in diameter in the shape of a cylindrical cross. This setup is illustrated in Fig. 3. The chamber was grounded and acted as the anode for the glow discharge. The cathode was pulsed negatively up to 15 kV by connecting a 25-nF capacitor through a triggered spark-gap or alternatively by using a pulse transformer providing voltages up to 5 kV. In the former case, a 10- $\Omega$  resistor was used in series with the discharge. The

Manuscript received December 19, 1985; revised February 25, 1986. This work was supported in part by the U.S. Air Force, the National Science Foundation under Grant ECS-8404727, and the NSF-CONICET (United States–Argentina) International Program under Grant INT-8402914. J. Rocca received support from an NSF Presidential Young Investigator Award.

B. Wernsman and J. J. Rocca are with the Electrical Engineering Department, Colorado State University, Fort Collins, CO 80523.

H. F. Ranea-Sandoval is on leave from CIOP (CIC-BA) Optical Research Center, Rep. Argentina.

H. Mancini is with CEILAP (CITEFA-CONICET), Rep. Argentina. IEEE Log Number 8609595.

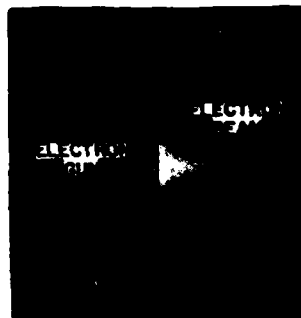


Fig. 2. Electron beam generated with the cathode of Fig. 1(b). Total current 3.9 A; discharge voltage 4 kV; He pressure 2.4 torr; pulsewidth 50  $\mu$ s; pulse repetition rate  $\approx$  670 Hz.

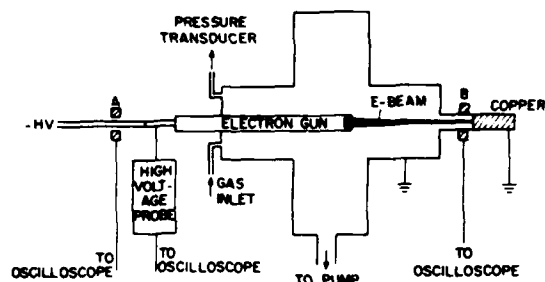


Fig. 3. Experimental setup used in the electron-beam generation experiments. *A* and *B* represent the pulse transformers used to measure the total discharge current and electron-beam current, respectively. Pulse transformer *B* is mounted on an insulating cylinder.

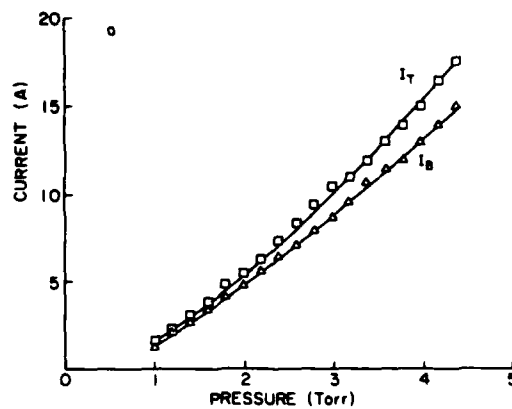
total discharge current was measured by monitoring the cathode current with a pulse transformer.<sup>1</sup> The discharge voltage was measured using a commercially available high voltage divider probe.<sup>2</sup> The electron-beam current was estimated by shooting the electron beam through a second pulse transformer as indicated in Fig. 3. The current probe was mounted around an insulating cylinder placed between a grounded copper collector and the rest of the vacuum chamber.

The variation of the total glow discharge and electron-beam currents as a function of helium pressure for both cathode geometries is shown in Fig. 4. To obtain these data, approximately 30 mtorr of oxygen was added to the discharge to maintain a stable oxide layer and to ensure efficient electron emission at high repetition rates. When the measurements were repeated without the addition of oxygen, slightly lower (20 percent) currents were obtained. Fig. 4(a) corresponds to the electron gun geometry represented in Fig. 1(a). The discharge voltage was 13 kV and remained approximately constant for all values of the pressure between 1 and 4 torr. The electron-beam current constitutes approximately 80 percent of the total discharge current. This is in agreement with the values of dc electron-beam generation efficiencies obtained from calorimetric measurements [1].

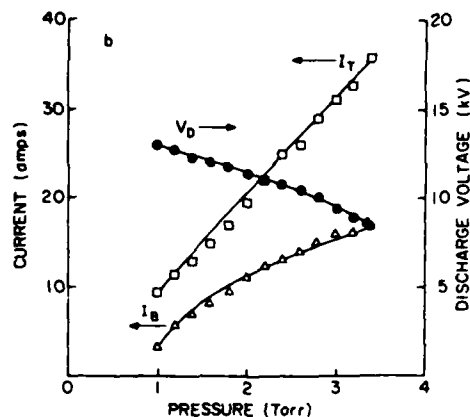
Fig. 4(b) corresponds to the electron gun having the cathode geometry shown in Fig. 1(b). Electron-beam cur-

<sup>1</sup>Pearson Electronics, Model 110 current monitor, 0.1 V/A output.

<sup>2</sup>Tektronix Inc., Model 6015 high-voltage divider probe, 40 kV, 4-ns rise time.



(a)



(b)

Fig. 4. Electron-beam current  $I_B$ , total discharge current  $I_T$ , and discharge voltage  $V_D$  as a function of He pressure; 30 mtorr of  $O_2$  was added to the discharge. (a) and (b) correspond to the electron gun geometries of Fig. 1(a) and (b), respectively. In (b),  $V_D$  was constant.

rents up to 18 A were obtained. However, the electron-beam generation efficiency is smaller and approximately equal to 50 percent. The discharge voltage also shows a different behavior. It decreases as the pressure is increased as illustrated in Fig. 4(b). The different behavior of both cathodes might be due to the fact that, as the pressure is increased, the cathode of Fig. 1(b) tends to develop a hollow cathode behavior. A dense plasma is created within the cathode cavity causing a decrease in the discharge impedance. This argument is supported by the fact that if the pressure is further increased or the cathode is made deeper (2 cm) the glow will behave as a lower impedance hollow cathode discharge.

Fig. 5(a) shows the discharge voltage and corresponding electron-beam current pulse for the electron gun of Fig. 1(a) operating at 4 torr. Fig. 5(b) shows a simultaneous recording of the total discharge current and electron-beam pulse obtained with the same electron gun.

Fig. 6 illustrates the current pulses obtained with the electron gun geometry of Fig. 1(b) operating at 2.6 torr. The peak electron-beam current in this photograph is 14 A for an applied voltage of 15 kV. By adding up to 0.1

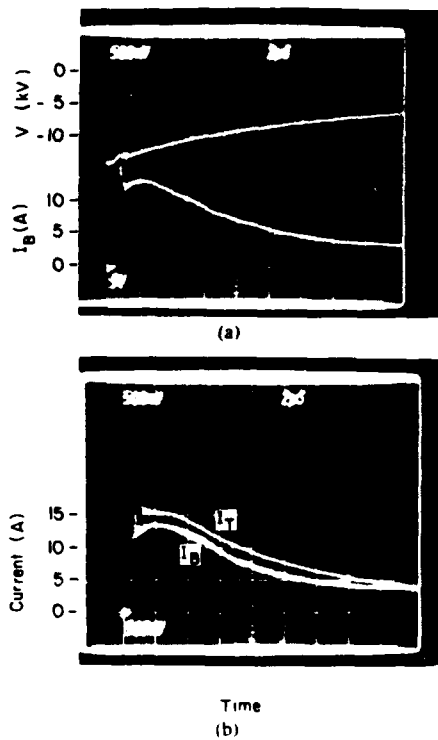


Fig. 5. (a) Discharge voltage (upper trace) and electron-beam current pulse (lower trace). Increasing discharge voltage is in a downward direction. He pressure: 4 torr. (b) Total current (upper trace) and electron-beam current (lower trace) pulses. He pressure: 4 torr. The discharge voltage at peak beam current is 13 kV. The electron gun geometry is represented in Fig. 1(a).

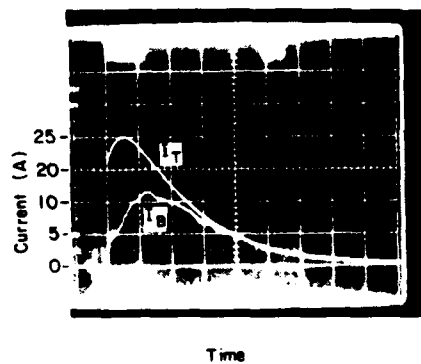


Fig. 6. Discharge current (upper trace) and electron-beam current (lower trace) pulses. He pressure: 2.6 torr. Peak discharge voltage 15 kV. The electron gun geometry is represented in Fig. 1(b). Peak beam current is 14 A.

torr of O<sub>2</sub> to the discharge, stable 20-A beam current pulses were obtained.

In order to use these electron guns for laser excitation, it is useful to have an optical path through the axis. In this way, the volume of the plasma excited with the electron beam can be overlapped with the volume of an optical resonator [2]. For this purpose, we opened a hole 0.5 cm in diameter through the axis of the 3-cm-diameter electron guns described above. The hole was insulated with a quartz tube to maintain the high impedance operation of

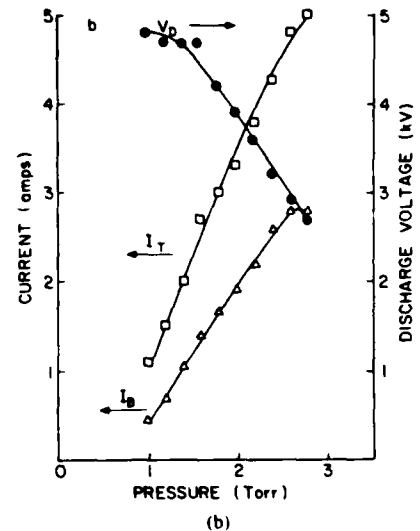
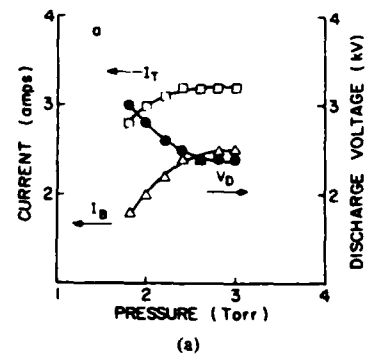


Fig. 7. Electron-beam current  $I_B$  and total discharge current  $I_T$  as a function of He pressure; 30 mtorr of O<sub>2</sub> was added to the discharge. (a) and (b) correspond to the electron gun geometries of Fig. 1(a) and (b), respectively, with the difference that they have a 0.5-cm diameter hole in their axis.

the glow discharge. The axial hole, however, limits the maximum electron-beam current that can be obtained from these guns, since at high discharge power, the discharge tends to collapse into an arc. With the axial hole, the gun of Fig. 1(b) was found to give slightly higher beam currents as compared to the one of Fig. 1(a). Its operation was also more reliable.

These electron guns were excited with the output from a pulse transformer driven by a pulse-forming network giving rectangular voltage pulses of controllable duration. Fig. 7(a) and (b) shows the variation of the total discharge current and electron-beam current of these guns as a function of helium pressure for an applied voltage of 5 kV.

Fig. 8 shows the discharge voltage and corresponding total discharge current for a gun similar to that shown in Fig. 1(b) but having a 0.5-cm diameter hole through its axis. Multiampere discharge current pulses can be obtained at 1-kHz repetition rates. We operated the electron gun at pulse rates up to 2 kHz and at pulsewidths between 5 and 100  $\mu$ s.

As an example of the use of these electron guns for laser pumping, we excited an He-Zn metal vapor mixture

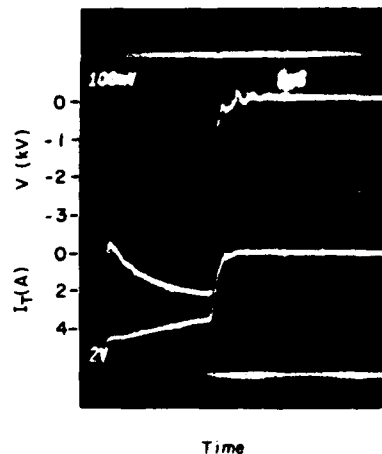


Fig. 8. Electron-beam discharge voltage (upper trace) and glow discharge current pulse (lower trace). Increasing discharge voltage is in the downward direction. The He pressure was 4 torr. Electron gun geometry corresponds to that of Fig. 1(b) with a 0.5-cm diameter hole in its axis.

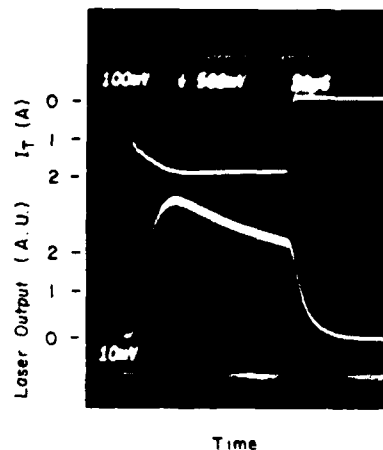


Fig. 9. Discharge current (upper trace) and ZnII laser output at 1.83133  $\mu\text{m}$  (lower trace) as a function of time. Discharge voltage 2 kV; pulse repetition rate  $\approx$  670 Hz. The time scale is 20  $\mu\text{s}$  div.

TABLE I  
NEW ZnII LASER LINES

Wavelength ( $\mu\text{m}$ )	Transition Assignment
1.83133	$6p \ ^2P_{3/2}^o - 6s \ ^2S_{1/2}$
2.15003	$5p \ ^2P_{3/2}^o - 4d \ ^2D_{5/2}$
2.24401	$5p \ ^2P_{1/2}^o - 4d \ ^2D_{3/2}$

and obtained laser action in three new ZnII laser transitions. The laser setup was similar to that previously used to excite CW metal vapor lasers using a dc electron beam [2]. The electron beam was injected into a stainless steel plasma tube 1 cm in diameter and 100 cm long. The tube was maintained at 600°C using an external heater, and Zn vapor was introduced by heating a reservoir to 450°C. An electromagnet surrounding the plasma tube provided an axial magnetic field of up to 2.5 kG to guide the electron beam. At a helium pressure of 1.5 torr, three new infrared laser transitions were observed in ZnII when a resonator was constructed using two, 2-m radius-of-curvature mirrors having high reflectivity in the 1.5–2- $\mu\text{m}$  spectral region. The transition wavelengths and level assignments are listed in Table I.

A 90- $\mu\text{s}$  electron-beam discharge current pulse and the corresponding laser output at 1.83133  $\mu\text{m}$  as observed through a monochromator are shown in Fig. 9. Laser action occurs during the entire electron-beam current pulse. The variation of the laser output power of the 1.83133- $\mu\text{m}$  ( $6p \ ^2P_{3/2}^o - 6s \ ^2S_{1/2}$ ) transition as a function of discharge current is shown in Fig. 10. The total discharge current threshold for oscillation of this line was found to be 600 mA. The laser upper levels are excited mainly by charge transfer collisions between helium ions and neutral zinc atoms.

The presence of the small amount of oxygen added into

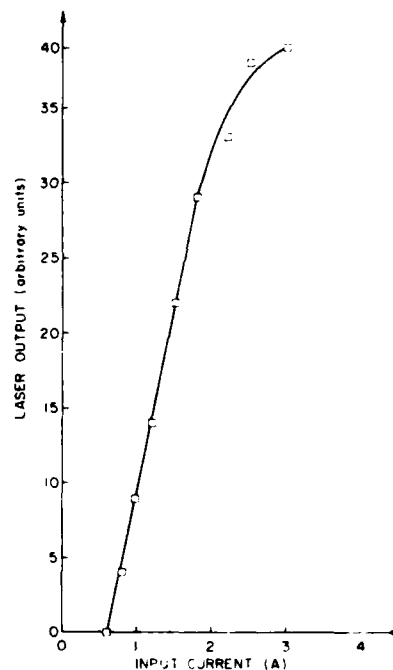


Fig. 10. Laser output power of the 1.83133- $\mu\text{m}$  line as a function of electron-beam discharge current. Zn reservoir temperature was 500°C. The average He pressure in the plasma tube was 1.5 torr.

the electron gun region was not observed to have any detrimental effect on the laser output. This result is in agreement with a previous experiment in which we used the same electron guns to obtain laser oscillation in CdI and CdII [4]. In the excitation of other laser transitions, such as the excitation of ultraviolet metal vapor lasers, the presence of oxygen in the active medium might present a more serious problem. In this case, sintered metal-oxide cathode materials (e.g., molybdenum-aluminum oxide) can be used. These materials have a high secondary emission coefficient and are able to operate in a pure noble gas

atmosphere without a degradation of their emissive characteristics [3].

The pulsed electron guns described here find an interesting application in the excitation of recombination lasers. The beam electrons can provide efficient ionization, and cold secondary electrons created by ionization can readily recombine to populate high-lying levels through three-body electron-ion recombinations. We have used the pulsed electron beams described above to obtain laser action in three transitions of CdI following electron-ion recombination. These results will be discussed in another publication [4].

In summary, we demonstrated the production of pulsed electron beams with currents up to 20 A, current densities of more than  $2.5 \text{ A/cm}^2$ , and energies up to 15 keV using

electron guns of simple construction having aluminum cathodes. Its application to the excitation of metal vapor lasers was also demonstrated.

#### REFERENCES

- [1] J. J. Rocca, J. Meyer, Z. Yu, M. Farrell, and G. J. Collins, "Multi-kilowatt electron guns for CW laser excitation," *Appl. Phys. Lett.*, vol. 41, pp. 811-813, Nov. 1, 1982.
- [2] J. J. Rocca, J. Meyer, and G. J. Collins, "1-W zinc ion laser," *Appl. Phys. Lett.*, vol. 43, pp. 37-39, July 1, 1983.
- [3] J. J. Rocca, J. Meyer, M. Farrell, and G. J. Collins, "Glow discharge created electron beams: Cathode materials, electron gun designs, and technological applications," *J. Appl. Phys.*, vol. 56, pp. 790-797, Aug. 1, 1984.
- [4] J. J. Rocca, H. Mancini, and B. Wernsman, "CD recombination laser in a plasma generated by an electron beam," *IEEE J. Quantum Electron.*, vol. QE-22, pp. 509-512, Apr. 1986.

# High current density hollow cathode electron beam source

J. J. Rocca, B. Szapiro, and T. Verhey

Electrical Engineering Department, Colorado State University, Fort Collins, Colorado 80523

(Received 23 January 1987; accepted for publication 16 March 1987)

An electron beam with current density greater than  $30 \text{ A/cm}^2$  and total current of  $92 \text{ A}$  has been generated in  $5 \mu\text{s}$  pulses by accelerating the electrons from a glow discharge in a narrow gap between two grids. The ratio of the extracted electron beam current to discharge current is approximately 1. The gun also operates in a dc mode.

Plasma cathodes that do not suffer diode closure (collapse of the anode-cathode gap) are of particular interest in the generation of high current density electron beam pulses with duration  $> 1 \mu\text{s}$ . Glow discharges have been previously used to produce electron beams at current densities  $< 2 \text{ A/cm}^2$ .<sup>1-4</sup> Humpries *et al.* obtained electron beam current densities up to  $15 \text{ A/cm}^2$  at energies  $< 300 \text{ eV}$  from a spark generated, grid controlled plasma cathode.<sup>5</sup> Recently, an electron beam current of  $30 \text{ A}$  ( $60 \text{ A/cm}^2$ ) was reported from a grid-stabilized plasma emitter.<sup>6</sup>

Here we report the generation of a high current density ( $> 32 \text{ A/cm}^2$ ) electron beam with a total current of  $92 \text{ A}$  by accelerating the electrons of a hollow cathode glow discharge in the narrow gap between two grids at energies up to  $2 \text{ keV}$ . The current of energetic electrons was measured at  $15 \text{ cm}$  from the acceleration grid, and does not include the electrons accelerated in the gap, but intercepted by the  $40\%$  opaque acceleration grid. The electron current density emitted by the plasma source is larger and approaches  $45 \text{ A/cm}^2$ .

Our experimental setup is schematically illustrated in Fig. 1. The plasma source is a  $5\text{-cm}$ -diam stainless-steel hol-

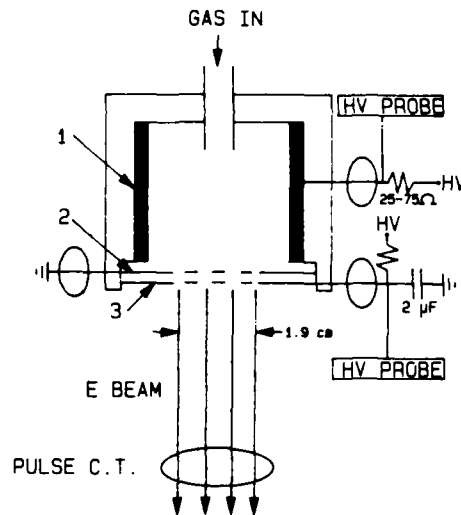


FIG. 1. Experimental setup. The vacuum chamber is not shown. The circles represent pulse current transformers. (1) The  $5 \text{ cm}$  i.d. hollow cathode, (2) the anode electrode, and (3) the acceleration electrode are indicated. The  $25\text{--}75 \Omega$  discharge ballast resistor was only used in the high current experiments, in series with a  $50\text{-nF}$  capacitor.

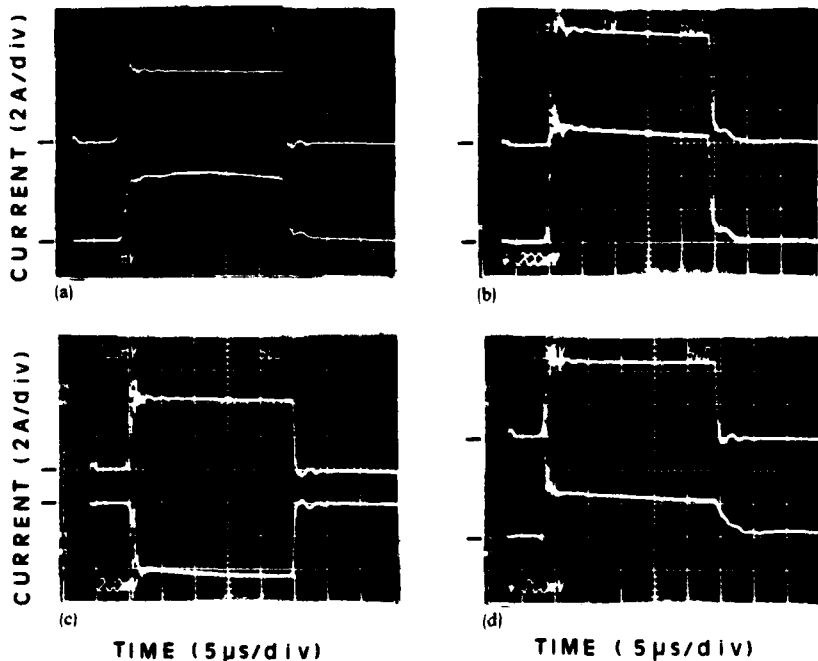


FIG. 2. (a) Upper trace: discharge current; lower trace: electron beam current. Acceleration voltage  $V_{\text{accel}} = 2 \text{ kV}$ . (b) Upper trace: sum of discharge and anode grid currents; lower trace: sum of electron beam and acceleration grid currents. (c) Upper trace: discharge current; bottom trace: anode grid current for  $V_{\text{accel}} = 0 \text{ kV}$ . (d) Upper trace: discharge current; lower trace: anode grid current for  $V_{\text{accel}} = 2 \text{ kV}$ . All vertical scales are  $2 \text{ A/div}$ , with the zero level indicated in the left margin. The helium pressure was  $0.45 \text{ Torr}$ .

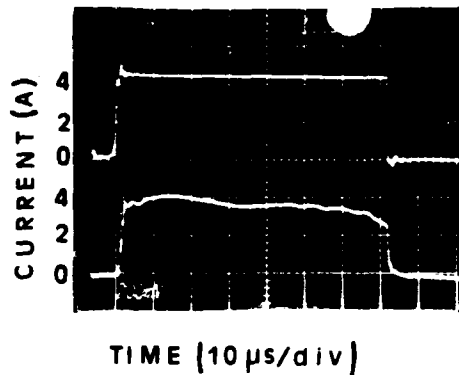


FIG. 3. Upper trace: discharge current; lower trace: electron beam current.  $V_{\text{anode}} = 2$  kV. The background helium pressure was 0.45 Torr. The slight current decrease at the end of the electron beam pulse is a consequence of the decrease in the accelerating voltage due to the charge lost by the biasing capacitor. Since the beam current is measured at 15 cm from the gun, a reduction in accelerating voltage results in increasing scattering leading to the slight current reduction.

low cathode discharge that was operated in helium. Emission is confined to the inner walls of the cylindrical cathode by a Teflon embodiment that surrounds the cathode. The Teflon piece also supports two grids that form the 2.5-mm-wide electron acceleration gap. Both the internal anode grid and the acceleration grid are made of number 42 stainless-steel mesh, having a transmissivity of approximately 60%. The grids are mounted in supporting stainless-steel plates having an orifice 19 mm in diameter that defines the diameter of the extracted beam. The entire electron gun structure was enclosed in a vacuum chamber and evacuated to a pressure of  $10^{-3}$  Torr. Helium was continuously introduced inside the electron gun and evacuated through the grids by a

rotatory pump connected to the vacuum chamber. The helium flow caused the pressure inside the electron gun structure to be approximately 1.2 times higher than that in the electron beam drift region of the vacuum chamber. The electron gun was operated at vacuum chamber pressures between 0.1 and 1 Torr. The hollow cathode discharge was excited with a pulse forming network and a high voltage pulsed transformer giving negative voltages up to 6 kV. The maximum current this source can provide is 7 A. In experiments at larger currents the hollow cathode discharge was initiated and maintained by discharging a 50-nF capacitor negatively charged up to 8 kV through a series spark gap. In the later case a ballast resistor (25–75  $\Omega$ ) was connected in series with the discharge circuit. The anode grid was grounded and the acceleration grid was directly connected to a 2- $\mu$ F capacitor charged to provide the desired electron beam energy (0–2 keV). No limiting resistor was added in series with the acceleration grid circuit. The cathode current and the grid currents were monitored with current transformers. The electron beam current was measured by monitoring the current flowing through another current transformer placed coaxial with the beam at 15 cm from the extraction grid. The voltage drop across the glow discharge and the acceleration gap were also simultaneously measured using commercially available high voltage dividers.

The ratio of the electron beam current to the discharge current is close to 1 as shown in Fig. 2(a). The sum of the electron beam current and extraction grid current was observed to be as high as 1.4 times the cathode current. The sum of the former two was measured to exactly match the sum of the discharge current and anode current [Fig. 2(b)]. When no acceleration voltage is applied a negligible current is collected by the acceleration grid, and the pulse of electron current collected by the anode grid is a good reproduction of

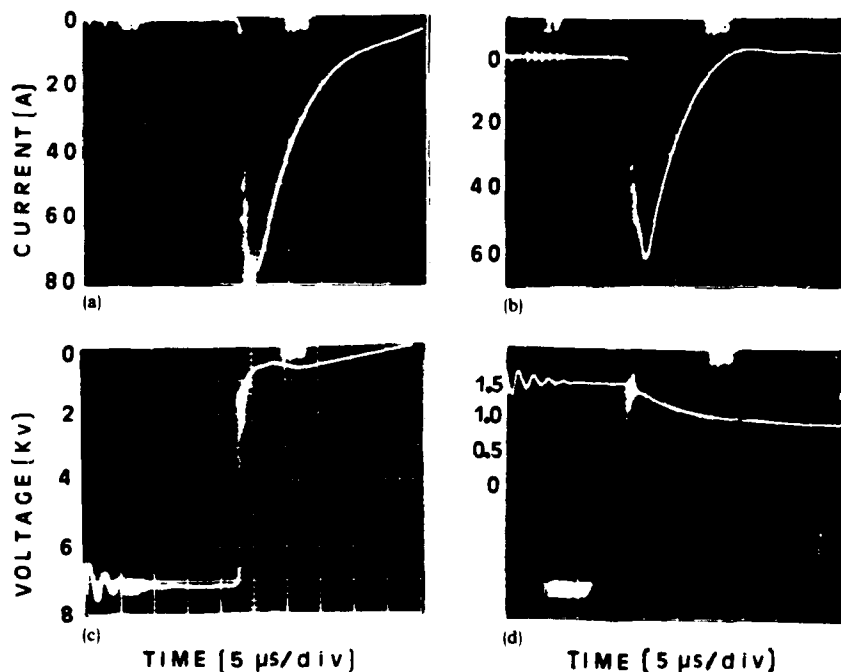


FIG. 4. (a) Discharge current. (b) Electron beam current. (c) Discharge voltage. (d) Acceleration voltage. The background helium pressure was 0.2 Torr. A 75- $\Omega$  ballast resistor was used in series with the hollow cathode discharge current.

the cathode current pulse [Fig. 2(c)] however, when an acceleration voltage greater than 60 V is applied across the gap, the anode current reverses sign and becomes an ion current as shown in Fig. 2(d). This behavior corresponds to that of grid-controlled plasma cathodes in which the wire spacing in the grids is larger than the width of the space-charge layer near the anode, and is consistent with the theory of Zharinov *et al.*<sup>7</sup>

The discharge current was observed to be practically unperturbed by the application of an acceleration voltage and the resulting electron beam extraction. Consequently, the electron beam current and energy can be controlled independently. Closure of the acceleration gap does not occur and long electron beam pulses can be obtained. Figure 3 shows a 70- $\mu$ s discharge pulse and the corresponding 2-keV electron beam pulse. The gun was also operated in a dc mode at electron beam currents of 50 mA.

Figures 4(a) and 4(b) show a 75-A discharge pulse and a 62-A ( $20 \text{ A/cm}^2$ ) electron beam pulse obtained charging the discharge capacitor to 7.2 kV. The voltage drop across the hollow cathode discharge is approximately 600 V, as shown by Fig. 4(c). The potential of the acceleration grid [Fig. 4(d)] is observed to decrease smoothly from 1.5 to 1 kV during the electron beam pulse due to the charge lost by the biasing capacitor. Electron beam current pulses as high as 92 A ( $32 \text{ A/cm}^2$ ) were obtained operating the gun at a background helium pressure of 0.2 Torr and an applied cathode voltage of 8 kV.

In conclusion, we have demonstrated the operation of a simple plasma gun at current densities  $> 30 \text{ A/cm}^2$  in  $5 \mu\text{s}$  pulses. The beam current was source limited and even larger beam currents should be possible. The gun does not present diode closure and was also operated at reduced currents in the dc mode.

This work is supported by the U.S. Air Force and a C. S. U. Graduate School grant. J. Rocca wants to acknowledge the support of a National Science Foundation Presidential Young Investigator Award and B. Szapiro the support from the Universidad Nacional de Buenos Aires for his fellowship.

<sup>1</sup>S. Humpries, Jr., S. Coffey, M. Savage, L. K. Len, G. W. Cooper, and D. M. Woodall, *J. Appl. Phys.* **57**, 709 (1985).

<sup>2</sup>B. Wernsman, H. Ranea Sandoval, J. J. Rocca, and H. Mancini, *IEEE Trans. Plasma Sci.* **PS-14**, 518 (1986).

<sup>3</sup>T. Fusayama, *Jpn. J. Appl. Phys.* **25**, L406 (1986).

<sup>4</sup>J. R. Bayless and R. C. Knechtli, *IEEE J. Quantum Electron.* **QE-10**, 213 (1974).

<sup>5</sup>S. Humpries, Jr., N. Savage, and D. M. Woodall, *Appl. Phys. Lett.* **47**, 468 (1985).

<sup>6</sup>A. V. Zharinov, Yu. A. Kovalenko, I. S. Roganov, and P. M. Tyuryukanov, *Sov. Phys. Tech. Phys.* **31**, 39 (1986).

<sup>7</sup>A. V. Zharinov, Yu. A. Kovalenko, I. S. Roganov, and P. M. Tyuryukanov, *Sov. Phys. Tech. Phys.* **31**, 413 (1986).

A REFLEX ELECTRON BEAM DISCHARGE AS A  
PLASMA SOURCE FOR ELECTRON BEAM GENERATION

C. Murray, J.J. Rocca and B. Szapiro

Electrical Engineering Department

Colorado State University

Fort Collins, CO 80523

ABSTRACT

A reflex electron beam glow discharge has been used as a plasma source for the generation of broad area electron beams. An electron current of 120 A (  $12 \text{ A/cm}^2$  ) was extracted from the plasma in 10  $\mu\text{sec}$  pulses and accelerated to energies greater than 1 keV in the gap between two grids. The scaling of the scheme for the generation of multikiloamp high energy electron beams is discussed.

We have demonstrated that the plasma created by a reflex electron beam glow discharge constitutes an efficient source of thermal electrons for subsequent acceleration into intense broad area electron beams. Electron currents of up to 120 A ( $12 \text{ A/cm}^2$ ) were extracted from the plasma of the reflex discharge and accelerated in the gap between two grids at kiloelectronvolt energies.

Several types of electron sources, including thermionic cathodes [1], photoelectric emitters [2], vacuum plasmas [3-5] and hollow cathode discharges [6-8] have been used and are currently being studied for broad area electron beam generation. Low pressure high voltage glow discharges have been demonstrated to generate high current density ( $> 10 \text{ A/cm}^2$ ) broad area electron beams [9-13]. In these glow discharges almost the entire discharge voltage drops in the cathode sheath [13], where the emitted electrons are accelerated to form the electron beam. Electron emission occurs following the bombardment by energetic ions and fast neutrals. Cold cathode glow discharge electron guns do not suffer the phenomena of diode closure and are of simple construction. They have been shown to produce electron beam current densities  $> 10 \text{ A/cm}^2$  at energies of 50-90 kV [10]. However, at energies  $> 100 \text{ kV}$  the electron beam current density is limited by frequent arcs to values on the order of  $1 \text{ A/cm}^2$  [10].

Here we present a novel electron beam generation scheme in which two glow discharge electron guns are used in a reflex configuration to create a dense and cold plasma on a large volume. The thermal

electrons created mainly by electron beam ionization are subsequently accelerated by an externally applied electric field in the gap between two grids to produce a broad area electron beam. The electron beam current density and energy are independently controlled by the voltage applied to the glow discharge guns and by the electric field sustained between the grids respectively.

Figure 1 is a schematic representation of the electron gun configuration used in the experimental demonstration of the concept reported here. Aluminum cathodes 3 cm in diameter surrounded by ceramic tubes constitute two glow discharge electron guns, that are placed 15 cm apart in a reflex configuration. Both electron guns are maintained at the same potential. At an operating pressure of 0.2 Torr of Helium the multikilovolt beam electrons produced by the glow discharge guns have a reaching distance that is several times longer than the distance between the guns. Consequently, the electrons can travel back and forth between the cathodes generating a dense negative glow plasma. This is: the electrons emitted by one of the cathodes are accelerated in the corresponding cathode sheath region and travel towards the opposite cathode, where they are reflected by the potential barrier presented by the cathode sheath. The beam electrons maintain this oscillatory motion until they become thermalized after suffering large number of ionizing and exciting collisions or are scattered outside the plasma. In their oscillatory motion the beam electrons ionize the gas creating an almost electric field free plasma in which the secondary electrons created by ionization thermalize to a very low electron temperature ( $< 1 \text{ eV}$ ) [14].

The process is similar to the operation of hollow cathode discharges. Hollow cathode discharges have been used as electron sources for broad area beams [6-8]. However, in the reflex electron beam discharge the electron production efficiency can be more than an order of magnitude larger. This is a consequence of the enhanced secondary emission of materials when bombarded by keV ions as compared to a few hundred eV ions in the hollow cathode discharges [18]. More important, the reflex glow discharge has less constraints to be scaled to large areas.

The electron guns of the reflex discharge were connected to a 50 nF capacitor through a 25 ohm ballast resistor and a triggered spark-gap. The capacitor was negatively charged to voltages up to 9 kV. Thermal electrons from the discharge diffuse to the 0.4 cm gap between two grids where they are accelerated to form a beam. The grids are rectangular with dimensions of 2 cm by 5 cm and are made of number 40 stainless-steel mesh with a transmissivity of 38 percent. In most of our tests the inner grid was grounded and the external grid was directly connected to a 20  $\mu$ F capacitor as shown in figure 1. This capacitor was positively charged to voltages corresponding to the desired energy of the extracted electron beam up to 1.5 keV. The total current of the glow discharge guns, the inner grid, and the outer acceleration grid were monitored using three commercially available pulse current transformers. The variation of the voltage applied to the glow discharge guns and the acceleration voltage applied between the two grids were monitored using two commercially available high voltage dividers. The entire electron gun structure

was enclosed in 10 cm diameter stainless steel chamber with several diagnostics ports and initially evacuated to a pressure of  $10^{-3}$  Torr by a rotary pump. Helium was continuously flown through the chamber and the pressure was maintained at 0.2 Torr with the use of a needle valve. A small amount of oxygen ( 5 mTorr ) was added to maintain the surface of the aluminum cathodes oxidized with the purpose of allowing a high emissivity in prolonged operation at high discharge current densities [15].

Above 1.5 kV of acceleration voltage a discharge was observed to develop between the positively biased acceleration grid and the metal vacuum envelope. By grounding the outer grid and negatively biasing the inner grid and the glow discharge electron guns with respect to the outer grid, we avoided this problem and were able to successfully operate the electron gun at acceleration voltages up to 5 kV. The reflex electron beam discharge was operated at discharge currents up to 100 A with pulse-widths of 10  $\mu$ sec. Figure 2(a) shows the variation of the voltage applied to the guns and the corresponding total current of the reflex discharge. The discharge voltage at the time of the peak current, 70 A, is 4 kV. If no voltage is applied to the external grid practically all the current is collected by the inner grid as shown by figure 2(b). When an acceleration voltage is applied to the outer grid the current to the inner grid reverses sign and becomes an ion current as shown in 2(c) for an acceleration voltage of 1200 V. The electron current accelerated through the grid gap then equals the sum of the glow discharge cathode current and the

inner grid current. The accelerated electron current was measured to be up to 1.5 times the glow discharge cathode current, as shown in figure 2(d). We observed a similar behavior in hollow cathode grid controlled electron guns [6]. As described by the theory of Zharinov et. al it corresponds to grid-controlled plasma cathodes in which the wire spacing in the grids is larger than the width of the space charge layer near the anode [16].

Figure 2(e) shows a 100 A (  $10 \text{ A/cm}^2$  ) electron flux collected by the outer grid after having been accelerated to 1.2 keV by the field maintained between the grids. Electron currents up to 120 A (  $12 \text{ A/cm}^2$  ) were emitted by the 3 cm diameter reflex discharge and accelerated to form a well collimated beam. The electron current density was measured using a pulse current transformer at 15 cm from the electron gun. At an accelerating voltage of 4 kV approximately 38 percent of the electron current accelerated in the grid gap was measured by this current transformer. This percentage is in agreement with the transmissivity of the acceleration grid.

In this experiment, the dimensions of the glow discharge and the values of the extraction voltage limited the discharge currents to 100 A and the electron beam current to 120 A. Also the maximum acceleration voltage applied was 5 kV. It should be possible to scale the concept discussed here to multikiloamp currents and high voltages (  $>100 \text{ kV}$  ). To create the reflex discharge reported in this work we employed glow discharge electron guns that in individual operation gave a maximum electron beam current of only 20 A. To scale the

concept to greater electron beam currents, the 3 cm in diameter guns could be replaced with larger diameter cathodes that with 50 kV excitation have produced currents of up to 900 A [13]. Two of these guns in a reflex configuration should be able to produce multikiloamp currents for subsequent acceleration to high energies in the gap between the two grids. As in other grid-controlled plasma guns that operate in a gaseous atmosphere, the maximum electron beam energy will ultimately be limited by Paschen or vacuum breakdown in the acceleration gap [8].

In summary, we have demonstrated the use of a reflex electron beam glow discharge as a plasma source for a grid-controlled electron gun. An electron current density of  $12 \text{ A/cm}^2$  was extracted from the plasma and accelerated to energies greater than 1 keV in 10  $\mu\text{sec}$  pulses. The electron gun does not present diode closure and should scale to provide multikiloamp electron beam currents at high energies.

Acknowledgments: This work was supported by the U.S. Air Force.

J.J. Rocca is a National Science Foundation Presidential Young Investigator. B. Szapiro wants to acknowledge the support from the Universidad Nacional de Buenos Aires for his fellowship.

## REFERENCES

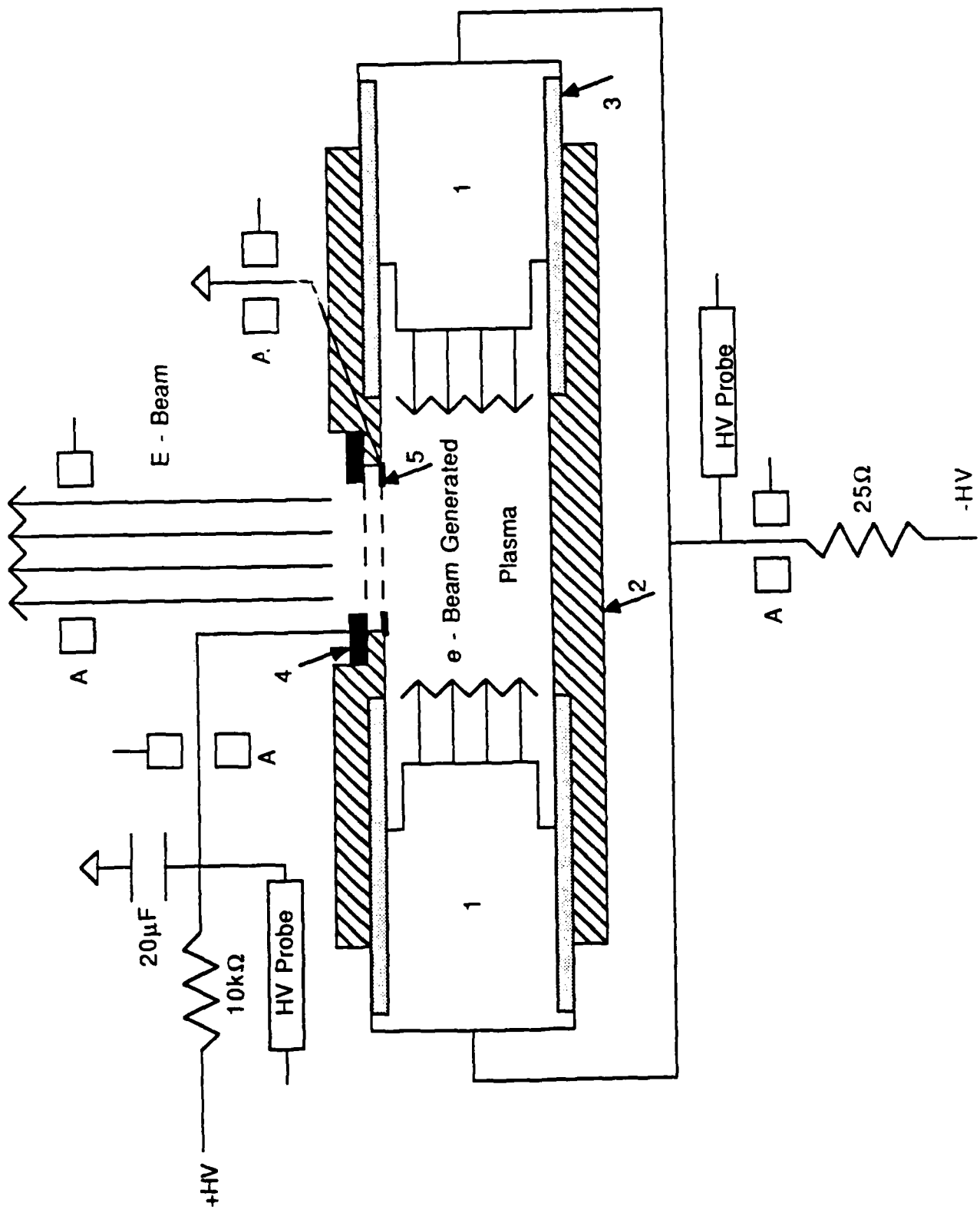
1. K. Amboss, Electron and Ion Beam Science and Technology, Sixth Int. Conference, p.497-517, Proc. Electrochem. Soc. Meet., San Francisco, Calif., Electrochem. Soc., Inc. Princeton, (1974).
2. C.H. Lee, P.E. Oettinger, E.R. Pugh, R. Klinkowstein, J.H. Jacob, J.S. Fraser, and R.L. Sheffield, IEEE Transactions on Nuclear Science, NS-32, 3045, (1985); and C.H. Lee, Appl. Phys. Lett., 44, 565, (1984).
3. H. Shields, R.L. Sandstrom and J.I. Levatter, Appl. Phys. Lett., 47, 681, (1985).
4. S. Humphries Jr., N. Savage and D.M. Woodall, Appl. Phys. Lett., 47, 468, (1985).
5. R.J. Adler, G.F. Kiuttu, B.E. Simpkins, D.J. Sullivan, and D.E. Voss, Rev. Sci. Instrum., 52, 766, (1985).
6. J.J. Rocca, B. Szapiro and T. Verhey, Appl. Phys. Lett., 50, 1334, (1987).
7. A.V. Zharinov, Yu. A. Kavalenko, I.S. Roganov and P.M. Tyuryukanov, Sov. Phys. Tech. Phys., 31, 39, (1986).
8. J.R. Bayless and R.C. Knechtli, IEEE J. Quantum Electronics, QE-10, 213, (1974).
9. G.W. McClure, Phys. Rev., 125, 969, (1961).
10. H. Ranea-Sandoval, N. Reesor, B. Szapiro, C. Murray and J.J. Rocca, IEEE Transactions on Plasma Science, To be Published August 1987.
11. B. O'Brien Jr., Appl. Phys. Lett., 22, 503, (1973).

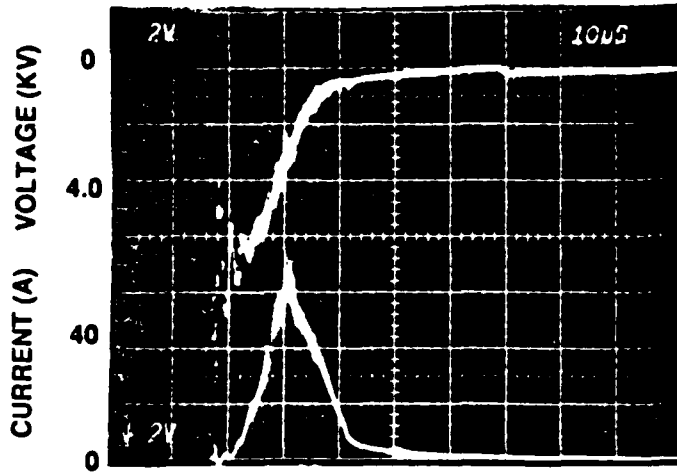
12. G.G. Isaacs, D.L. Jordan and P.J. Dooley, *J. Phys. E.: Sci. Instrum.*, **72**, 115, (1979).
13. S.A. Lee, L.V. Andersen, J.J. Rocca, M. Marconi and N. Reesor, *Appl. Phys. Lett.*, **51**, 409, (1987).
14. Z. Yu, J.J. Rocca, G.J. Collins, and C.Y. She, *Phys. Lett.*, **96A**, 125, (1983).
15. J.J. Rocca, J.D. Meyer, M. Farrell and G.J. Collins, *J. Appl. Phys.*, **52**, 790, (1984).
16. A.V. Zharinov, Yu.A. Kovalenko, I.S. Roganov and P.M. Tyuryukanov, *Sov. Phys. Tech. Phys.*, **31**, 413, (1986).
17. B. Wernsman, H.F. Ranea-Sandoval, J.J. Rocca and H. Mancini, *IEEE Transactions on Plasma Science*, **PS-14**, 518, (1986).
18. G. Carter and J.S. Colligon, *Ion Bombardment of Solids*, Elsevier, New York, (1968).

## FIGURE CAPTIONS

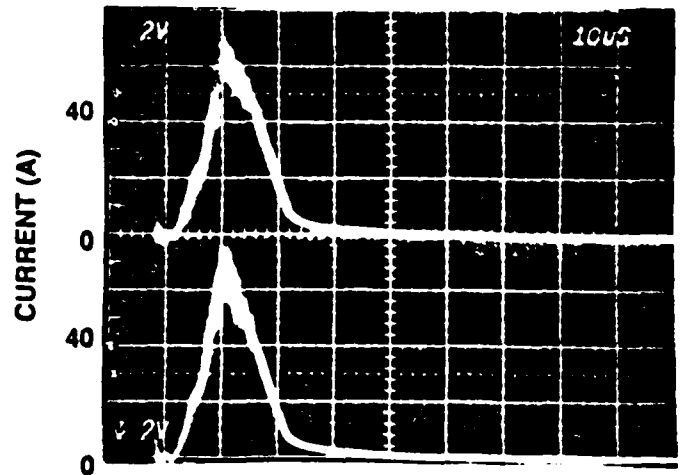
Figure 1. Schematic diagram of the electron gun and excitation circuit. 1) Cylindrical glow discharge aluminum cathodes, 2) delron support body, 3) ceramic tube, 4 and 5) stainless steel grids and metal supports. Pulse current transformers are identified with an A. The vacuum enclosure is not shown.

Figure 2. a) Upper trace: discharge voltage; lower trace: current of the reflex discharge, b) Upper trace: inner grid current, lower trace corresponding reflex discharge current pulse. Acceleration voltage  $V_{\text{accel}} = 0\text{kV}$ , c) Upper trace: inner grid current; lower trace: reflex discharge current,  $V_{\text{accel}} = 1.2\text{ kV}$ , d) Upper trace: accelerated (outer grid) electron current at 1.2 kV; lower trace: reflex discharge current, e) upper trace: accelerated electron current; lower trace: voltage across the acceleration gap. The helium pressure was 0.2 Torr.

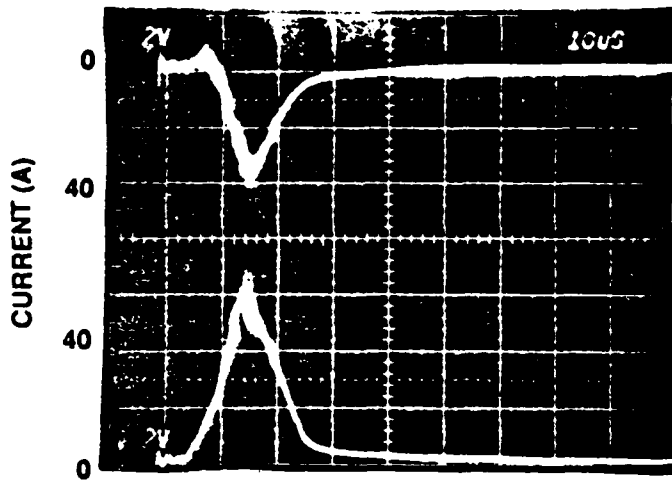




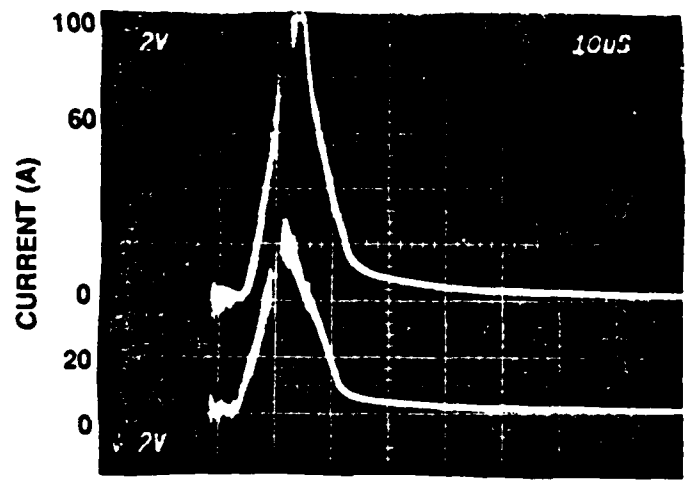
(a)



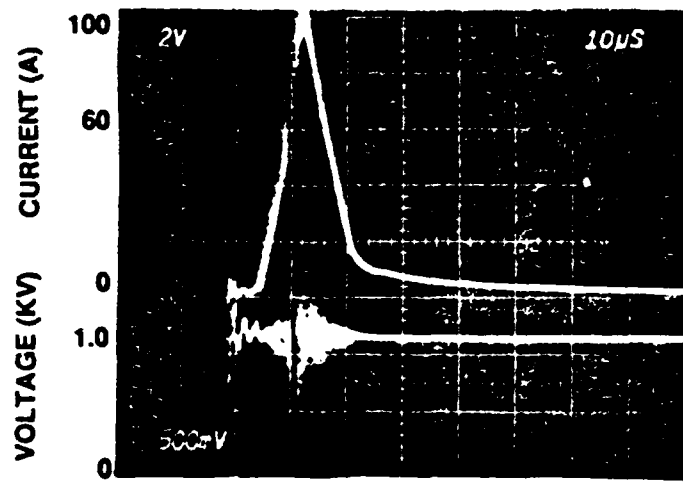
(b)



(c)



(d)



(e)

TIME (10µs/div)

HIGH CURRENT DENSITY HOLLOW CATHODE ELECTRON BEAM SOURCE

J.J.Rocca, B.Szapiro and T.Verhey

Electrical Engineering Department

Colorado State University

Fort Collins, Colorado 80523

An electron beam with current density greater than  $30 \text{ A/cm}^2$  and total current of 92 A has been generated in  $5 \mu\text{s}$  pulses by accelerating the electrons from a glow discharge in a narrow gap between two grids. The ratio of the extracted electron beam current to discharge current is approximately 1. The gun also operates in a d.c. mode.

Plasma cathodes that do not suffer diode closure are of particular interest in the generation of high current density electron beam pulses with duration  $> 1 \mu\text{s}$ . Glow discharges have been previously used to produce electron beams at current densities  $< 2 \text{ A/cm}^2$  [1-4]. Humpries et al. obtained electron beam current densities up to  $15 \text{ A/cm}^2$  at energies  $< 300 \text{ eV}$  from a spark generated, grid controlled plasma cathode [5]. Recently, an electron beam current of 30 A ( $60 \text{ A/cm}^2$ ) was reported from a grid-stabilized plasma emitter [6].

Here we report the generation of a high current density ( $> 32 \text{ A/cm}^2$ ) electron beam with a total current of 92 A by accelerating the electrons of a hollow cathode glow discharge in the narrow gap between two grids at energies up to 2 keV. The current of energetic beam electrons was measured at 15 cm from the acceleration grid, and does not include the electrons accelerated in the gap, but intercepted by the 40 percent opaque acceleration grid. The electron current density emitted by the plasma source is larger and approaches  $45 \text{ A/cm}^2$ .

Our experimental setup is schematically illustrated in Fig.1. The plasma source is a 5 cm diameter stainless steel hollow cathode discharge that was operated in helium. Emission is confined to the inner walls of the cylindrical cathode by a teflon embodiment that surrounds the cathode. The teflon piece also supports two grids that form the 2.5 mm wide electron acceleration gap. Both the internal anode grid and the acceleration grid are made of number 42 stainless steel mesh, having a transmissivity of approximately 60 percent. The grids are mounted in supporting stainless steel plates having an orifice 19 mm in diameter that defines the diameter of the extracted beam. The entire electron gun structure was enclosed in a vacuum envelope and evacuated to a pressure of  $10^{-3}$  Torr. Helium was continuously introduced inside the hollow cathode and evacuated by a rotatory pump. The pressure inside the cathode chamber exceeded the pressure in the electron beam drift region by a factor of 1.2. The electron gun was operated

at chamber pressures between 0.1 and 1 Torr. The hollow cathode discharge was excited with a pulse forming network and a high voltage pulsed transformer giving negative voltages up to 6 kV. The maximum current this source can provide is 7 A. In experiments at larger currents the hollow cathode discharge was initiated and maintained by discharging a 50 nF capacitor negatively charged up to 8 kV through a series spark-gap. In the later case a ballast resistor (25-75  $\Omega$ ) was connected in series with the discharge circuit. The anode grid was grounded and the acceleration grid was directly connected to a 2  $\mu$ F capacitor charged to provide the desired electron beam energy (0-2 keV). No limiting resistor was added in series with the acceleration grid circuit. The cathode current and the grids currents were monitored with current transformers. The electron beam current was measured by monitoring the current flowing through another current transformer placed coaxial with the beam at 15 cm from the extraction grid. The voltage drop across the glow discharge and the acceleration gap were also simultaneously measured using commercially available high voltage dividers.

The ratio of the electron beam current to the discharge current is close to 1 as shown in Fig.2a. The sum of the electron beam current and extraction grid current was observed to be as high as 1.4 times the cathode current. The sum of the former two was measured to exactly match the sum of the discharge current and anode current (Fig.2b). When no acceleration voltage is applied a negligible current is collected by the acceleration grid, and the pulse of electron current collected by the anode grid is a good reproduction of the cathode current pulse (Fig.2c). However, when an acceleration voltage greater than 60 V is applied across the gap, the anode current reverses sign and becomes an ion current as shown in Fig.2d. This behavior corresponds to that of grid controlled plasma cathodes in which the wire spacing in the grids is larger than the width

of the space charge layer near the anode, and is consistent with the theory of Zharinov et al. [7].

The discharge current was observed to be practically unperturbed by the application of an acceleration voltage and the resulting electron beam extraction. Consequently, the electron beam current and energy can be controlled independently. Closure of the acceleration gap does not occur and long electron beam pulses can be obtained. Fig.3 shows a 70  $\mu$ s discharge pulse and the corresponding 2 keV electron beam pulse. The gun was also operated in a d.c. mode at electron beam currents of 50 mA.

Figs. 4a and 4b show a 75 A discharge pulse and a 62 A ( $20 \text{ A/cm}^2$ ) electron beam pulse obtained charging the discharge capacitor to 7.2 kV. The voltage drop across the hollow cathode discharge is approximately 600 V, as shown by Fig.4c. The potential of the acceleration grid (Fig.4d) is observed to decrease smoothly from 1.5 to 1 kV during the electron beam pulse due to the charge lost by the biasing capacitor. Electron beam current pulses as high as 92 A ( $32 \text{ A/cm}^2$ ) were obtained operating the gun at a background helium pressure of 0.2 Torr and an applied cathode voltage of 8 kV.

In conclusion, we have demonstrated the operation of a simple plasma gun at current densities  $> 30 \text{ A/cm}^2$  in 5  $\mu$ s pulses. The beam current was source limited and even larger beam currents should be possible. The gun does not present diode closure and was also operated at reduced currents in the d.c. mode.

ACKNOWLEDGMENTS. This work is supported by the U.S. Air Force and a C.S.U. Graduate School grant. J.Rocca wants to acknowledge the support of a National Science Foundation Presidential Young Investigator Award and B.Szapiro the support from the Universidad Nacional de Buenos Aires for his fellowship.

## FIGURE CAPTIONS.

Figure 1. Experimental set up. The vacuum chamber is not shown. The circles represent pulse current transformers. The 5 cm ID hollow cathode (1), the anode electrode (2), and the acceleration electrode (3) are indicated. The 25-75  $\Omega$  discharge ballast resistor was only used in the high current experiments, in series with a 50 nF capacitor.

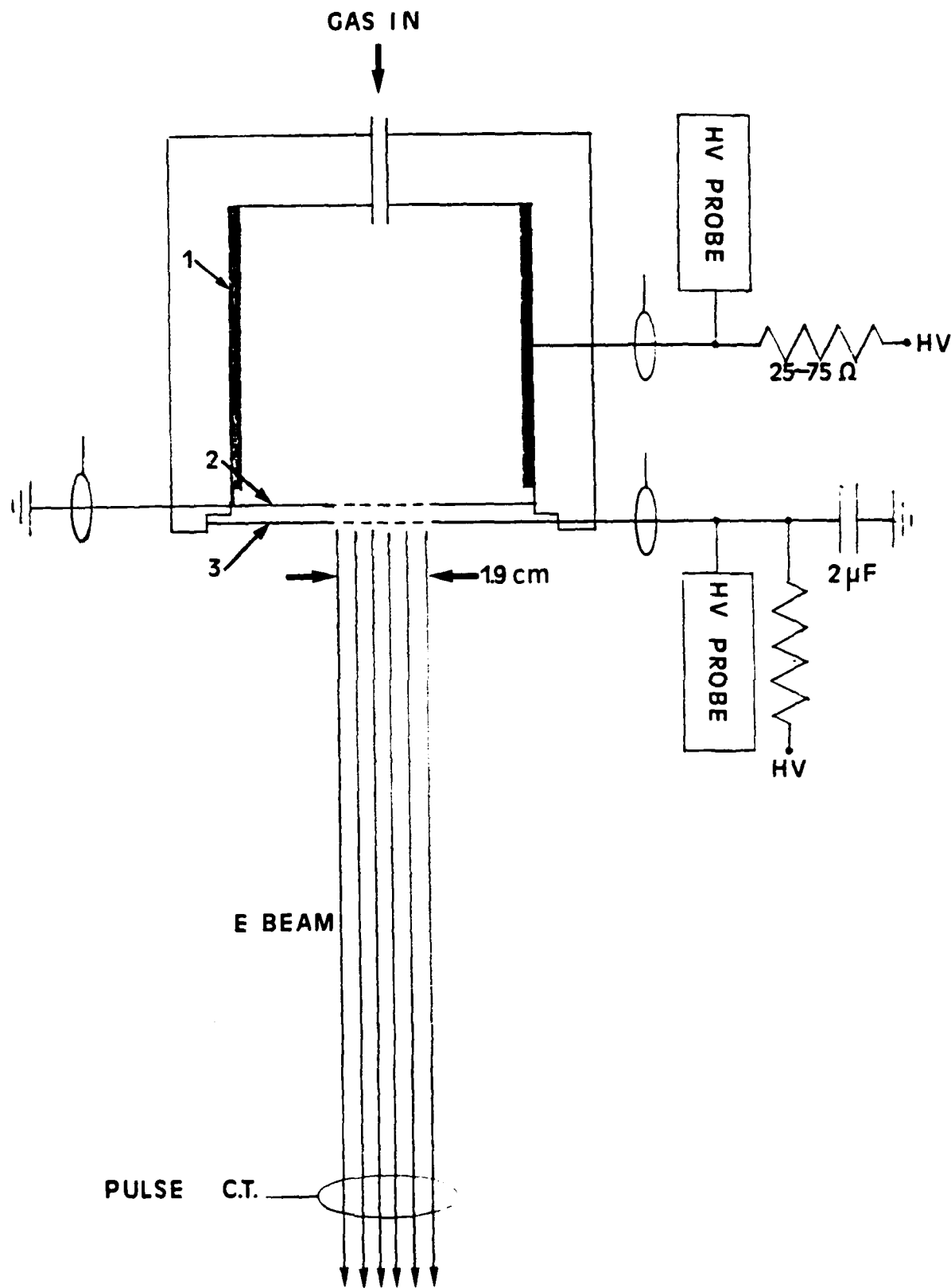
Figure 2. a) Upper trace: discharge current; lower trace: electron beam current. Acceleration voltage,  $V_{\text{accel}} = 2$  kV. b) Upper trace: sum of discharge and anode grid currents; lower trace: sum of electron beam and acceleration grid currents. c) Upper trace: discharge current; bottom trace: anode grid current for  $V_{\text{accel}} = 0$  kV. d) Upper trace: discharge current; lower trace: anode grid current for  $V_{\text{accel}} = 2$  kV. All vertical scales are 2 A/div, with the zero level indicated in the left margin. The helium pressure was 0.45 Torr.

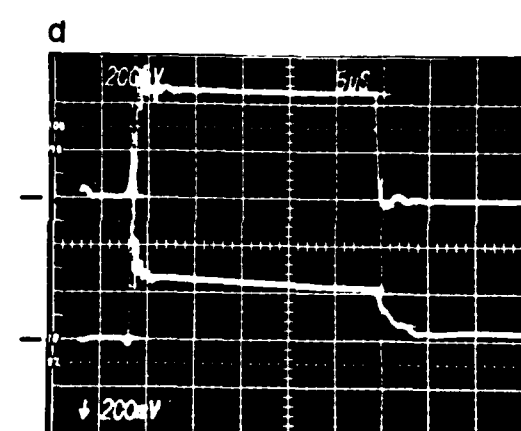
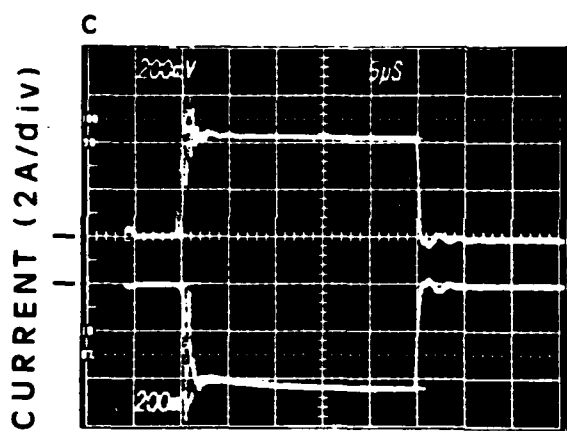
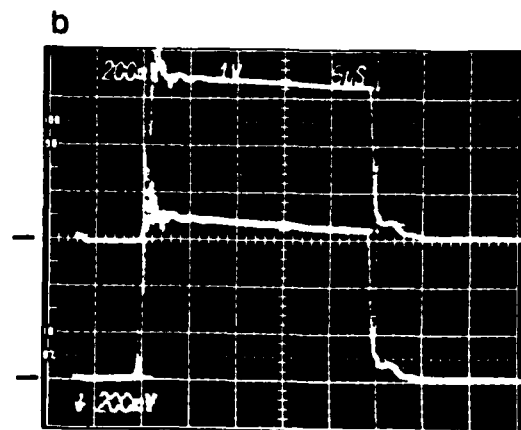
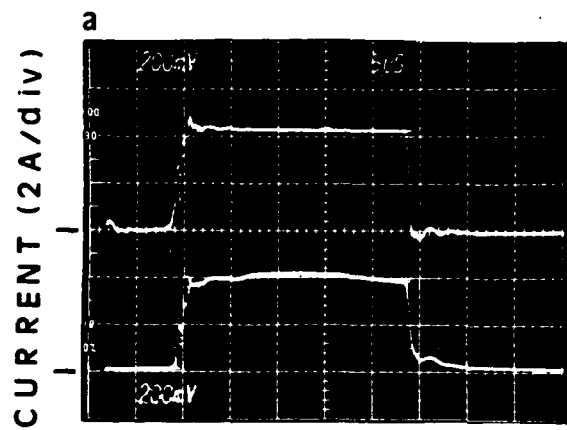
Figure 3. Upper trace: discharge current; lower trace: electron beam current.  $V_{\text{accel}} = 2$  kV. The background helium pressure was 0.45 Torr. The slight current decrease at the end of the electron beam pulse is a consequence of the decrease in the accelerating voltage due to the charge lost by the biasing capacitor. Since the beam current is measured at 15 cm from the gun, a reduction in accelerating voltage results in increasing scattering leading to the slight current reduction.

Figure 4. a) Discharge current. b) Electron beam current. c) Discharge voltage.  
d) Acceleration voltage. The background helium pressure was 0.2 Torr.  
A 75  $\Omega$  ballast resistor was used in series with the hollow cathode  
discharge current.

## REFERENCES.

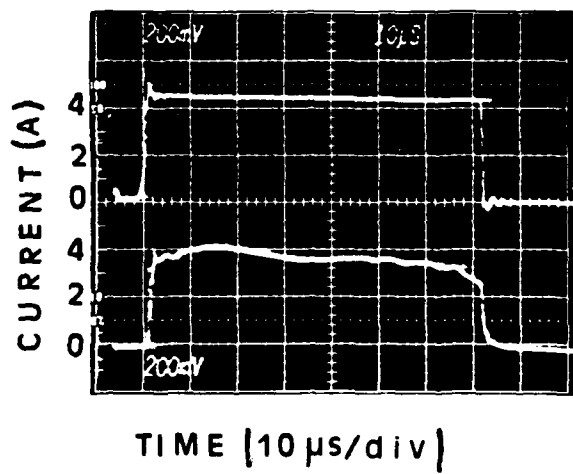
- 1) S.Humpries,Jr., S.Coffey, M.Savage, L.K.Len, G.W. Cooper, and D.M.Woodall. J.Appl.Phys. 57, 709(1985).
- 2) B.Wernsman, H.Ranea Sandoval, J.J.Rocca, and H.Mancini. IEEE Trans.Plasma Sci. PS-14, 518(1986).
- 3) T.Fusayama. Jap.J.Appl.Phys. 25, L 406(1986).
- 4) J.R.Bayless, and R.C. Knechtli. IEEE J.Q.Elect. 213, QE-10 (1974).
- 5) S.Humpries,Jr., M.Savage, and D.M.Woodall. Appl.Phys.Lett. 47, 468(1985).
- 6) A.V.Zharinov, Yu.A.Kovalenko, I.S.Roganov, and P.M.Tyuryukanov. Sov.Phys.Tech.Phys. 31, 39(1986).
- 7) A.V.Zharinov, Yu.A.Kovalenko, I.S.Roganov, and P.M.Tyuryukanov. Sov.Phys.Tech.Phys. 31, 413(1986).

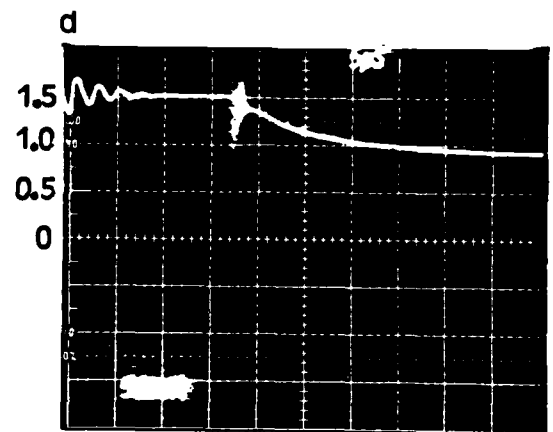
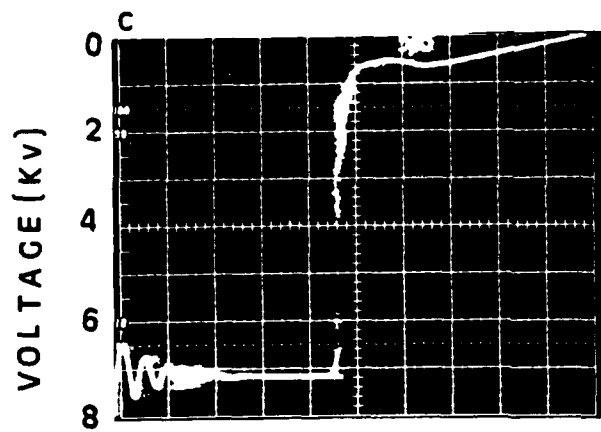
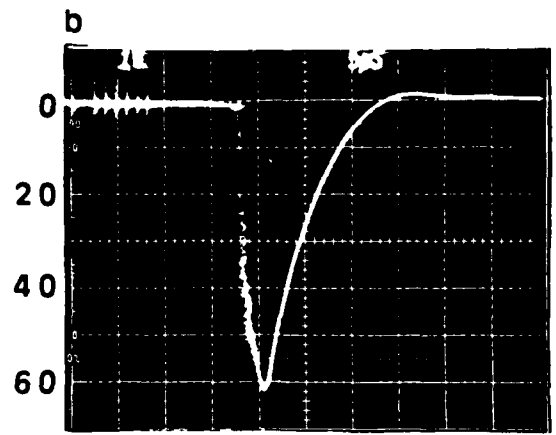
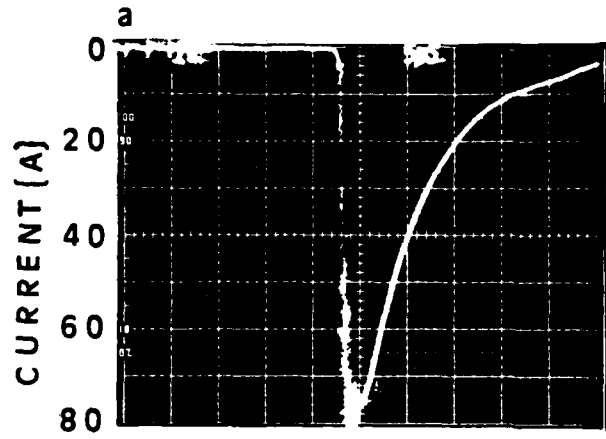




TIME (5µs/div)

TIME (5µs/div)





TIME [5  $\mu$ s/div]

TIME [5  $\mu$ s/div]

STUDY OF INTENSE ELECTRON BEAMS PRODUCED BY HIGH VOLTAGE PULSED GLOW DISCHARGES

H.F. RANEA-SANDOVAL<sup>(1)</sup>, N. REESOR, B.T. SZAPIRO<sup>(2)</sup>, C. MURRAY, AND J.J. ROCCA

Electrical Engineering Department  
Colorado State University  
Fort Collins, CO 80523

We report the generation of high current density (20 A/cm<sup>2</sup>) pulsed electron beams from high voltage (48-100 kV) glow discharges using cathodes 7.5 cm in diameter. The pulse duration was determined by the energy of the pulse generator and varied between 0.2  $\mu$ s and several  $\mu$ s, depending on the discharge current. The largest electron beam current (900 A) was obtained with an oxidized aluminum cathode in a helium-oxygen atmosphere. An oxidized magnesium cathode produced similar results, and a molybdenum cathode operated at considerably lower currents. A small diameter (<1 mm), well collimated beam of energetic electrons of very high current density (>1 kA/cm<sup>2</sup>) was also observed to develop in the center of the discharge. Electrostatic probe measurements show that the negative glow plasma density and the electron beam current have a similar spatial distribution. Electron temperatures of 1 to 1.5 eV were measured at 7 cm from the cathode. The plasma density ( $8.5 \times 10^{11} \text{ cm}^{-3}$  at 450 A) was found to depend linearly on the discharge current. In discharges at high currents a denser and higher temperature plasma region was observed to develop at approximately 20 cm from the cathode. We have modeled the process of electron beam generation and we predicted the energy distribution of the electron beam. More than 95 % of the electron beam energy is calculated to be within 10 % of that corresponding to the discharge voltage.

## I. INTRODUCTION

Glow discharges can be used to generate energetic beams of electrons by accelerating through the cathode fall the electrons emitted at the cathode surface by the bombardment of ions and fast neutrals [1-4]. There is no limit to the duration of the electron beam pulse, and it is possible to produce d.c. electron beams at current densities of  $> 0.1 \text{ A/cm}^2$  [5]. A detailed study of pulsed high voltage glow discharges (40-80 KV) at currents of the order of 10 mA/cm<sup>2</sup> was conducted by McClure [6]. O'Brien [7] has generated electron beam current densities in excess of 1 A/cm<sup>2</sup> over large areas, for durations of the order of 20  $\mu\text{s}$ . His results were obtained using aluminum or stainless steel electrodes in different gaseous atmospheres. The largest current densities he obtained were 5 A/cm<sup>2</sup> (in nitrogen at 20 mTorr) and 3 A/cm<sup>2</sup> (in helium at 180 mTorr).

In the generation of d.c. electron beams by glow discharges it is known that oxidation of an aluminum cathode can significantly increase the electron beam current density and efficiency [3]. Surface nitridisation causes a similar effect. This is a consequence of an increased secondary electron emission at the cathode surface. Thus, high secondary electron emission cathode materials are desirable. This work puts emphasis on studying the use of high electron yield cathode materials in the generation of intense pulsed electron beams.

We present in Section III results of operating aluminum and magnesium

cathodes in helium, nitrogen and oxygen atmospheres at pressures up to 720 mTorr and at voltages between 48 kV and 100 kV. A small amount of oxygen (<10 mTorr) was added to maintain the cathode oxidation in the helium discharges during long periods of operation. Electron beams with currents up to 900 A were produced at 65 kV using cathodes with an emitting surface area of 44 cm<sup>2</sup>. This corresponds to a current density at the cathode of nearly 20 A/cm<sup>2</sup>. A current density of 9 A/cm<sup>2</sup> was measured passing through a 7.7  $\mu$ m thick aluminum foil in the axis of the beam operating the discharge at 100 kV. The beam generation is very efficient; the electron beam current and the total discharge current were measured to differ in only a few percent. The duration of the electron beam current pulses was limited by the energy stored in the capacitors (5 nF erected capacitance) of the pulse generator. At large electron beam current densities (20 A/cm<sup>2</sup>) the pulse duration is approximately 200 ns, while at small current densities (1 A/cm<sup>2</sup>), it is several  $\mu$ s. We compare these results with those obtained using a molybdenum cathode that does not form a high secondary electron yield oxide or nitride layer.

In Section III.B the radial and axial distribution of the electron beam current is discussed. The radial profiles show the presence of a high current density (> 1 kA/cm<sup>2</sup>), small diameter (<1 mm) beam in the axis of the discharge. This phenomenon is further discussed in Section III.D. Measurements of the plasma density and electron temperature in the negative glow region of the discharge were obtained using electrostatic probes. The results are presented in Section III.C. The model of Section IV uses these data and predicts the electron energy distribution.

## II. EXPERIMENTAL APPARATUS

A two-stage Marx generator capable of delivering 25 J at 100 KV was built using commercially available spark gaps, pressurized with dry nitrogen. Both stages of the Marx generator are triggered by a transmission line discharged by a third spark-gap. This spark-gap is switched by discharging a second transmission line through a grounded-grid hydrogen thyatron.

The experimental setup is shown in Fig. 1. The Marx generator is enclosed in a metal tank filled with transformer oil. The vacuum chamber consists of a stainless steel cylinder 50 cm long, 20 cm ID in which the cathode is placed 13 cm apart from one end. The vacuum chamber is grounded and constitutes the anode of the discharge. The electron gun is connected to the Marx generator by a high-voltage, high-vacuum feedthrough. The cathode holder includes a water refrigeration system for high repetition rate operation. However, most of the results presented herein were obtained at 1 Hz repetition rate.

The vessel is pumped to  $10^{-6}$  Torr by a 200 l/s turbomolecular pump (3). Pressure is measured by an ionization gauge. The gases are flowed at a small rate into the chamber through needle valves, and circulated by means of a mechanical pump to minimize impurities in the gas mixture. Working gas pressures are measured with a capacitance manometer (4).

A diagram of the electron gun is presented in Fig. 2. The cathode is enclosed in a closely spaced (1 mm) dielectric shield to avoid emission from

surfaces other than the front one. The enclosure was made of polycarbonate due to its ability to support surface flashover without significant deterioration. A ceramic shield protects the plastic from direct exposure to the discharge by avoiding possible carbon sputtering from the polycarbonate, due to ion bombardment. The electron gun structural design allows for the easy replacement of cathodes. Cathodes made of oxidized aluminum, magnesium and molybdenum were tested. They are 7.5 cm in diameter, 3.5 cm long cylinders with rounded edges at their front surfaces.

The front cathode surfaces are hand-polished but the results do not show any significant dependence on the surface finishing, except when pores are present. Pores can cause the development of arcs on the cathode front surface, and consequently the collapse of the higher impedance glow discharge. In the case of magnesium, development of pores was observed as a consequence of the chemical attack caused by a detergent used during the cleaning procedure. After this was realized, only acetone and methanol were used as cleaning agents.

The electron beam current was measured using a commercially available pulse current monitor coil (5) mounted inside the discharge chamber. The coil inside diameter is 5 cm. It was placed coaxial with the beam, 7 cm from the cathode surface, and gave a signal proportional to the electron beam current passing through it. The calibrated sensitivity of the coil is 0.1 V/A. A second coil (6) having an inner diameter of 1.25 cm and a sensitivity of 1 V/A was also used in measuring electron beam current density profiles. The coils could be displaced along the diameter of the beam by a dynamic vacuum feedthrough shown in Fig 1. The smaller coil can also be displaced along the axis of the

discharge chamber when mounted in a second vacuum feedthrough which could be placed at the end of the chamber, and not shown in Fig. 1. The total discharge current was measured by a third coil (5) mounted inside the tank of the Marx generator. The discharge voltage was monitored using a 5000:1 resistive voltage divider.

The plasma density and electron temperature were measured using electrostatic probes. Both single and double probes were used in these measurements. They were made of 0.25 mm diameter tungsten wire, and were biased with batteries. Probe currents were measured with a commercially available current transformer. Spatially resolved plasma parameter measurements were obtained by displacing the probes with dynamic vacuum feedthroughs.

### III. EXPERIMENTAL RESULTS

#### A. Electron beam generation

Glow discharges created using three different cathode materials were studied. Cathodes made of aluminum, magnesium and molybdenum were alternately tested in oxygen, nitrogen and helium-oxygen atmospheres. The largest electron beam current, 900 A, was obtained at 65 kV from an aluminum cathode in a helium-oxygen gas mixture. The electronic component of the glow discharge current was measured with the 5 cm diameter current monitoring coil placed at 7 cm from the cathode surface. The active area of the coil is 20 cm<sup>2</sup>,

approximately half of the cathode area. It is shown in Section 3.B that at low currents (<100 A) the electron beam current density distribution across the cathode is approximately uniform. Consequently, at low beam currents the electron flux measured by the coil represents nearly half of the electron beam current generated by the electron gun. At high currents almost all the electron beam flux is measured by the coil due to the self-constriction of the electron beam.

Fig. 3 shows the dependence of the electron beam current generated by an aluminum cathode in a helium-oxygen atmosphere on the discharge conditions. The variation of the electron beam current  $I(A)$  with pressure  $P(\text{Torr})$  and discharge voltage  $V(\text{kV})$  can be described by the empirical expression:  $I = C V^k P^m$ , where  $C = (4.8 \pm 0.1) \times 10^{-3}$ ,  $k = (3 \pm 0.15)$  and  $m = (2.2 \pm 0.2)$ .

The electron beam current increases sharply with increasing pressure and discharge voltage. The maximum values of voltage and pressure at which the electron beam discharge may be operated is limited by the occurrence of arcs in the gap between the cathode and the ceramic shield. At a Marx generator voltage of 65 KV, the discharge was operated at pressures up to 600 mTorr. At these conditions the electron current measured through the monitoring coil was 900 A. This value corresponds to an electron beam current density at the cathode of approximately 20 A/cm<sup>2</sup>. At a voltage of 100 KV the maximum operating pressure at which an electron beam was obtained was 320 mTorr, resulting in an electron beam current of 300 A.

Figs. 4(a) and 4(b) show a 680 A electron beam current pulse obtained operating the discharge at a pressure of 720 mTorr and the corresponding discharge voltage, respectively. The electron beam pulse width of 200 ns FWHM is limited by the charge stored in the Marx generator. Figs. 5(a) and 5(b) illustrates a lower current electron beam pulse of 1.6  $\mu$ s FWHM and the corresponding discharge voltage variation. At lower discharge currents electron beam pulses of longer duration, lasting a few tens of us, were recorded.

The electron beam current passing through a 7.7  $\mu$ m thick aluminum foil was measured using the 5 cm ID current monitor. The foil was mounted on a stainless steel plate having an orifice of 2.8 cm in diameter placed in the axis of the discharge between the cathode and the coil. Results obtained operating the discharge at 100 KV at pressures between 100 mTorr and 300 mTorr are shown in Fig. 6. A transmitted beam current density of 9 A/cm<sup>2</sup> was measured at 300 mTorr. The results of the sheath model presented in Section IV and the foil beam profile measurements discussed in the next section show that the major part of the electron beam current is due to high energy electrons.

The aluminum cathode was also operated in pure oxygen and pure nitrogen atmospheres. Figs. 7(a) and 7(b) show the variation of the electron beam current passing through the 5 cm diameter current monitoring coil as a function of discharge pressure and voltage. For both molecular gases the maximum pressures at which an electron beam was generated were below 60 mTorr, and the maximum electron beam current obtained in both cases is below 200 A.

The use of magnesium as cathode material was also investigated. As

aluminum, magnesium forms oxide or nitride layers that constitute efficient emitters of electrons following ion bombardment. Fig. 8 shows the variation of the electron beam current as a function of discharge voltage and pressure. As in Fig. 3, the gas mixture contained 10 mTorr of oxygen, the balance being helium. The electron beam currents passing through the 5 cm monitoring coil are comparable to the values obtained with the aluminum cathode. A maximum current of 700 A was obtained at 65 kV and a pressure of 520 mTorr.

Figures 9(a) and 9(b) show the electron beam currents obtained operating the magnesium cathode in pure oxygen and nitrogen atmospheres, respectively. In these experiments the maximum electron beam current measured through the 5 cm coil was below 200 A. As in the case of aluminum, the electron beam currents obtained in the oxygen and nitrogen atmospheres are considerably lower than those obtained in the helium-oxygen mixture.

We also studied glow discharges generated using a molybdenum cathode. In contrast with aluminum and magnesium, molybdenum does not form oxide or nitride layers that significantly increase electron emission. Fig. 10 summarizes the electron beam currents obtained in a helium atmosphere. Figs. 11(a) and 11(b) show the results obtained in experiments in pure oxygen and nitrogen atmospheres, respectively. In all cases the currents emitted by the molybdenum cathode are significantly lower than those obtained with the oxidized cathodes. All the results discussed in the following sections were obtained using aluminum cathodes.

## B. Spatial distribution of the electron beam current

We have studied the radial and axial variation of the electron beam current. All the experiments discussed in this section were performed in a helium-oxygen atmosphere. The radial distribution was measured displacing the 1.25 cm diameter coil masked by a stainless steel plate across a cathode diameter by means of a vacuum feedthrough. The plate supported two blades defining a  $1.25 \times 0.2$  cm<sup>2</sup> slot. The electron beam current profile was generated measuring the current passing through the slot at different positions.

Fig. 12 shows the radial distributions of the electron beam current measured at 7 cm from the cathode corresponding to discharge currents of 80 A and 400 A. At the lower current the electron beam profile is only slightly more intense at the axis. This relatively uniform distribution is in good agreement with the shape of the profiles measured by O'Brien [7] for an 180 cm<sup>2</sup> aluminum cathode operated at a current of 34 A. In contrast, the measurements performed at a discharge current of 400 A show a distribution that is sharply peaked at the axis. The current obtained by integrating the 5 cm central region under the respective profiles agrees within 10 % with the current measured with the 5 cm diameter pulse transformer, at the same discharge conditions.

Fig. 13 shows the current density variation along the electron beam axis for four values of the discharge current. The electron beam current density at the axis is seen to increase as a function of the distance from the cathode due to the self-constriction of the electron beam by the self-generated magnetic

field. At 300 A the entire beam focuses into a spot of a few cm<sup>2</sup> at 17.5 cm from the cathode surface. The location of the region of maximum current density at the axis approaches the cathode as the electron beam current increases.

At high currents (>150 A) a bright, pink plasma is observed in the region where the highest current densities are attained. The electrostatic probe measurements discussed in Section III.C confirm that a higher density plasma ( $>5 \times 10^{12} \text{ cm}^{-3}$ ) develops in this region. Strong beam-plasma interactions are likely to occur there. This phenomenon was previously observed in the focal region of glow discharge generated d.c. electron beams [8]. By this mechanism a significant fraction of the electron beam energy is transferred to the plasma, which increases both its density and temperature. Simultaneously, the electron beam spectrum degrades [8] and the beam diverges.

We have also studied the radial profiles of the beam after passing through a 7.7  $\mu\text{m}$  thick aluminum foil. Figs. 14 and 15 compare the beam profiles with and without the foil at the same set of discharge voltage and He-O<sub>2</sub> operating pressure: at 100 kV and 100 mTorr; and at 100 kV and 200 mTorr, respectively. In both cases the integrated current passing through the foil is approximately 80 % of the current evaluated from the profile without the foil. However, the model presented in Section IV predicts that 95 % of the electrons have energy greater than 60 keV, and should pass through the foil. The scattering of electrons by the foil can be responsible for this discrepancy. The acceptance angle of our detection system composed by the slot and the pulse transformer is rather small (12°) and, consequently, electrons scattered at larger angles are not detected.

Sharp peaks in the electron beam current density distributions are observed at the axis of the electron beam in Figs. 14 and 15. The origin of this phenomenon is the presence of a very small diameter ( $< 1$  mm) beam of energetic electrons approximately coincident with the axis of the high current density discharge. Thus, during the high current density measurements with the foil we avoided the axial region because the mini-beam could perforate the foil. For this reason, the lower trace in Fig. 15 is open. The narrow peak due to the mini-beam does not appear in the profiles of Fig. 12 because it has been intentionally subtracted. This phenomenon is further discussed in Section III.D.

### C. Electron density and temperature

The electron energy distribution in the negative glow of the discharge is non-Maxwellian, containing high-speed electrons that have been accelerated in the cathode fall [9]. A large fraction of these electrons have an energy corresponding to approximately the entire discharge voltage. The calculated energy distribution of these high-speed electrons is discussed in Section IV. Nevertheless, the majority of the electrons in the negative glow region have low energy. This low energy group, which practically determines the plasma density, is made of secondary electrons been produced by the beam electrons in ionizing collisions [9]. The energy distribution of these slow electrons is approximately Maxwellian [6-8].

The knowledge of the plasma density and electron temperature in the negative glow region of the discharge is relevant to the process of electron beam generation. These parameters determine the ion flux passing from the negative glow to the cathode fall region. These ions, which are subsequently accelerated in the cathode fall region, and the fast neutral atoms created by charge transfer collisions, are responsible for the emission of secondary electrons at the cathode surface. In the rest of this section we discuss the measurement of the temperature and density of the thermalized electrons. In Section IV we use these experimental values in a model of the discharge to predict the energy distribution and density of beam electrons produced in the glow discharge.

McClure [6] and O'Brien [7] have previously measured the plasma density and electron temperature in the negative glow region of pulsed discharges. Their measurements correspond to low discharge current densities ( $<0.3 \text{ A/cm}^2$ ). We have measured these parameters at glow discharge current densities up to  $10 \text{ A/cm}^2$ .

Our measurements were made using single and double electrostatic probes. The probe traces were obtained by sequentially changing the probe bias on a shot by shot basis. The double probe was used to measure in the high density plasma region, where the electron beam focuses. The single probe, giving a larger signal, was used to measure in the lower density regions. Our double probe has a better frequency response than our single probe. However, in measurements made in the plasma regions where it was possible to compare both probes, the values of the plasma parameters agree within a factor of two. Fig. 16 is a

typical single probe trace, and corresponds to a measurement taken at 20 cm from the cathode.

Radial profiles of the plasma densities measured at 7 cm from the cathode using a single probe are shown in Fig. 17. The measurements were made at a discharge voltage of 72 kV and at currents of 180 A and 450 A. The general shape of the plasma density profiles resemble the radial distribution of the electron beam current density shown in Fig. 12. The maximum plasma density is at the axis of the beam, where the electron beam current density peaks. Values of the electron temperature obtained from the same measurements were all between 1 and 1.5 eV.

The variation of the plasma density on the axis of the beam, at 7 cm from the cathode, as a function of discharge current is illustrated in Fig. 18. The measurements were obtained at a discharge voltage of 56 kV. In the range of currents investigated the plasma density was observed to increase linearly with the current, from a value of  $6 \times 10^{10} \text{ cm}^{-3}$  at 40 A to  $8.5 \times 10^{11} \text{ cm}^{-3}$  at 450 A. The electron energy values obtained from the same probe traces were also between 1 and 1.5 eV. In all the measurements made in the negative glow region of the discharge the plasma potential was between 5 and 10 V above anode potential, confirming that practically all the discharge voltage drops in the cathode sheath.

We also measured the plasma parameters 20 cm from the cathode where at high currents a high luminosity plasma is observed. This is the region where, as shown in Fig. 13, the electron beam current density increases due to

self-constriction. The energy of the thermal electrons in this region was observed to be consistently higher than closer to the cathode, where the electron beam current density is considerably lower. The measured electron energies in the high luminosity region are between 2 eV and 6 eV. Secondary electrons produced by ionization in the high luminosity region are likely to be heated as a result of beam-plasma interactions [8]. The plasma density in this region is also significantly higher. Values between  $5 \times 10^{12}$  and  $7 \times 10^{13} \text{ cm}^{-3}$  were measured at electron beam currents between 160 A and 400 A.

Measurements were also made in a pure nitrogen atmosphere at 7 cm from the cathode and 72 kV of discharge voltage. At a pressure of 30 mTorr and discharge current of 60 A (1.3 A/cm<sup>2</sup>), we obtained an electron temperature  $kT_e = 1.2 \text{ eV}$  and a plasma density of  $1.1 \times 10^{11} \text{ cm}^{-3}$ . At a pressure of 40 mTorr and discharge current of 100 A (2.2 A/cm<sup>2</sup>), these values were 1.4 eV and  $2 \times 10^{11} \text{ cm}^{-3}$ . These electron temperatures compare well with the value of  $kT_e = 1 \text{ eV}$  measured by O'Brien [7] at lower current densities (0.3 A/cm<sup>2</sup>). The plasma densities measured in both experiments indicate a linear increase with the current density.

#### D. High current density mini-electron beam

As mentioned in Section III.B, a high current density electron beam of small diameter develops approximately in the axis of the discharge. This small beam made marks of less than 1 mm in diameter in the stainless steel blades used as collimators in the current profile measurements. As the coil was moved vertically across the cathode diameter, a line of similar dots was etched on the

stainless-steel plate used to protect the pulse transformer from electron bombardment.

Where this well collimated mini-beam impinges on a metallic surface, a bright plasma spot is observed. This effect is shown in Fig. 19. To obtain this photograph the coil was rotated  $45^\circ$  respect to the axis of the discharge to permit viewing of the mini-beam -created plasma. The photograph was obtained at a discharge voltage of 82 kV, in a He-O<sub>2</sub> mixture at 375 mTorr.

When the time evolution of the electron beam in the axial region of the beam was measured, the pulse shape shown in Fig. 20 was observed. This signal was obtained with a 1.25 cm diameter current monitoring coil aligned with the axis of the discharge. A short pulse, having a width of approximately 20 ns, is apparent in the leading edge of the electron beam pulse. This feature is only observed when the mini-beam is present, and consequently it is attributed to it.

Using data from Figs. 15 and 20 it is possible to obtain a rough estimate of the current and energy density of the mini-beam. In Fig. 15 the current density at the center of the profile made without the aluminum foil is out of scale. The value there is 32 A/cm<sup>2</sup>, and the major fraction is attributed to the mini-beam. The corresponding measured current through the 0.2x1.25 cm<sup>2</sup> slot was 8 A. The base of the narrow peak in Fig. 15 can be estimated to be 7.5 A/cm<sup>2</sup>, corresponding to a current of approximately 2 A. Consequently, the current of the mini-beam at these discharge conditions is estimated to be 6 A. From the marks left in the stainless steel plate the diameter of the mini-beam is estimated to be 0.5 mm. The corresponding current density is of the order of 1

kA/cm<sup>2</sup>. Considering a pulse width of 20 ns and a discharge voltage of 100 kV, the energy density of this small beam can be estimated to be of the order of several J/cm<sup>2</sup>.

Similar effects were also observed in magnesium cathodes when the discharge currents were above a few hundreds amperes. Moreover, the plasma spot shown in Fig. 19 was found independent of the axial position of the target. A more detailed study is needed to determine the mechanism of formation of this high current density, very small area electron beam.

#### IV. MODEL OF THE ELECTRON BEAM GENERATION

The pulsed glow discharges discussed in the previous section were operated at high current densities (1-20 A/cm<sup>2</sup>) and at relatively high helium pressures. The mechanisms of electron beam generation at these conditions have not been previously studied.

We have modeled the process of electron beam generation in these high current densities helium glow discharges. The model was used to predict the density and energy distribution of the electron beam. The results also show that fast neutral atoms bombarding the cathode make a major contribution to the total electron emission. We constructed a model of the cathode fall region similar to that previously developed by McClure [10] for a deuterium discharge. Experimental values of the negative glow plasmas were used to calculate the flux of ions entering the cathode sheath. The electric field and the fluxes of

charged particles in the cathode fall region are calculated in a self-consistent manner. Charged particle pair creation in the sheath resulting from ionization by fast ions and beam electrons was included. The collisional processes considered in the cathode fall region include the creation of fast neutral atoms by charge transfer and are summarized in Table I. The sources of the cross sections data used are also indicated.

The secondary electron emission coefficients for aluminum under He<sup>+</sup> bombardment measured by Bourne et al. [11] were used. The secondary emission yields due to fast helium atoms and ions of the same energy were assumed to be equal for energies above 20 keV [12], but electron emission due to atoms was assumed to be negligible for energies below 500 eV.

The electron beam energy distribution resulting from running our model at 52 kV and 370 mTorr of helium is shown in Fig. 21. The conditions correspond to a measured negative glow plasma density of  $4.5 \times 10^{11} \text{ cm}^{-3}$ , and electron energy of 1.5 eV. By integrating the data shown in Fig. 21, we calculated that 97 % of the electron beam energy is carried by electrons having an energy that is within 10 % of that corresponding to the discharge voltage. The low energy peak is due to electrons created by ionization in the sheath. The integration of the total electron flux density amounts to a current density of 4.1 A/cm<sup>2</sup>. This value is in good agreement with the experimentally measured of 4.5 A/cm<sup>2</sup>.

Figs. 22.(a) and 22.(b) are the predicted energy spectra of the fluxes of He<sup>+</sup> and fast He atoms at the cathode. The emission rate of electrons is calculated by the convolution of these curves with the corresponding secondary

electron emission data. For the above conditions the emission of electrons at the cathode due to fast neutrals is calculated to be 65 % of the total electron emission at the cathode.

The model results can be summarized as follows. The electron beam current densities predicted using measured negative glow plasma parameters are of the same order of the experimental values. Fast neutral atoms, created by charge transfer in the cathode sheath, are at least as important as ions in causing the emission of electrons from the cathode surface. The emission due to neutrals results in electron beam current densities above those corresponding to the Child-Langmuir space charge limited ion flux for a given voltage and sheath thickness. More than 95 % of the electron beam energy is carried by electrons having an energy that is within 10 % of that corresponding to the discharge voltage.

#### V. SUMMARY

We studied the generation of intense pulsed electron beams in glow discharges at voltages between 48 kV and 100 kV using cathodes 7.5 cm in diameter. An aluminum cathode in a helium-oxygen atmosphere produced electron currents up to 900 A (20 A/cm<sup>2</sup>). Pulse duration was limited by the stored energy in the Marx generator. A current density of 9 A/cm<sup>2</sup> was measured through a 7.7  $\mu$ m thick aluminum foil in the axis of a 100 kV discharge. Similar current densities were obtained using an oxidized magnesium cathode. Arcs developing

between the cathode and the ceramic shield set a limit for the maximum electron beam current and voltage. The electron beam currents obtained operating the discharge in pure oxygen and nitrogen atmospheres were lower than those obtained in the helium-oxygen mixture. A molybdenum cathode, that does not have a high electron yield oxide layer, delivered considerably lower current densities.

Simultaneously, the glow discharges were observed to generate a small diameter ( $<1$  mm), short duration (20 ns) beam of energetic electrons of very high current density ( $>1$  kA/cm<sup>2</sup>) in the axis. Its energy density ( $>1$  J/cm<sup>2</sup>) is enough to etch marks on metallic targets. The understanding of the mechanism of formation of this intense small beam requires further studies.

Electron beam current distribution measurements show that the beam is relatively uniform at low ( $<100$  A) currents. At large currents, self-constriction increases the axial beam density. Electrostatic probe measurements show that the negative glow plasma density and the electron beam current have a similar radial distribution. The plasma density measured at the axis of the discharge at 7 cm from the cathode increases linearly with discharge current. The electron temperature in the same region was measured to be between 1 eV and 1.5 eV. A bright, high density plasma was observed in the region where the highest electron beam current densities occur. Electrostatic probe measurements show that both the plasma density and the electron temperature are higher there than in the other regions of the discharge. This is possibly due to the onset of beam-plasma instabilities.

A model of the cathode sheath predicts electron beam current densities

values in agreement with the experiments. According to the model results, more than half of the electron current emitted at the cathode is due to the bombardment of fast neutral created by charge transfer in the cathode sheath. The calculated energy distribution shows that >95 % of the electron beam is carried by electrons having an energy within 10 % of the discharge voltage.

#### VI. ACKNOWLEDGMENTS

This work was supported by the U.S. Air Force. J.Rocca wants to thank the support of an N.S.F. Presidential Young Investigators Award. B.Szapiro is gratefully indebted to the Universidad Nacional de Buenos Aires for his fellowship. The authors also want to thank the experimental assistance of Ben Wernsman and the skilfull machining by Jerry Davis. The support and the helpful comments by A. Garscadden and P. Haland are gratefully acknowledged.

- (1) On leave from CIOp (CIC-BA) Centro de Investigaciones Opticas, Rep. Argentina.
- (2) On leave from PROFET (UNCPBA) Programa de Fisica Experimental Tandil, Rep. Argentina.
- (3) Edwards Turbomolecular pump, Model ETP6/200.
- (4) MKS Baratron, Type 227 A.
- (5) Pearson Electronics, Model 110 current monitor, 0.1 V/A sensitivity.

(6) Pearson Electronics, Model 411 current monitor, 1 V/A sensitivity.

## REFERENCES

- [1] A.S.Pokrovskaya-Soboleva and B.N.Kliarfel'd, "Ignition of the high voltage discharge in hydrogen at low pressures," Soviet Physics JETP, vol.5, pp.812-818, Dec. 1957.
- [2] R.A.Dugdale,"Soft vacuum processing of materials with electron beams," J.Mater.Sci.,vol.10,pp.896-902,1975.
- [3] J.J.Rocca,J.D.Meyer,M.R.Farrell,and G.J.Collins,"Glow-discharge- created electron beams: cathode materials,electron gun designs, and technological applications," J.Appl.Phys.,vol.56,pp.790-797,Aug.1984.
- [4] B.Wernsman,H.F.Ranea-Sandoval,J.J.Rocca,and H.Mancini,"Generation of pulsed electron beams by simple cold cathode plasma guns," IEEE Trans.Plasma Sci.,vol.PS-14,pp.518-522,Aug.1986.
- [5] J.J.Rocca,J.D.Meyer,Z.Yu,M.Farrell,and G.J.Collins,"Multikilowatt electron beams for pumping CW lasers," Appl. Phys. Lett., vol.41,pp.811-813,Nov.1982.
- [6] G.W.McClure,"High-voltage glow discharges in D2 gas.I.Diagnostic measurements,"Phys.Rev.,vol.124, pp.969-982,Nov.1961.
- [7] B.B.O'Brien,Jr., "Characteristics of a cold cathode plasma electron gun," Appl.Phys.Lett.,vol.22,pp.503-505,May.1973.

- [8] Z.Yu, J.J.Rocca, G.J.Collins, "Studies of a glow discharge electron beam," J.Appl.Phys., vol.54, pp.131-136, Jan.1983
- [9] Z.Yu, J.J.Rocca, G.J.Collins and C.Y.She, "The energy of thermal electrons in electron beam created helium discharges," Phys. Lett., vol. 96A, pp. 125-127, Jun. 1983.
- [10] G.W.McClure and K.D.Granzow, "High-voltage glow discharges in D<sub>2</sub> gas. II. Cathode fall theory," Phys.Rev., vol.125, pp.3-10, Jan.1962.
- [11] H.C.Bourne, Jr., R.W.Cloud, and J.G.Trump, " Role of positive ions in high-voltage breakdown in vacuum," J.Appl.Phys., vol. 26, pp.596-599, May 1955.
- [12] F.Schwartzke, "Ionisierungs- und Umladequerschnitte von Wasserstoff-Atomen und Ionen von 9 bis 60 keV in Wasserstoff," Z.Physik, vol.157, pp.510-522, 1960.
- [13] W.Lotz, "Electron-impact ionization cross sections and ionization rate coefficient for atoms and ions," Astrophys. J. Suppl. Ser. XIV, No 128, pp. 207-237, May 1967.
- [14] L.J.Kiefer and G.H.Dunn, "Electron impact ionization cross section data for atoms, atomic ions and diatomic molecules: I. Experimental data," Rev. Mod. Phys., vol. 38, pp. 1-35, Jan. 1966.
- [15] M.J.Van Der Wiel, F.J. DeHeer, and G. Wiebes, "Double ionization of

helium," Phys. Lett., vol. 24A, pp. 423-424, Apr. 1967.

[16] S.K.Allison, "Experimental results on charge-changing collisions of Hydrogen and Helium atoms and ions at kinetic energies above 0.2 keV," Rev. Mod. Phys., vol. 30, pp. 1137-1138, Oct. 1958.

[17] L.J.Pucket, G.O.Taylor, and D.W.Martin, "Cross sections for ion and electron production in gases by 0.15-1.00 MeV hydrogen and helium ions and atoms," Phys. Rev. , vol. 136, pp. 379-385 , Oct. 1964.

[18] R.A.Langley, D.W.Martin, D.S.Harmer, J.W.Hooper, and E.W.McDaniel, "Cross sections for ion and electron production in gases by fast helium (0.133-1.0 MeV): I. Experimental," Phys. Rev., vol. 36, pp. 379-385, Oct. 1964.

[19] S.W.Nagy, W.J.Savloa, Jr., and E.Poylack, "Measurements of the total cross section for symmetric charge exchange in Helium from 400-2000 eV," Phys. Rev., vol. 177, pp. 71-76, Jan. 1969.

[20] J.B.Hasted, "Atomic and molecular processes," D.R.Bates,Ed., (Academic Press,1962), pp. 496-720.

[21] K.H.Berkner, R.V.Pyle, J.W.Stearns, and J.C.Warren, "Single and double electron capture by 7.2 to 181 keV He<sup>++</sup> ions in He," Phys. Rev., vol. 166, pp. 44-46, Feb. 1968.

[22] G.R.Hertel, and W.S.Koski, "Cross sections for the single charge transfer of

TABLE I  
COLLISIONAL PROCESSES IN THE CATHODE SHEATH

REACTION	PROCESS	REFERENCE
$e + \text{He} \rightarrow \text{He}_s^+ + 2e$	Ionization by electrons	[13],[14]
$e + \text{He} \rightarrow \text{He}_s^{++} + 3e$	Double ionization by electrons	[15]
$\text{He}_f + \text{He} \rightarrow \text{He}_f^+ + \text{He} + e$	Ionization by fast neutrals	[16],[17]
$\text{He}_f^+ + \text{He} \rightarrow \text{He}_f^+ + \text{He}^+ + e$	Ionization by fast ions	[16],[17],[18]
$\text{He}_f^{++} + \text{He} \rightarrow \text{He}_s^+ + \text{He}_f^{++} + e$	Ionization by double ions	[15]
$\text{He}_f^+ + \text{He} \rightarrow \text{He}_f^{++} + \text{He} + e$	Ionization of fast ions	[16]
$\text{He}_f^+ + \text{He} \rightarrow \text{He}_f^+ + \text{He}^+$	Ion-neutral charge-transfer	[16],[19],[20]
$\text{He}_f^{++} + \text{He} \rightarrow \text{He}_f^+ + \text{He}^{++}$	Double ion-neutral double charge transfer	[21],[22],[23]
$\text{He}_f^{++} + \text{He} \rightarrow \text{He}_f^+ + \text{He}^+$	Double ion charge-transfer	[21],[22],[23]

s : slow particle  
f : fast particle

## FIGURE CAPTIONS

Fig. 1. Experimental apparatus.

Fig. 2. Schematic diagram of the electron gun and high voltage vacuum feedthrough. The cathode diameter is 7.5 cm.

Fig. 3. Electron beam current vs. voltage, with pressure as a parameter. An aluminum cathode was used in He + 10 mTorr of O<sub>2</sub>. A 5 cm I.D. pulse transformer was used to measure the current at 7 cm from the cathode.

Fig. 4. (a) Electron beam current pulse. (b) Corresponding evolution of the discharge voltage. An aluminum cathode was used at 710 mTorr of He + 10 mTorr of O<sub>2</sub>.

Fig. 5. (a) Electron beam current pulse. Three superimposed traces can be seen. (b) Corresponding evolution of the discharge voltage. An aluminum cathode was used at 190 mTorr of He + 10 mTorr of O<sub>2</sub>.

Fig. 6. Electron beam current density passing through a 7.7  $\mu\text{m}$  thick aluminum foil as function of discharge pressure. Measurements were made through an on-axis aperture 2.8 cm in diameter. Increasing pressure corresponds to increasing electron beam discharge current. An aluminum cathode was used in a He + 10 mTorr O<sub>2</sub> atmosphere. The Marx output voltage was 100 kV.

Fig. 7. Electron beam current vs. voltage, with pressure as a parameter.

An aluminum cathode was used in (a) pure O<sub>2</sub>, (b) pure N<sub>2</sub>. In both cases a 5 cm I.D. pulse transformer was used to measure the current at 7 cm from the cathode.

Fig. 8. Electron beam current vs. voltage, with pressure as a parameter. A magnesium cathode was used in He + 10 mTorr of O<sub>2</sub>. A 5 cm I.D. pulse transformer was used to measure the current at 7 cm from the cathode.

Fig. 9. Electron beam current vs. voltage, with pressure as a parameter. A magnesium cathode was used in (a) pure O<sub>2</sub>, (b) pure N<sub>2</sub>. In both cases a 5 cm I.D. pulse transformer was used to measure the current at 7 cm from the cathode.

Fig. 10. Electron beam current vs. voltage, with pressure as a parameter. A molybdenum cathode was used in He + 10 mTorr of O<sub>2</sub>. A 5 cm I.D. pulse transformer was used to measure the current at 7 cm from the cathode.

Fig. 11. Electron beam current vs. voltage with pressure as a parameter. A molybdenum cathode was used in (a) pure O<sub>2</sub>, (b) pure N<sub>2</sub>. In both cases a 5 cm I.D. pulse transformer was used to measure the current at 7 cm from the cathode.

Fig. 12. Radial distribution of electron beam current measured at 7 cm in front of the aluminum cathode. The shadowed region in the abscissas identifies the relative position of the cathode. Discharge currents are indicated.

Fig. 13. Electron beam current density profile along the axis of the beam. A change of scale was used in the current density axis, to allow the comparison of the four curves. Discharge currents are indicated.

Fig. 14. Electron beam current profile measured with (lower trace) and without (upper trace) a  $7.7 \mu\text{m}$  thick Al foil placed between the cathode and the coil. The profile was measured with a slotted aperture of  $0.2 \times 1.25 \text{ cm}^2$  placed in front of a current monitoring coil. The discharge current was 70 A.

Fig. 15. Electron beam current profile measured with (lower trace) and without (upper trace) the  $7.7 \mu\text{m}$  thick Al foil placed between the cathode and the coil. The profile was measured with a slotted aperture of  $0.2 \times 1.25 \text{ cm}^2$  placed in front of a current monitoring coil. The discharge current was 250 A.

Fig. 16. Langmuir single probe characteristic yielding plasma density and electron temperature.

Fig. 17. Radial profiles of the plasma density measured at 7 cm from the cathode. Discharge currents are indicated.

Fig. 18. On-axis plasma density as a function of the discharge current.

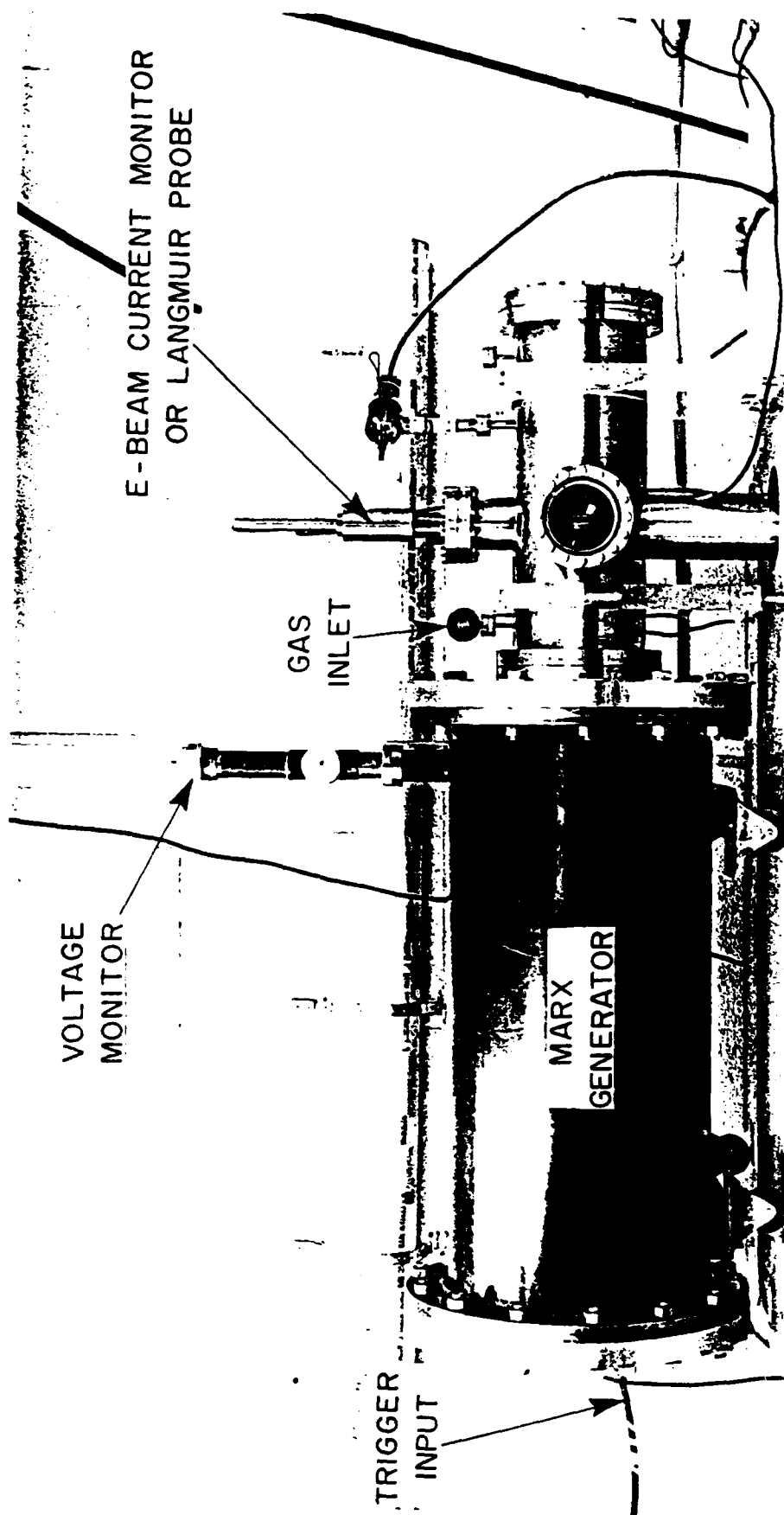
Fig. 19. Photograph of the plasma spot (arrow) generated when the mini-beam impinges the brass wall of the 1.25 cm ID pulse transformer. The coil was rotated  $45^\circ$  respect of the beam axis to make it more visible. Discharge voltage was 82 kV, and the He + 10 mTorr O<sub>2</sub> pressure was 375 mTorr. The beam

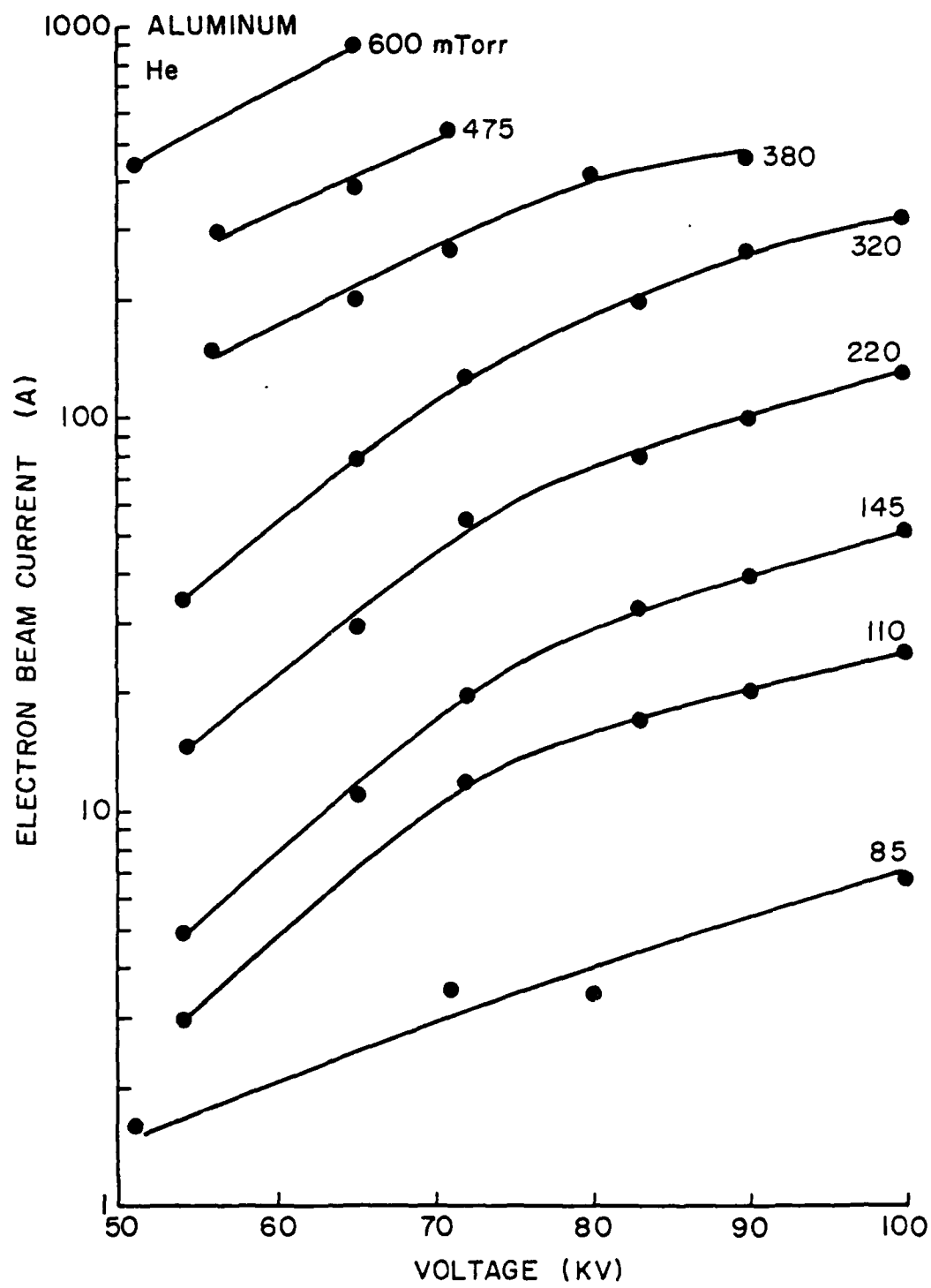
current was 300 A.

Fig. 20. Time evolution of the current in the central region of the electron beam. The signal was digitized in 512 channels with 5 ns resolution. The mini-beam is apparent between the arrows, and lasts about 20 ns. The He + 10 mTorr O<sub>2</sub> pressure was 430 mTorr and the discharge voltage was 72 kV.

Fig. 21. Calculated electron flux energy distribution corresponding to a discharge voltage of 52 kV and a helium pressure of 350 mTorr.

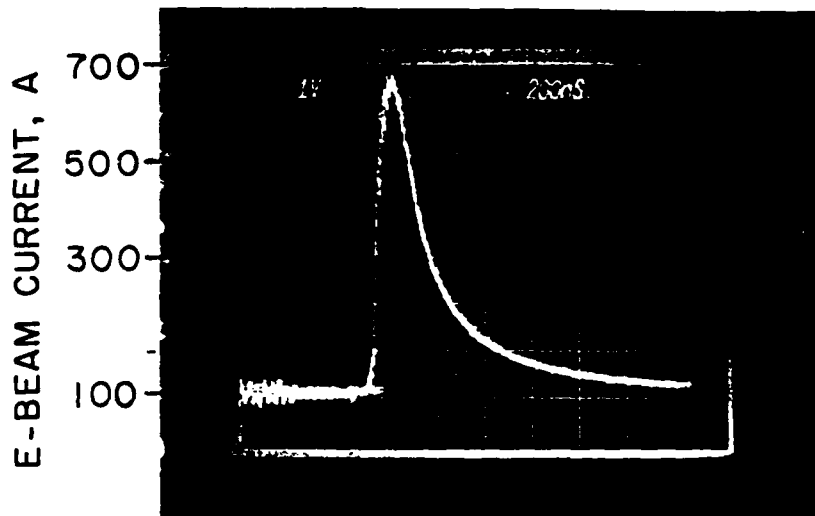
Fig. 22. (a) Calculated He<sup>+</sup> flux energy distribution at the cathode surface. (b) Calculated neutral helium flux energy distribution at the cathode surface. The distributions corresponds to a discharge voltage of 52 kV and a helium pressure of 350 mTorr.



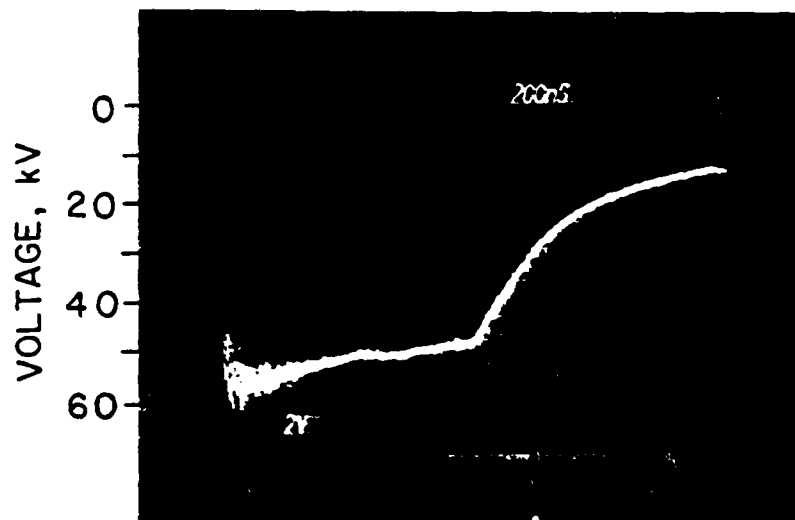


0.72 Torr, He

a)



b)



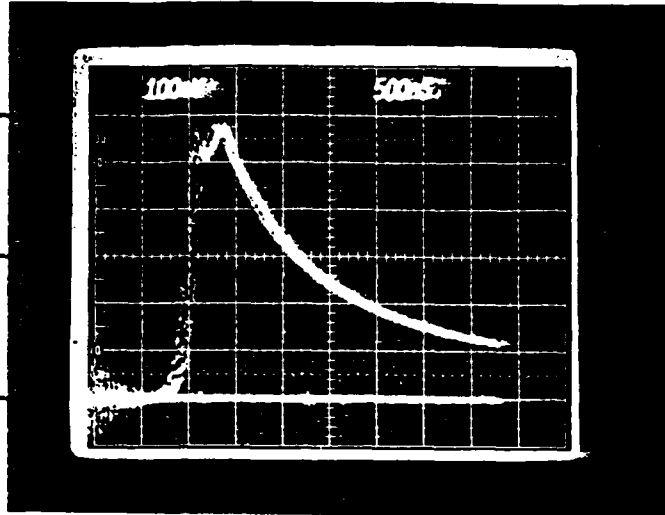
TIME

0.2 Torr, He

a)

E-BEAM CURRENT, A

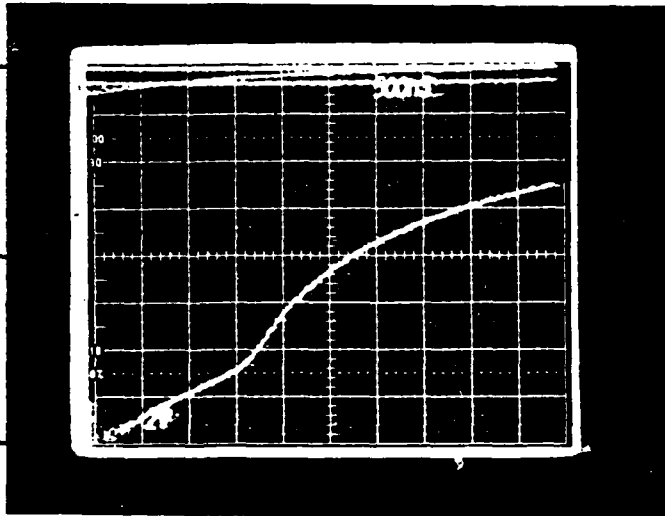
60  
30  
0



b)

VOLTAGE, kV

0  
40  
80



TIME

